

Dissertation

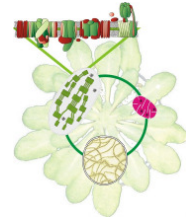
TAP38 - a key player in LHCII
dephosphorylation

A genetic approach in *Arabidopsis thaliana*



Mathias Pribil

13.07.2009



TAP38 - a key player in LHCII dephosphorylation

A genetic approach in *Arabidopsis thaliana*

Dissertation

zur Erlangung des Doktorgrades der Fakultät für Biologie
der Ludwig-Maximilians-Universität München

Mathias Pribil

Juli 2009

(Tag der mündlichen Prüfung: 27.08.2009)

Erstgutachter: Prof. Dr. Dario Leister

Zweitgutachter: Prof. Dr. Jörg Nickelsen

Summary

Short-term changes in illumination or in the spectral composition of light elicit alterations in phosphorylation of thylakoid proteins and a reorganisation of the photosynthetic machinery. Phosphorylation of the light-harvesting complex (LHC) of photosystem II (PSII) facilitates relocation of LHCII to PSI and consequently permits redistribution of excitation energy between the photosystems (State Transitions). In the green alga *Chlamydomonas reinhardtii* and the flowering plant *Arabidopsis thaliana* the orthologous thylakoid protein kinases, Stt7 and STN7 respectively, are required for LHCII phosphorylation and State Transitions. The phosphorylation of LHCII is a reversible process and therefore requires a protein phosphatase. Previous biochemical efforts to identify the involved phosphatase have been without success so far. In this thesis it was shown, that the Thylakoid-Associated Phosphatase of 38 kDa (TAP38) is required in *A. thaliana* for dephosphorylation of LHCII and for the transition from state 2 to state 1. In *tap38* mutants, levels of LHCII phosphorylation are constitutively high, the PSI antenna is enlarged and thylakoid electron flow is enhanced, resulting in more rapid growth under low light regimes compared to wild type. Overexpression of the TAP38 gene (*oeTAP38*) markedly decreases LHCII phosphorylation and inhibits the shift from state 1 to state 2, thus mimicking the *stn7* phenotype in which LHCII phosphorylation is suppressed. The dependence of LHCII dephosphorylation upon TAP38 protein amount as well as the strong phenotypic resemblance of *oeTAP38* and *stn7* mutant plants suggest, that TAP38 and STN7 act antagonistic at the same regulatory level regarding short term photosynthetic adaptation. This could be accomplished by TAP38 and STN7 either via direct (de-) phosphorylation of LHCII or by forming part of a phosphorylation cascade, which controls the activity of the LHCII kinase or phosphatase. In this respect an involvement of TAP38 in the adjustment of photosystem stoichiometry is discussed, which plays a role in long-term acclimation of photosynthesis.

Zusammenfassung

Kurzzeitige Lichtschwankungen in Intensität oder spektraler Zusammensetzung führen zu veränderter Thylakoidproteinphosphorylierung und zu einer Restrukturierung des Photosyntheseapparates. Die Phosphorylierung des Lichtsammelkomplexes (LHC) des Photosystems II (PSII) induziert die Anlagerung von LHCII an das Photosystem I (PSI) und ermöglicht „State Transitions“: eine Umverteilung der Anregungsenergie zwischen den Photosystemen. Die orthologen, Thylakoidmembran-assoziierten Proteinkinasen Stt7 und STN7 der Grünalge *Chlamydomonas reinhardtii* und der Blütenpflanze *Arabidopsis thaliana* sind für die LHCII Phosphorylierung und damit für „State Transitions“ erforderlich. Die LHCII Phosphorylierung ist ein reversibler Prozess und bedarf daher einer Proteinphosphatase. Bisherige biochemische Ansätze die beteiligten Proteinphosphatasen zu identifizieren, blieben jedoch erfolglos. In dieser Arbeit wurde gezeigt, dass die Thylakoidmembran-assoziierte Proteinphosphatase mit einer Größe von 38 kDa (TAP38) in *A. thaliana* für die LHCII Dephosphorylierung und den Übergang von State 2 zu State 1 erforderlich ist. *Tap38* Mutanten weisen einen konstitutiv erhöhten Level an phosphoryliertem LHCII auf, einen stabileren Elektronenfluss in der Thylakoidmembran und besitzen eine vergrößerte PSI Antenne. Unter Schwachlichtbedingungen führt dies verglichen zum Wildtyp zu einem schnelleren Wachstum. Die Überexpression von TAP38 (*oeTAP38*) bedingt eine merkliche Phosphorylierungsabnahme des LHCII, hemmt den Übergang von State 1 zu State 2 und ähnelt insofern stark dem Phänotyp der *stn7* Mutante, in der die LHCII Phosphorylierung unterdrückt ist. Die Abhängigkeit der LHCII Phosphorylierung von der TAP38 Proteinmenge sowie die starke Ähnlichkeit der *oeTAP38* und *stn7* Mutantenphänotypen lassen folgern, dass TAP38 und STN7 in der kurzfristigen Photosyntheseadaptation antagonistisch auf derselben regulatorischen Ebene wirken. TAP38 und STN7 könnten LHCII direkt (de-)phosphorylieren oder als Elemente einer Phosphorylierungskaskade wirken, welche die Aktivität der LHCII Kinase bzw. Phosphatase reguliert. Daher wird für TAP38 eine Funktion bei der Langzeitadaptation des Photosyntheseapparates diskutiert.

Index

Summary	ii
Zusammenfassung	iii
Index	iv
List of Figures	vii
List of Tables	ix
Abbreviations	x
1. Introduction	1
1.1 Photosynthesis	1
1.2 Mechanisms for the adaptation of photosynthesis to changing light conditions.....	5
1.3 Short-term acclimation – State Transitions	5
1.4 Long-term acclimation – Long-term response (LTR)	8
1.5 Protein phosphorylation in chloroplasts	10
1.6 Chloroplast protein import and its bioinformatic prediction	12
1.7 Aims of the thesis	13
2. Materials and Methods	14
2.1 Database analysis and prediction of subcellular targeting.....	14
2.2 Subcellular localisation of PCP-dsRED fusions in Arabidopsis protoplasts.....	14
2.3 LHCII phosphorylation assay	15
2.4 Plant materials and growth conditions	16
2.5 Screening for T-DNA insertion lines	17
2.6 TAP38 overexpressor and complementing lines	18
2.7 Generation of polyclonal TAP38 antibodies.....	19
2.8 Transcript profiling of <i>TAP38</i> in different genetic backgrounds.....	19
2.9 Chlorophyll fluorescence and spectroscopic measurements	20
2.9.1 Standard photosynthetic parameters.....	20
2.9.2 State Transition measurements.....	21
2.9.2.1 State Transition measurements via PAM fluorometry.....	21
2.9.2.2 77K fluorescence emission spectroscopy.....	21
2.10 <i>In vitro</i> import of TAP38 into pea chloroplasts	22

2.11	Total protein preparation.....	23
2.12	Isolation of intact chloroplasts.....	24
2.13	Immunoblot analyses.....	24
2.14	Blue Native (BN) - PAGE.....	25
2.15	2D polyacrylamide gel electrophoresis (2D-PAGE)	25
2.16	Sucrose gradient centrifugation	26
3.	Results	30
3.1	Prediction and experimental validation of putative cpPPs	30
3.2	At4g27800 gene model and expression of splice variants.....	36
3.3	Subcellular localisation of TAP38	37
3.4	Comparison of TAP38 with related protein sequences from higher plants and moss	37
3.5	Expression of TAP38 in <i>tap38</i> mutant and TAP38 overexpressors.....	40
3.6	State Transitions and 77K measurements.....	40
3.7	Reversible phosphorylation of LHCII	44
3.8	Association of TAP38 with a low molecular weight complex.....	48
3.9	Growth characteristics and photosynthetic performance	49
4.	Discussion	52
4.1	cpPPs - bioinformatic prediction vs experimental confirmation.....	52
4.2	Splice variants of TAP38	55
4.3	LHCII dephosphorylation - thylakoid associated TAP38 vs biochemically identified stromal PP	55
4.4	TAP38 - possible modes of action	56
4.4.1	Model A	58
4.4.2	Model B	58
4.4.3	Model C	59
4.4.4	Arguments in favour of models B and C	59
4.5	Uncoupling of LHCII phosphorylation from PQ redox state	59
4.6	Putative interaction partners of TAP38	60
4.7	Does TAP38 - like STN7 - function in LTR?	62
4.8	Which protein took over the function of TAP38 in <i>Chlamydomonas</i> ?.....	64

4.9	Enhanced photosynthetic performance and growth phenotype of tap38 mutants.....	64
Appendix 1	66
Appendix 2	67
References	68
Acknowledgements	87
Curriculum vitae	88
Declaration / Ehrenwörtliche Versicherung	90

List of Figures

Figure 1.1	The absorption spectra of the chlorophylls (Chl a + Chl b) plus carotenoids (A) correlates well with the observed photosynthetic output (B)	2
Figure 1.2	Scheme of linear electron transport (LEF).....	4
Figure 1.3	State Transitions	7
Figure 1.4	Concept of LTR signalling	10
Figure 3.1	Fluorescence micrographs of <i>Arabidopsis thaliana</i> protoplasts transfected with N-terminal fusions of the predicted transit peptides of the respective cpPPs to RFP....	33
Figure 3.2	Gene structures including T-DNA insertion sites of chloroplast localised protein phosphatases.....	34
Figure 3.3	Comparison of the level of PSII core and LHCII protein phosphorylation between different T-DNA insertion lines and WT plants	35
Figure 3.4	Insertion alleles of <i>At4g27800</i> and splice variant expression.....	36
Figure 3.5	Subcellular localisation of TAP38.....	38
Figure 3.6	Comparison of the TAP38 sequence with those of related proteins from higher plants and moss	39
Figure 3.7	TAP38 transcript and protein levels in different genetic backgrounds.....	41
Figure 3.8	TAP38 is required for State Transitions.....	42
Figure 3.9	Low-temperature (77K) fluorescence emission spectra of thylakoids	43
Figure 3.10	Levels of LHCII phosphorylation correlate inversely with TAP38 concentrations	45
Figure 3.11	Quantification of PSI-LHCI and PSI-LHCI-LHCII complexes under state 2 conditions	47
Figure 3.12	TAP38 is constantly expressed under all investigated light conditions	48

Figure 3.13	TAP38 occurs mainly as a monomer or associated with a low molecular weight complex.....	49
Figure 3.14	Growth characteristics of <i>tap38</i> mutant plants	50
Figure 3.15	Photosynthetic performance of <i>tap38</i> mutant plants	51
Figure 4.1	Models for potential modes of action of TAP38.....	57
Appendix Figure 1	Collection of fluorescence micrographs of <i>A. thaliana</i> protoplasts transfected with N-terminal fusions of the predicted transit peptides of the respective cpPPs to dsRED	66
Appendix Figure 2	Thylakoid proteins extracted from <i>tap38-2</i> plants fractionated by SDS- and BN-PAGE.	67

List of Tables

Table 2.1	List of primers used to amplify the N-terminal coding sequences of the 27 candidate genes to generate the respective dsRED fusion constructs.....	28
Table 2.2	AGI accession numbers of genes coding for the experimentally identified cpPPs and the corresponding T-DNA insertion lines.....	28
Table 2.3	Primers used for the identification of the homozygous T-DNA insertion lines listed in Table 2.1.....	29
Table 3.1	Protein phosphatase sequences were retrieved from TAIR	31
Table 3.2	List of 26 candidate genes selected for the <i>in vivo</i> localisation assay with RFP-fusion proteins in <i>Arabidopsis</i> protoplasts	32
Table 3.3	Energy distribution between PSI and PSII measured as the fluorescence emission ratio at 730 nm and 685 nm (F_{730}/F_{685}) under state 1 and state 2 promoting light conditions.....	44

Abbreviations

<i>A. thaliana</i>	<i>Arabidopsis thaliana</i>
ATP	adenosine triphosphate
ATPase	ATP synthase
β -DM	n-dodecyl β -D-maltoside
BN	blue-native
Bis-Tris	bis(2-hydroxyethyl)-imino-tris(hydroxymethyl)-methane
bp	base pair
BSA	bovine serum albumin
cDNA	complementary deoxyribonucleic acid
CEF	cyclic electron flow
Chl (a/b)	chlorophyll (a/b)
Co-IP	complex-immunoprecipitation
cpPP	chloroplast protein phosphatase
<i>C. reinhardtii</i>	<i>Chlamydomonas reinhardtii</i>
cTP	chloroplast transit peptide
cyt	cytochrome
D	dark
DNA	deoxyribonucleic acid
dsRED	red fluorescence protein from a <i>Discosoma</i> coral
DTT	dithiothreitol
EDTA	ethylene diamine tetraacetic acid
EGTA	ethylene glycol tetraacetic acid
EST	expressed sequence tag
Fd	Ferredoxin
F_M / M'	maximum fluorescence in the dark / light
F_0	fluorescence after dark adaptation
F_s	steady-state fluorescence
F_v	variable fluorescence
FNR	Ferredoxin-NADP ⁺ -oxido-reductase
FR	far-red (light)
HEPES	4-(2-hydroxyethyl)-1-piperazineethanesulfonic acid

IPTG	isopropyl β -D-1-thiogalactopyranoside
LB	Left border
LED	light-emitting diode
LEF	linear electron flow
LHC (I/II)	light harvesting complex (I/II)
LL	low light
LTR	long-term response
mRNA	messenger ribonucleic acid
MES	2-(N-morpholino)ethanesulfonic acid
NADP ⁺ /H	Nicotinamide adenine dinucleotide phosphate
NDH	NADPH dehydrogenase complex
oe	overexpressor
o/n	overnight
P680	PSII reaction centre
P700	PSI reaction centre
PA	polyacrylamide
PAGE	polyacrylamide gel electrophoresis
PAM	pulse amplitude modulation
PAR	photosynthetically active radiation
PC	plastocyanin
PCP	putative chloroplast
PCR	polymerase chain reaction
PEG	polyethyleneglycol
PFD	photon flux density
PK	protein kinase
pLHC (I/II)	phosphorylated LHC (I/II)
pmf	proton motive force
PP	phosphatase
PP2C	protein phosphatase 2 C
PP2A	protein phosphatase 2 A
PQ(H ₂)	plastoquinone oxidised (reduced)
PS (I/II)	photosystem (I/II)
qP	photochemical quenching
qT	State Transitions

RB	right border
RFP	red fluorescent protein
RNA	ribonucleic acid
RT-PCR	reverse transcriptase PCR
SD	standard deviation
SDS	sodium dodecyl sulphate
TAP	thylakoid associated protein phosphatase
T-DNA	transfer-DNA
TM	transmembrane domain
Tris	tris (hydroxymethyl) aminomethane
UBI	Ubiquitin
vs	versus
WT	wild type
2D	2-dimensional

Units

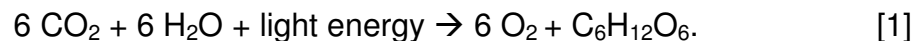
°C	degree Celcius
cm	centimetre
δ	delta
Da	Dalton
g	gram
<i>g</i>	gravity
h	hour
K	Kelvin
k	kilo
l	litre
μ	micro
M	molar
m	metre
mA	milliampere
min	minutes
ml	millilitre
mM	millimolar
mol	molar

nm	nanometre
Φ_{II}	effective quantum yield of photosystem II
rmp	rounds per minute
s	second
V	volt
v	volume
w	weight

1. Introduction

1.1 Photosynthesis

Life on earth is driven by sunlight which is used by photoautotrophic organisms to assimilate organic molecules from carbon dioxide. This process is called photosynthesis and occurs in chloroplasts, organelles found in all green parts of plants but mainly in leaf cells (Campbell, 1997). The overall reaction of oxygen-generating photosynthesis is



The principal end products are two different carbohydrates. Sucrose is synthesised in the cytosol from three carbon precursors generated in the stroma of the chloroplast and is then transported from the leaf to other parts of the plant. Leaf starch, the second product, is transitorily stored in the chloroplast (Lodish et al., 2000).

Three membranes are characteristic for chloroplasts. The outer membrane contains proteins that form large aqueous channels and therewith is permeable to small metabolites. The inner membrane represents a permeability barrier with transporters regulating the metabolite movement in and out of the organelle. The third membrane, the thylakoid membrane, represents the site of photosynthesis. The compartment surrounded by the thylakoid membranes is called the thylakoid lumen. Integral membrane proteins bind prosthetic groups and light-absorbing pigments, such as chlorophyll (Lodish et al., 2000).

The process of photosynthesis can be divided into two functional and regional separated reactions. The first is the absorption of light energy by photosynthetic pigments, attached to proteins in the thylakoid membranes. The finally produced ATP and NADPH are used in the second step, the Benson-Calvin cycle, taking place in the stroma (Lodish et al., 2000).

The absorption spectra of chlorophyll a (Chl a) and chlorophyll b (Chl b) cover wave lengths between 400 and 700 nm. The measured rate of photosynthesis as a function of absorbed wavelength correlates well with the absorption frequencies of chlorophylls, but makes it evident that there are some other contributors to the absorption, which refers to carotenoids (Figure 1.1). However, only Chl a is directly involved in the light reaction. Most of the Chl a form a complex together with Chl b and carotenoids. Due to their antennae function these complexes are called light-harvesting-complexes (LHCs). The absorption of photons by LHCs and their transfer to the reaction centres is the fundamental mechanism driving linear electron transport (LEF) in thylakoid membranes (Campbell, 1997) (see Figure 1.2).

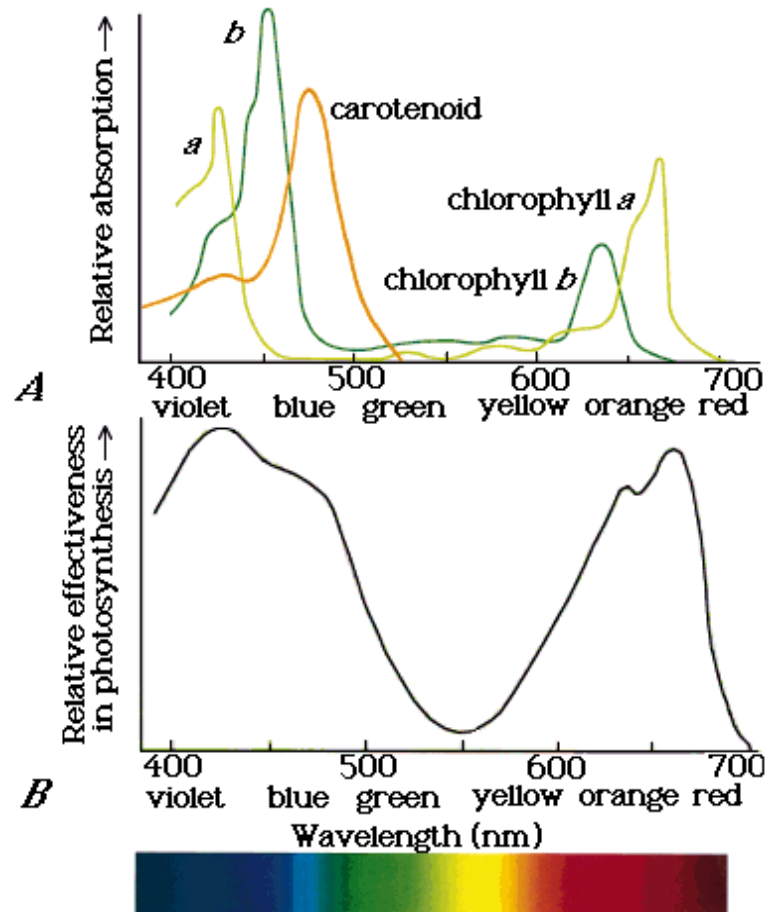


Figure 1.1 The absorption spectra of the chlorophylls (Chl a + Chl b) plus carotenoids (A) correlates well with the observed photosynthetic output (B). The measure of photochemical efficiency is made by measuring the amount of oxygen produced by leaves following exposure to various wavelengths.

Two types of photosystems are integral to the thylakoid membrane: photosystem I (PSI) and photosystem II (PSII). The two photosystems show maximum light absorbing efficiencies in two different spectral ranges: PSI in the far-red light, at wavelengths of 700 nm and PSII in the low-red light, at wavelengths of 680 nm. Both systems contain similar Chl a molecules. However, the binding to different proteins in the thylakoid membrane causes a difference in electron distribution and therewith a slightly different light absorption behaviour (Campbell, 1997).

The electron transport starts at PSII (Figure 1.2). The absorption of photons causes excitation of the reaction centre of P680. Two electrons are transferred to the primary electron acceptor, Pheophytin a. The electron gap at the oxidised Chl a is counterbalanced when a photon is absorbed by the LHC of PSII (LHCII). Resonance transfer then guides the photon to the reaction centre of Chl a. Consequently water is split into two protons, $\frac{1}{2}$ O₂ and two electrons which will subsequently close the electron gap. The primary electron acceptor transfers the electron to a fixed plastoquinone (Q_A), which in turn transfers the electron to a reversibly bound plastoquinone (Q_B). By the uptake of two protons from the stroma, Q_B becomes a mobile carrier, which subsequently transfers the electron to the cytochrome b₆/f complex (Cyt b₆/f). The final mobile luminal carrier plastocyanin (PC) injects the electron to PSI. PSI is also associated with a LHC (LHCI), which contains less Chl b than LHCII. The transferred electrons close the electron gap of P700, which occurs similar to the procedure described for P680. The further electron transport chain leads from ferredoxin (Fd) to a ferredoxin-NADP-reductase (FNR) which reduces NADP⁺ with two electrons and two protons to NADPH and H⁺ (Campbell, 1997).

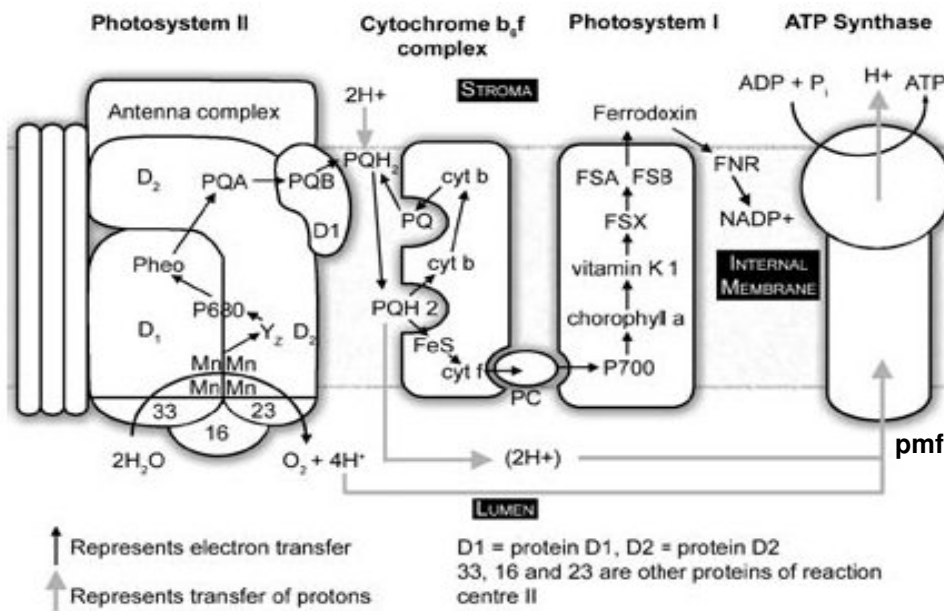


Figure 1.2 Scheme of linear electron transport (LEF). Pheophytin a (Pheo); oxidised/reduced form of plastoquinone (PQ/PQH₂); plastocyanin (PC); ferredoxin-NADPH-oxidoreductase (FNR); proton motive force (pmf); adapted from Hankamer et al. (1997).

The ATP synthase (ATPase) produces ATP at the expense of the proton motive force (pmf) formed by light-driven electron-transfer reactions and by Cyt b₆/f, which mediates electron transport between PSII and PSI and converts the redox energy into part of the proton gradient used for ATP formation. Both, function and structure of the integral thylakoid membrane complexes were extensively studied and reviewed (Nield et al., 2000; Ben-Shem et al., 2003; Nelson and Yocum, 2006; Baniulis et al., 2008).

The assimilation of CO₂ in the Benson-Calvin cycle requires ATP and NADPH in a 3:2 ratio (Allen, 2002). This ratio cannot be ensured by LEF itself, as the pH gradient does not allow for a higher ATP production. There are different alternative electron pathways that play a role in the fine-tuning of the ATP:NADPH ratio, known as cyclic electron flow (CEF) around PSI (Eberhard et al., 2008). Electrons generated at the acceptor side of PSI can be reinjected at its donor side to specifically increase the generation of ATP. It is assumed that this reaction increases under stress conditions such as low temperature and drought. The existence of at least two possible routes, via ferredoxin (Fd) (Munekage et al., 2002; DalCorso et al., 2008) and via

the plastidial NADPH dehydrogenase (NDH) (Shikanai, 2007), is generally accepted but their interconnections and interactions are still obscure.

1.2 Mechanisms for the adaptation of photosynthesis to changing light conditions

Owing to their sessile life style, plants have to cope with the changes of biotic and abiotic factors of their habitats, like the density of plant stand, temperature, nutrient and water availability as well as fluctuating light intensities and qualities. Changes in light quality result in imbalanced excitation of the two photosystems and a decrease in the efficiency of the photosynthetic light reactions. Plants counteract such changing conditions by performing acclimatory responses which elicit modifications of thylakoid proteins and reorganisation of the photosynthetic machinery (Kanervo et al., 2005; Walters, 2005). In the short-term (up to several minutes), this involves the so-called State Transitions, which depend on the reversible association of the mobile pool of LHCII with PSII or PSI in state 1 and state 2, respectively (Figure 1.3). As a long-term response (LTR), imbalances in energy distribution are adjusted by changing the stoichiometry of the photosystems (Pfannschmidt, 2003).

1.3 Short-term acclimation – State Transitions

Under light conditions preferentially exciting PSII (e.g. low light), the redox state of the PQ pool is changed to a more reduced state. A reduced state of the PQ pool promotes docking of plastoquinol (PQH₂) to the Q_o site of Cyt b₆/f, which in turn leads to the activation of a thylakoid protein kinase able to phosphorylate the LHCII complex (Vener et al., 1997; Zito et al., 1999). Upon phosphorylation conformational changes within LHCII occur (Nilsson et al., 1997) which trigger the association of LHCII with PSI in the stroma lamellae, grana ends and grana margins. This leads to a direction of additional excitation energy to PSI and thus balancing the light excitation

energy between the two photosystems (Allen and Forsberg, 2001; Haldrup et al., 2001; Wollman, 2001; Rochaix, 2007; Eberhard et al., 2008). The state in which the mobile part of LHCII is associated with PSI is called state 2 (Figure 1.3). The docking of phosphorylated LHCII (pLHCII) to PSI most likely involves the H, L and O subunits of PSI, as demonstrated by the impairment of this process in the corresponding *Arabidopsis* mutants (Lunde et al., 2000; Jensen et al., 2004). Conversely, when plants or algae are illuminated by light preferentially exciting PSI, the PQ pool becomes oxidised, leading to the inactivation of the LHCII kinase. An as yet unknown phosphatase catalyses the dephosphorylation of pLHCII associated with PSI and with it the return of the mobile LHCII fraction to PSII. This state is called state 1 (Allen, 1992; Wollman, 2001) (Figure 1.3).

The ability of photosynthetic organisms to rapidly respond to changes in light quality and quantity by varying the relative sizes of their PSI and PSII antennae cross-sections, is known as State Transitions (Allen, 1992; Wollman, 2001). This mechanism involved in balancing the absorbed light energy between the two photosystems was first reported almost 30 years ago in unicellular photosynthetic organisms (Bonaventura and Myers, 1969; Murata, 1969). The lateral movement of LHCII upon phosphorylation, which was proposed to be caused either by changes in the affinity to PSI and PSII due to conformational changes or by electrostatic repulsion due to an increase in negative charges (Allen, 1992), is also accompanied by rapid and reversible changes in thylakoid membrane and protein complex organisation (Chuartzman et al., 2008; Tikkanen et al., 2008).

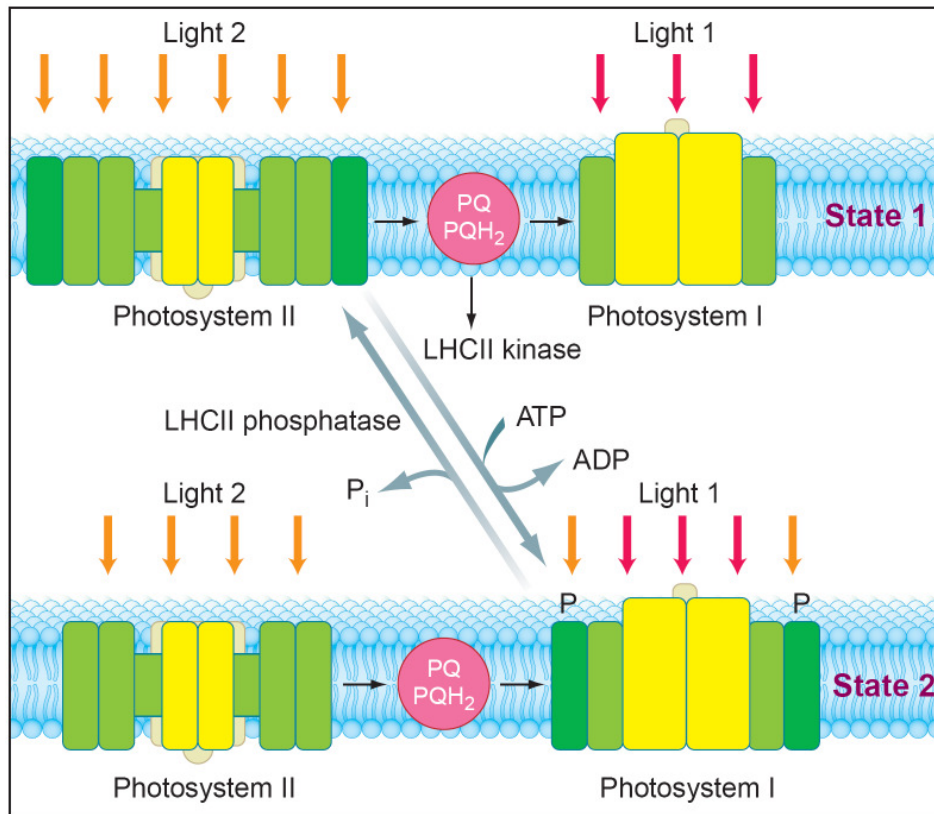


Figure 1.3 State Transitions. When photosystem II is preferentially excited, the plastoquinone pool becomes reduced (PQH_2), leading to an activation of the LHCII kinase. Thus, the mobile fraction of LHCII becomes phosphorylated and is relocated to PSI (state 2). Contrarily, if photosystem I is preferentially excited, the plastoquinone pool becomes oxidised (PQ), leading to an inactivation of the LHCII kinase. The LHCII phosphatase then catalyses the dephosphorylation and movement of LHCII back to PSII (state 1). PSII specific light (light 2); PSI specific light (light 1); light-harvesting protein pigment complexes specific to the respective PS (light green); mobile light-harvesting complex - LHCII (dark green); P (phosphate group); from Allen (2003).

The impact of State Transitions on energy balancing between PSII and PSI as well as promoting cyclic electron flow around PSI is well evidenced in *C. reinhardtii* (Wollman, 2001; Eberhard et al., 2008). With a PSII / PSI transfer rate of about 80% of the total excitation energy absorbed by LHCII (Delosme et al., 1996), *Chlamydomonas* is an ideal model system for studying photosynthetic State Transitions. In flowering plants, however, its physiological significance is still under debate. In *A. thaliana* the transfer rate of the mobile LHCII fraction comprises only 15-20%, which is significantly lower compared to green algae (Allen, 1992; Delosme et al., 1994). Moreover, plants are only marginally affected in their development

and fitness when impaired in State Transitions (Lunde et al., 2000; Bonardi et al., 2005; Tikkanen et al., 2006), even under light conditions permanently triggering its mechanism (Bellafiore et al., 2005; Frenkel et al., 2007). Contrarily, recent studies propose a stronger physiological relevance of State Transitions also in flowering plants, in particular when plants are perturbed in linear electron flow (LEF) (Pesaresi et al., 2009).

To elucidate the nature of the LHCII kinase, screens for mutants deficient in State Transitions were performed in *C. reinhardtii* (Fleischmann et al., 1999), which resulted in the isolation of mutants defective in a serine-threonine protein kinase, called Stt7 (Depege et al., 2003). The *stt7* mutant was blocked in state 1 and failed to phosphorylate LHCII under conditions that favour state 2. Stt7 possesses two homologues in the *Arabidopsis* genome – *STN7* and *STN8*. While *stn7* mutants were shown to be defective in LHCII phosphorylation and the redistribution of LHCII to PSI at the expense of PSII (Bellafiore et al., 2005; Bonardi et al., 2005), *stn8* mutants failed to phosphorylate PSII core proteins (Bonardi et al., 2005; Vainonen et al., 2005).

Recent studies on Stt7 propose a topology that is characterised by a transmembrane region separating a stroma-exposed catalytic kinase domain from its lumen-located N-terminal end with two conserved cysteine residues that are critical for the activity of Stt7 and State Transitions (Lemeille et al., 2009). Also an interaction with Cyt b_6/f , PSI and LHCII was revealed by co-immunoprecipitation assays. The question, whether the Stt7 / STN7 kinase is part of a kinase cascade or directly phosphorylates LHCII remains to date unresolved. Also the identity of the LHCII phosphatase(s) or phosphatases involved in the dephosphorylation of pLHCII is still unknown.

1.4 Long-term acclimation – Long-term response (LTR)

In the long-term, light conditions that preferentially excite PSI or PSII generate an imbalance in the excitation energy distribution between the two photosystems which the plant counteracts by adjusting its photosystem stoichiometry. This involves changes in the abundance of reaction centre

and light-harvesting proteins that take place within hours and days (long-term response, LTR) (Melis, 1991; Fujita, 1997).

Similar to State Transitions, the LTR is triggered by the redox state of the PQ pool. However, while the mechanism underlying State Transitions solely depends on post-translational modifications, the adjustment of photosystem stoichiometry involves changes in the expression of the corresponding plastid- and nucleus-encoded proteins and in the accumulation of chlorophyll *a* and *b* (Pfannschmidt et al., 2001). In *A. thaliana* as in most other species investigated, LTR was shown to be mediated predominantly by changes in the number of PSI complexes, demonstrated by an increased expression of the PSI reaction centre operon *psaAB* upon reduction of the PQ pool or a respective repression upon its oxidation (Fey et al., 2005a; Dietzel et al., 2008). Those changes in expression are followed by an extensive restructuring of the thylakoid membrane system, including enhanced formation of grana stacks and reduced accumulation of transitory starch in plastids upon exposure to PSI light (Dietzel et al., 2008). Studies of the *A. thaliana stn7* mutant uncovered a defect in both, State Transitions and LTR (Bonardi et al., 2005; Tikkanen et al., 2006). This implies that the STN7 kinase represents a common redox sensor and / or signal transducer for both responses, which is in accordance with earlier suggestions that the two processes are subject to regulatory coupling (Allen, 1995; Allen and Pfannschmidt, 2000; Pursiheimo et al., 2001) (see Figure 1.4). Recently, the Arabidopsis TSP9 protein, a thylakoid soluble phosphoprotein of 9 kDa, has been reported to be phosphorylated in a STN7-dependent manner and to be involved in State Transitions (Fristedt et al., 2009). Upon phosphorylation, TSP9 is released from the thylakoid membranes into the stroma and has therefore been suggested to be a possible component of the redox-dependent signaling cascade for the adjustment of photosynthetic gene expression (Carlberg et al., 2003; Zer and Ohad, 2003). The latest findings, however contradict this idea as *TSP9* RNA interference lines exhibit a normal LTR (Pesaresi et al., 2009). Therefore another so far unknown component has to exist, that mediates the redox signal to the nucleus. Pesaresi et al. (2009) could further exclude that the phosphorylation of

LHCII *per se* or conformational changes of thylakoid membrane components associated to State Transitions play any role in LTR.

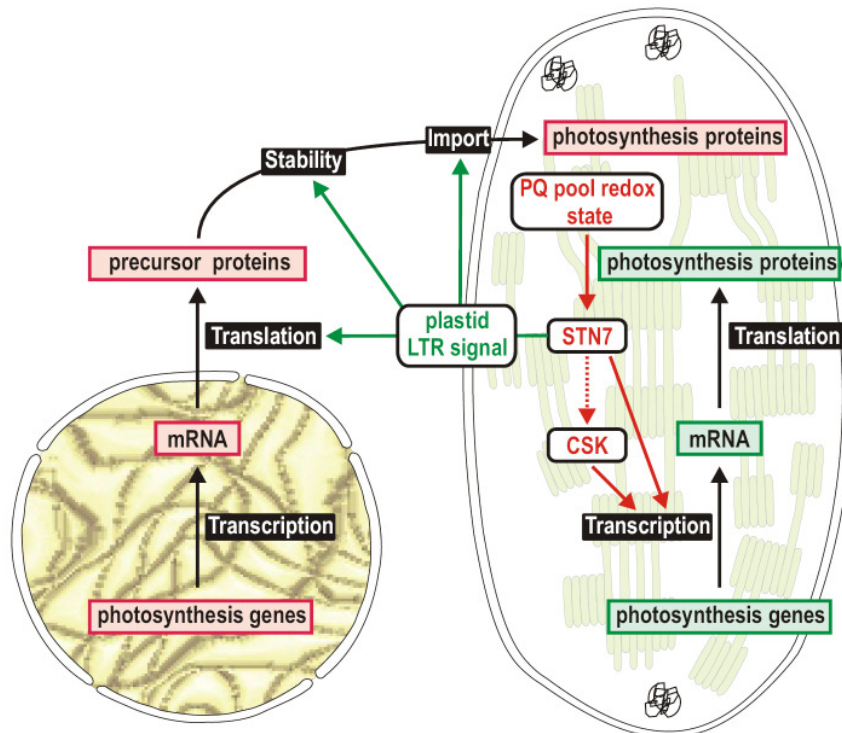


Figure 1.4 Concept of LTR signalling. The LTR signalling pathway is triggered by the STN7 kinase. Its activity is modulated by the redox state of the PQ pool. The signalling pathway can be divided in two main branches. One branch addresses chloroplast gene expression and is responsible for the transcriptional regulation of PSI-related genes (e.g. *psaAB* operon) (red arrows). The Chloroplast Sensor Kinase (CSK) (Puthiyaveetil et al., 2008), reported to regulate the transcription of the *psaAB* operon, might be a component of this branch. A second branch (green arrows) is responsible for the regulation of the accumulation of products of nuclear photosynthesis-related genes. These regulatory processes occur most likely after the transcription and might take place at the level of protein translation or degradation, or protein import efficiency and specificity. From Pesaresi et al. (2009).

1.5 Protein phosphorylation in chloroplasts

With around one-third of all eukaryotic proteins undergoing reversible phosphorylation (Olsen et al., 2006), phosphorylation of amino acid side chains is the major post translational modification that can modulate the

conformation, activity, localisation and stability of proteins. Proteins of eukaryotic cells become predominantly phosphorylated at their serine, threonine or tyrosine residues (Laugesen et al., 2004), whereas phosphorylation of important elements of the two-component signalling pathway in prokaryotes and eukaryotes are also reported to occur at histidine and aspartate residues (Saito, 2001). The major group of eukaryotic serine and threonine phosphatases is represented by two families, PPP and PPM phosphatases. While members of the PPP family are sensitive to the toxins okadaic acid and microcystin (PP1 and PP2A) or cyclosporin A (PP2B), members of the PPM family (PP2C and PP2C-like) are dependent on the presence of divalent cations (e.g. Mg^{2+} or Mn^{2+}) for their activity and are insensitive to microcystin and okadaic acid (Cohen, 1989). In chloroplasts, reversible phosphorylation of proteins can predominantly be detected at serine and threonine residues and is known to regulate prominent processes like the photosynthetic light reaction (Vener et al., 1998; Vener, 2007), starch metabolism (Tetlow et al., 2004) or transcription (Baginsky et al., 1997; Kleffmann et al., 2007). To date, the reversible phosphorylation of thylakoid proteins associated with the regulation of the migration of LHCII between the photosystems during State Transitions (Haldrup et al., 2001; Wollman, 2001), as well as with the turnover of PSII proteins (Rintamäki et al., 1996; Rintamäki et al., 1997), has been subject of extensive investigation. However, the complement of the involved chloroplast protein phosphatases (cpPPs), in comparison to the chloroplast protein kinases (cpPKs), is virtually unknown. AtRP1, a bifunctional protein kinase / protein phosphatase involved in the regulation of *Arabidopsis* pyruvate, orthophosphate dikinase (PPDK) is the only experimentally identified cpPP so far (Chastain et al., 2008). For many years, attempts were undertaken to elucidate the nature of the PPs involved in the dephosphorylation of photosynthesis related phosphoproteins (i.e. PSII core and LHCII proteins). By means of biochemical approaches (Sun et al., 1989; Hammer et al., 1995a; Hast and Follmann, 1996) it could be shown, that phosphatases of different families must be involved in the reversible phosphorylation of thylakoid phosphoproteins. While a PP2A-like phosphatase was postulated to be responsible for the desphosphorylation of

the PSII core proteins (Vener et al., 1999), the LHCII phosphatase activity was shown to be dependent on the presence of divalent cations and not to be inhibited by microcystin and okadaic acid (Sun et al., 1989; Hammer et al., 1995a). Both findings strongly suggest an involvement of a PP2C-type phosphatase (Cohen, 1989). The identification of novel cpPPs with a strong emphasis on the PSII core and LHCII protein phosphatase(s) was the superior motif for the work presented in this thesis.

1.6 Chloroplast protein import and its bioinformatic prediction

The protein import translocons, present in the outer envelope of the chloroplast (Toc complex) and the inner envelope (Tic complex), mediate the translocation of the vast majority of nuclear-encoded pre-proteins destined for the chloroplast (Jarvis, 2004; Stengel et al., 2007).

Most of these nucleus-encoded, organellar proteins initially bear an amino-terminal targeting signal - called a presequence or chloroplast transit peptide (cTP) - which guides these proteins through the post-translational targeting pathway to their final destination (Jarvis and Soll, 2002). After import, the cTP is proteolytically removed. The transit sequence is both necessary and sufficient for organelle recognition and translocation initiation. For the prediction of cTPs various algorithms have been developed preferentially using sequence-based methods (Casadio et al., 2008). The algorithms analyse the protein sequences for characteristics like hydrophobicity of certain domains or the amino acid composition in respect to their charges. By applying several prediction algorithms on the same dataset the accuracy of prediction can be improved (Richly and Leister, 2004).

1.7 Aims of the thesis

The project's goal was the identification of the LHCII phosphatase(s). To achieve this aim novel and so far unknown chloroplast protein phosphatases (cpPPs) were systematically identified in *Arabidopsis*.

In a prediction algorithm-based *in vivo* localisation assay, the entire complement of known protein phosphatases was screened for the presence of cTPs followed by the subcellular localisation of the identified candidate genes by RFP-fusions in *Arabidopsis* protoplasts.

In a second approach, published data of various mass spectrometric analyses of the chloroplast proteome or its subfractions were analysed for proteins with a clear or putative phosphatase motif followed by the confirmation of their localisation via RFP-fusions.

For the true cpPPs, identified in this thesis, loss-of-function mutants were characterised with respect to defects in the reversible phosphorylation of thylakoid membrane proteins. The main focus was on loss-of-function mutants with distinct differences in the phosphorylation behaviour of LHCII and PSII core proteins in comparison to WT plants.

2. Materials and Methods

2.1 Database analysis and prediction of subcellular targeting

To analyse gene models and their coverage by full-length mRNAs or ESTs, the NCBI (<http://www.ncbi.nlm.nih.gov/>) and TAIR databases (<http://www.arabidopsis.org/>; genome release 7) were used. Predictions of chloroplast targeting sequences were performed with the following nine algorithms: Predotar (Small et al., 2004), TargetP (Emanuelsson et al., 2000), Protein Prowler (Boden and Hawkins, 2005), AAIndexLOC (Tantoso and Li, 2007), PredSL (Petsalaki et al., 2006), SLP-Local (Matsuda et al., 2005), WoLF PSORT (Horton et al., 2007), MultiLOC (Hoglund et al., 2006) and PCLR (Schein et al., 2001). For mass spectrometry database searches an in-house database on chloroplast membrane and soluble proteins (Dr. Bernd Müller, unpublished data), as well as publicly available datasets on high purity chloroplast subfractions (Kleffmann et al., 2004; Zybailov et al., 2008) were employed.

2.2 Subcellular localisation of PCP-dsRED fusions in Arabidopsis protoplasts

The red fluorescent protein (RFP) from the reef coral *Discosoma* (dsRED) (Jach et al., 2001) was used as a reporter to determine the intracellular localisation of the putative chloroplast protein phosphatases (PCPs) in a transient gene expression assay. For that, the first 300 base pairs (bps) of the N-terminal coding regions of the selected candidate PCPs, containing the predicted cTPs, were cloned in frame with, and immediately upstream of the sequence coding for dsRED. The primers, which were used to amplify the N-terminal gene sequences by PCR, are listed in Table 2.1. PCR conditions for amplification were as described in 2.5. The coding sequences were ligated into the pGJ1425 vector after digestion with the restriction

enzyme *NcoI* (MBI Fermentas). In the case of TAP38 (At4g27800.1), additionally the entire coding region was cloned into the corresponding vector (pGJ1425) using the primers TAP38_RFPs (5'-A TCC ATG GCG CTT CTG AGG CCG CAT C-3') and TAP38_RFPas (5'-TAC CAT GGC AGA GGA CGA CCC AGC GTG G-3'). Cotyledons of two-week-old *Arabidopsis* plants from tissue culture (ecotype Col-0) were cut and incubated overnight at 23°C in the dark in an appropriate cell wall lysis solution (10 mM MES, 20 mM CaCl₂, 0.5 M mannitol pH 5.8, 0.1 g/ml macerozyme [Duchefa], 0.1 g/ml cellulase [Duchefa]). Protoplasts were collected by centrifugation at 50 *g* for 10 min after filtration through a nylon mesh (Ø 75 µm), followed by resuspension in 8 ml of MSC solution (10 mM MES, 20 mM CaCl₂, 0.5 M mannitol, 120 g/l sucrose, pH 5.8). Subsequently 2 ml of MMM solution (10 mM MES, 10 mM CaCl₂, 10 mM MgSO₄, 0.5 M mannitol, pH 5.8) were added on top of the protoplasts and intact protoplasts were recovered at the interface between the two solutions after centrifugation at 70 *g* for 10 min as described in Dovzhenko and Koop (2003). 40 µg of plasmid DNA were used for protoplast transfection employing PEG in solution (40 % PEG solution, 70 mM Ca(NO₃)₂) as previously described by Koop et al. (1996). Microscopic analyses were carried out after overnight incubation at 23°C in the dark using an Axio Imager fluorescence microscope with integrated ApoTome (Zeiss). Fluorescence was excited via an X-Cite Series 120 fluorescence lamp (EXFO) and detected at wavelength ranges of 565 - 620 nm (dsRED fluorescence) and 670 - 750 nm (chlorophyll autofluorescence).

2.3 LHCII phosphorylation assay

Four-week-old plants of the different T-DNA insertion lines of the experimentally confirmed chloroplast PPs and WT plants were kept overnight in the dark, subsequently exposed to low light (80 µmol m⁻² s⁻¹) for 2 h (8 h in the case of TAP38) and then to far-red light (4.5 µmol m⁻² s⁻¹, 740 nm (LED)) for 2 h (for 30, 60 and 120 min in the case of TAP38). After each light treatment plant material was snap frozen in liquid N₂ and thylakoids

were prepared in the presence of 10 mM NaF as described by Bassi et al. (1985). Leaf material was blended in cold homogenisation buffer (0.5% milk powder, 0.4 M Sorbitol, 0.1 M Tricine pH 7.8), filtrated through a double layer of Miracloth (Calbiochem) and centrifuged at 1400 *g* for 10 min at 4°C. Afterwards the pellet was resuspended in cold resuspension buffer (20 mM HEPES / KOH pH 7.8, 10 mM EDTA pH 8.0) followed by centrifugation at 10.000 *g* for 10 min. The pellet was then resuspended in a small volume of TMK buffer (10 mM Tris-HCl pH 6.8, 10 mM MgCl₂, 20 mM KCl) and the concentration of thylakoid membrane proteins was determined according to the total chlorophyll content (Porra, 2002). Protein amounts equivalent to 2 µg of chlorophyll for each genotype and condition were fractionated using SDS-PAGE (15% polyacrylamide gel) according to Laemmli (1970). After overnight run at 100 V (12-20 mA, anode and cathode buffer: 25 mM Tris-HCl, 190 mM Glycine, 0.1% SDS, pH 8.3) the proteins were transferred to Immobilon-P PVDF membranes (Millipore, Eschborn, Germany) using a semi-dry blotter (Biorad) according to Towbin et al. (1979). For protein transfer a current corresponding to 0.8 mA cm⁻² was applied and a transfer buffer containing 96 mM Glycine, 10 mM Tris and 10% v/v methanol was used. Phosphorylated threonine residues were identified using phosphothreonine-specific antibodies raised in rabbits (Cell Signaling, Beverly, MA). Immunodecoration of the filters was performed according to standard protocols (Sambrook et al., 1989). Signals were detected by enhanced chemiluminescence (ECL kit, Amersham Biosciences).

2.4 Plant materials and growth conditions

AGI accession numbers of confirmed chloroplast PPs and the corresponding T-DNA insertion lines are listed in Table 2.2. At4g27800 insertion mutant line *tap38-2* (SALK_025713) bearing a T-DNA insertion 77 bp upstream of the start codon was identified in the SALK collection (Alonso et al., 2003) which contains flank-tagged ROK2 T-DNA lines (ecotype Col-0). The At4g27800 insertion mutant line *tap38-1* (SAIL_514_C03) derived

from the SAIL collection (Sessions et al., 2002). It possesses a flank-tagged DAP101 T-DNA insertion 49 bp upstream of the start codon (ecotype Col-0). All T-DNA insertion lines were identified by screening the insertion flanking database SIGNAL (http://signal.salk.edu/cgi-bin/tdna_express). Seeds of *A. thaliana* WT (ecotype Col-0) and mutant lines were placed on water soaked Whatman paper in Petri dishes and incubated for three days at 4°C in the dark. This stratification step was performed in order to break dormancy and to synchronise germination. Plants were grown on soil under controlled climate chamber conditions (PFD: 80 $\mu\text{mol m}^{-2}\text{s}^{-1}$, 12 / 12 h dark / light cycle). Fertilisation with “Osmocote Plus” (Scotts Deutschland GmbH, Nordon Germany) was performed according to manufacturer’s instructions. To determine the growth rates of WT and *tap38* mutant plants, the leaf areas of twenty plants of each genotype were measured over a period of four weeks after germination using the free software ImageJ (Abramoff et al., 2004).

2.5 Screening for T-DNA insertion lines

Arabidopsis DNA was isolated from leaf tissue as described (Liu et al., 1995). Insertion junction sites were identified by sequencing the amplicons of PCRs using a combination of gene and T-DNA insertion specific primers. The primers, which were used for the different T-DNA insertion lines of the confirmed chloroplast PPs, are listed in Table 2.3. PCR runs were performed with Taq polymerase (Qiagen) and the following cycling conditions: 3 min at 94°C initial denaturation, followed by 32 cycles of 20 sec denaturation at 94°C, 30 sec annealing at 55°C and 1 min 30 sec elongation at 72°C. After a final elongation step of 5 min at 72°C, the PCR products were separated by a 1% agarose gel. The primer combination used for the *tap38-1* T-DNA insertion derived from pDAP101 was LB1 (5'-GCC TTT TCA GAA ATG GAT AAA TAG CCT TGC TTC C-3') and TAP38-as (5'-CGC TGC GTA GGA GAA GCT AT-3'). Primer specific for the *tap38-2* T-DNA insertion derived from pROK2 were LBB1 (5'-GCG TGG ACC GCT TGC TGC AAC TC-3') and TAP38-as (5'-CGC TGC GTA GGA GAA GCT

AT-3'). A corresponding gene specific primer combination for TAP38 in WT was TAP38-s (5'-CCA CAT AAT TTA CAG ACA TGA GGA A-3') and TAP38-as (5'-CGC TGC GTA GGA GAA GCT AT-3').

2.6 TAP38 overexpressor and complementing lines

To generate TAP38 overexpressing lines (*oeTAP38*) the coding sequence of TAP38 was cloned into the plant expression vector pH2GW7 (Invitrogen). This was accomplished by a cloning strategy based on the GATEWAY Technology (Invitrogen) using the primers TAP38_GATE_s (5'-G GGG ACA AGT TTG TAC AAA AAA GCA GGC TTC ACC ATG GCG CTT CTG AGG CCG CAT C-3') and TAP38_GATE_as (5'-GGG GAC CAC TTT GTA CAA GAA AGC TGG GTG TCA TTA AGA TAG ATG TGA AGA CAT C-3') with additional 5'-terminal attB sites to amplify the TAP38 coding sequence. The coding sequence was then cloned into an entry vector (pDONR201) and subsequently subcloned into the destination vector (pH2GW7) in which TAP38 is under the control of a Cauliflower Mosaic Virus 35S promoter.

For complementation of the *tap38-1* mutant the TAP38 genomic DNA, together with 1 kb of its natural promoter, was ligated into the plant expression vector pP001-VS. Both constructs were used to transform Col-0 or *tap38-1* mutant plants using the floral dipping technique described in Clough and Bent (1998). Flowers were immersed in *Agrobacterium* suspension (strain GV3101, carrying the respective binary vector) containing 5% sucrose and the surfactant Silwet-77 (0.0005% v/v) for 25 sec. Afterwards, plants were transferred to the greenhouse and seeds were collected after approximately 3 weeks.

After selection for resistance to hygromycin (*oeTAP38*) or Basta herbicide (complemented *tap38-1*) the transgenic plants were grown on soil in a climate chamber under controlled conditions (PFD: 80 $\mu\text{mol m}^{-2}\text{s}^{-1}$, 12 / 12 h dark / light cycles). The T2 generation of the *oeTAP38* plants was used for the experiments reported. TAP38 overexpression was confirmed by real-time PCR (see 2.8) and increased levels of TAP38 protein were detected by probing with specific antibodies (see 2.13). Successful complementation of

tap38-1 mutants was confirmed by measurements of chlorophyll fluorescence and LHCII phosphorylation levels under light regimes promoting State Transitions as described in 2.9.2.1 and 2.3.

2.7 Generation of polyclonal TAP38 antibodies

The coding sequence of TAP38 without its predicted cTP was cloned into the pET151-Topo vector (Invitrogen) using the primers TOPO_TAP38_s (5'-C ACC GCG ATT GCG ATC GAC GCT C-3') and TAP38_as (5'-T TAA GAT AGA TGT GAA GAC ATC-3'), providing TAP38 with an N-terminal His-Tag. This construct was used to transform the *E.coli* strain BL21 which is suitable for the overexpression of recombinant proteins. Overexpression of TAP38 was induced with 1 mM IPTG and bacterial cells were harvested after 4 h at 37°C. His-tagged TAP38 protein was purified according to a Ni-NTA batch purification protocol under denaturing conditions (Qiagen). The purified TAP38 protein was injected into rabbits to generate polyclonal antibodies. The injections and maintenance of the animals were kindly taken over by Prof. Dr. Roberto Barbato (Alessandria, Italy) and Dr. Paolo Pesaresi (Milan, Italy).

Additionally, an epitope antibody was generated against a specific peptide sequence (VQGFRDEMEDDIVI) located at the N-terminus of TAP38. Peptide synthesis, the required injections and maintenance of the rabbits as well as monospecific purification of the antibody were performed by Biogenes (Berlin).

2.8 Transcript profiling of TAP38 in different genetic backgrounds

For the determination of *TAP38* transcript levels, total leaf RNA was extracted with TRIzol reagent (Invitrogen, Karlsruhe, Germany) from snap frozen tissue of WT, *tap38-1*, *tap38-2* and *oeTAP38* plants. RNA isolation and first-strand cDNA synthesis from 1 µg of total RNA using the iScript cDNA Synthesis Kit (Bio-Rad) were performed according to manufacturer's instructions. For reverse-transcriptase (RT)-PCR, cDNA was diluted 10-fold,

and 3 μl of the dilution was used in a 20 μl reaction. Thermal cycling consisted of an initial step at 95 °C for 3 min, followed by 30 cycles of 10 s at 95 °C, 30 s at 55 °C and 10 s at 72 °C. For real-time PCR analysis 3 μl of the diluted cDNA was mixed with iQ SYBR Green Supermix (Bio-Rad). Thermal cycling consisted of an initial step at 95 °C for 3 min, followed by 40 cycles of 10 s at 95 °C, 30 s at 55 °C and 10 s at 72 °C, after which a melting curve was performed. Real-time PCR was monitored using the iQ5™ Multi Color Real-Time PCR Detection System (Bio-Rad). All reactions were performed in triplicate with at least two biological replicates. The following primers were used to discriminate between the three potential At4g27800 splice forms: At4g27800.1/TAP38-At4g27800.2-specific primer (No. 1 in Figure 3.3) (5'-ACA TGG GAA TGT GCA GCT TG-3'); At4g27800.1/TAP38-At4g27800.2-At4g27800.3 (No. 2 in Figure 3.3) (5'-GTG AAG ACA TCC ATA TGC CA-3'); At4g27800.2-specific primer (No. 3 in Figure 3.3) (5'-AAT ACC CTC CTC AGC CTT TC-3'); At4g27800.3-specific primer (No. 4 in Figure 3.3) (5'-ACA TGG GAA TGT GCA GGC AA-3'). To compare the *TAP38* expression levels between the different genotypes the housekeeping gene Ubiquitin was chosen for normalisation: Ubiquitin forward primer (5'-GGA AAA AGG TCT GAC CGA CA-3'); Ubiquitin reverse primer (5'-CTG TTC ACG GAA CCC AAT TC-3').

2.9 Chlorophyll fluorescence and spectroscopic measurements

Five plants of each genotype were analysed and mean values and standard deviations were calculated.

2.9.1 Standard photosynthetic parameters

In vivo chlorophyll a fluorescence of single leaves was measured using the Dual-PAM 100 (Walz) according to Pesaresi et al. (2009). The fluorescence of dark adapted leaves was measured (F_0), followed by the application of pulses (0.5 s) of red light ($5000 \mu\text{mol m}^{-2} \text{s}^{-1}$) to determine the maximum fluorescence in the dark (F_M) and therewith the ratio F_V/F_M , a measure for the functionality of PSII. F_V is the variable fluorescence.

$$(F_M - F_0)/F_M = F_V/F_M. \quad [2]$$

The light dependence of the photosynthetic parameters 1-qP and the effective quantum yield of PSII (Φ_{II}) were determined by applying increasing red light intensities (0-2000 $\mu\text{mol m}^{-2} \text{s}^{-1}$) in 15 min intervals before the steady state fluorescence (F_S) was measured and a red light pulse (5000 $\mu\text{mol m}^{-2} \text{s}^{-1}$) was given to determine F_M' . The values were calculated according to the following equations (Maxwell and Johnson, 2000):

$$\Phi_{II} = (F_M' - F_S)/F_M' \quad [3]$$

$$\text{qP (photochemical quenching)} = (F_M' - F_S)/(F_M' - F_0). \quad [4]$$

2.9.2 State Transition measurements

State Transitions were measured using both pulse amplitude modulation fluorometry (Jensen et al., 2000) and 77K fluorescence emission analysis (Bellafiore et al., 2005; Tikkanen et al., 2006).

2.9.2.1 State Transition measurements via PAM fluorometry

Quenching of chlorophyll fluorescence due to State Transitions (qT) was determined by illuminating dark-adapted leaves for 15 min with red light (35 $\mu\text{mol m}^{-2} \text{s}^{-1}$) and subsequently measuring the maximum fluorescence in state 2 (F_{M2}). Next, state 1 was induced by adding far-red light (maximum light intensity corresponding to level 20 in the Dual-PAM setting) for 15 min and recording F_{M1} . qT was calculated according to the following equation (Jensen et al., 2000):

$$\text{qT} = (F_{M1} - F_{M2})/F_{M2}. \quad [5]$$

2.9.2.2 77K fluorescence emission spectroscopy

For 77K fluorescence emission spectroscopy, the fluorescence spectra of thylakoids were recorded after irradiation of plants with light that favoured excitation of PSII (80 $\mu\text{mol m}^{-2} \text{s}^{-1}$, 8 h) or PSI (LED light of 740 nm wavelength, 4.6 $\mu\text{mol m}^{-2} \text{s}^{-1}$, 2 h). After illumination, the leaves were snap frozen in liquid N_2 and grinded in buffer containing 50 mM Hepes / KOH pH 7.5, 100 mM sorbitol, 10 mM MgCl_2 , and 10 mM NaF. After filtration, the samples were diluted to a final chlorophyll concentration of 10 $\mu\text{g/ml}$ as described by Tikkanen et al. (2006). 77 K fluorescence emission spectra

were immediately measured using a Spex Fluorolog mod.1 fluorometer (Spex Industries, Texas, USA). Fluorescence was excited at 475 nm and the emission between 600 and 800 nm was recorded. Spectra were normalised relative to the peak height at 685 nm (PSII peak). The fluorescence emission ratio F_{730}/F_{685} was calculated as an indicator of energy distribution between PSI and PSII. More than ten independent measurements were made from each of the differently light treated WT, *tap38* mutant and *oeTAP38* plants.

2.10 *In vitro* import of TAP38 into pea chloroplasts

The coding sequences of TAP38 and At4g27800.2 were amplified by PCR using the following primer combinations [TAP38-At4g27800.2_FWD (5'-ATG GCG CTT CTG AGG CCG CAT C-3') / TAP38_REV (5'-TTA AGA TAG ATG TGA AGA CAT C-3') and TAP38-At4g27800.2_FWD (5'-ATG GCG CTT CTG AGG CCG CAT C-3') / At4g27800.2_REV (5'-CTA TTT TAC CAA AGC TAC-3')]. The coding sequences were cloned into the pGEM-Teasy vector (Promega) downstream of its SP6 promoter region, and mRNA was produced *in vitro* using SP6 RNA polymerase (MBI Fermentas). The TAP38 and At4g27800.2 precursor proteins were synthesised in a Reticulocyte Extract System (Flexi®, Promega) in the presence of [³⁵S] methionine within 1 h at 30°C. Aliquots of the translation reaction were centrifuged at 50000 *g* for 1 h at 4°C prior to import experiments. Intact chloroplasts were isolated from 10-day-old pea leaves (*Pisum sativum*, var. Golf) and purified by Percoll-gradient centrifugation as described in Waegemann and Soll (1991). Import assays were performed in 100 µl of import buffer (10 mM methionine, 10 mM cysteine, 20 mM potassium gluconate, 10 mM NaHCO₃, 330 mM sorbitol, 50 mM HEPES / KOH pH 7.6, 5 mM MgCl₂) with chloroplasts equivalent to 20 µg of chlorophyll (Nada and Soll, 2004). The import reaction was carried out at 25°C for 30 min, followed by a repurification step of the chloroplasts using a 40% Percoll cushion. For thermolysin treatment, chloroplasts were washed with 330 mM sorbitol, 50 mM HEPES pH 7.6, 0.5 mM CaCl₂ and subsequently incubated with 20 µg/ml thermolysin

(Calbiochem, Darmstadt, Germany) for 20 min on ice. The reaction was stopped by adding 5 mM EDTA. For the subfractionation of chloroplasts after protein import, aliquots of ten import reactions were combined. Intact chloroplasts of all ten reactions were pooled by resuspension in 0.65 M sucrose, 10 mM sodium phosphate pH 7.9. After two freeze and thaw cycles, chloroplasts were ruptured by 30 strokes in a Dounce homogeniser and diluted 1:1 in 10 mM sodium phosphate pH 7.9. Chloroplast fractions were separated by sucrose step gradient centrifugation (134.000 *g* at 4°C for 3 h) using 0.465 M and 0.996 M sucrose layers. Stromal proteins on top of the 0.465 M sucrose layer were precipitated with 20% trichloroacetic acid (TCA) and washed twice with 80% acetone before being resuspended in SDS-loading buffer. Mixed envelope vesicles collected from the interphase and pelleted thylakoids were resuspended in SDS-loading buffer and used for SDS-PAGE analysis without further treatment. Labelled proteins were separated using SDS-PAGE and detected by phosphor-imaging (Typhoon; Amersham Biosciences).

2.11 Total protein preparation

Leaves of four-week-old plants were snap frozen in liquid nitrogen and subsequently ground in solubilisation buffer (100 mM Tris pH 8, 50 mM EDTA pH 8, 0.25 M NaCl, 1 mM DTT and 0.7% SDS). The homogenate was incubated at 68°C for 10 min and centrifuged at 16000 *g* for 10 min at room temperature (RT) to remove cellular debris. The protein concentration was determined using the BIORAD Protein Assay (Bio-Rad). Prior to electrophoresis, proteins were precipitated with ice-cold acetone and resuspended in SDS-loading buffer (6 M Urea, 50 mM Tris-HCl pH 6.8, 100 mM DTT, 2% SDS, 10% glycerol, 0.1% bromophenol blue).

2.12 Isolation of intact chloroplasts

Leaves of four-week-old plants were blended in homogenisation buffer (330 mM sorbitol, 20 mM Tricine pH 7.6, 5 mM EGTA, 5 mM EDTA, 10 mM NaHCO₃, 0.1% BSA and 330 mg/l ascorbate). The homogenate was filtrated through a double layer of Miracloth (Calbiochem). Chloroplasts were collected by centrifugation at 2000 *g* for 5 min at 4°C. The pellet was carefully resuspended in washing buffer (330 mM sorbitol, 20 mM HEPES / KOH pH 7.6, 5 mM MgCl₂ and 2.5 mM EDTA). Chloroplasts were loaded on top of a two-step Percoll gradient as described by Aronsson and Jarvis (2002). Intact chloroplasts at the interface between the two Percoll phases were lysed by incubation for 30 min on ice in four times the volume of lysis buffer (20 mM HEPES / KOH pH 7.5, 10 mM EDTA). To separate thylakoids from the stroma, ruptured chloroplasts were centrifuged at 42000 *g* for 30 min at 4°C. Stromal proteins were recovered from the supernatant, whereas thylakoids were represented by the pellet.

2.13 Immunoblot analyses

Comparative analyses of TAP38 expression were performed for different genetic backgrounds (WT, *tap38* mutants and *oeTAP38*) and different chloroplast subfractions. For the analysis of different genetic backgrounds, thylakoid proteins were isolated as described in 2.3. Protein amounts equivalent to 10 µg (WT, *tap38-1* and *tap38-2*), 5 µg (WT) or 2.5 µg of chlorophyll (WT and *oeTAP38*) were separated on SDS-PAGE after resuspension in loading buffer (6 M Urea, 50 mM Tris-HCl pH 6.8, 100 mM DTT, 2% SDS, 10% glycerol, 0.1% bromophenol blue). Also chloroplast subfractions of *tap38-1* and WT were subject to TAP38 expression analysis. The following protein amounts were separated on SDS-PAGE after resuspension in loading buffer equally for *tap38-1* and WT plants: 15 µg of total protein (2.11), 15 µg of stromal proteins (2.12), thylakoid and total chloroplast proteins (2.12) each corresponding to 10 µg of chlorophyll. For immunoblot analyses, proteins were transferred to Immobilon-P membranes

(Millipore, Eschborn, Germany) and were incubated with a polyclonal antibody raised against the mature TAP38 protein (2.7) as previously described in 2.3.

2.14 Blue Native (BN) - PAGE

Leaves were harvested from four-week-old plants after being kept overnight in the dark, subsequently exposed to low light ($80 \mu\text{mol m}^{-2} \text{s}^{-1}$) for 8 h, and then to far-red light ($4.5 \mu\text{mol m}^{-2} \text{s}^{-1}$, 740 nm (LED)) for 30, 60 and 120 min. Thylakoids were prepared in the presence of 10 mM NaF as described by Bassi et al. (1985) (see also 2.3). Aliquots corresponding to 100 μg of chlorophyll were washed with TMK buffer (10 mM Tris-HCl pH 6.8, 10 mM MgCl_2 and 20 mM KCl) and subsequently solubilised in solubilisation buffer (750 mM 6-aminocaproic acid; 5 mM EDTA, pH 7; 50 mM NaCl; 1.5% digitonin) for 1 h at 4°C. After centrifugation for 1 h at 21000 g the solubilised material was supplemented with 5% w/v Coomassie-blue in 750 mM aminocaproic acid and fractionated by non-denaturing BN-PAGE (4-12% polyacrylamide gels, containing 500 mM 6-aminocaproic acid, 50 mM Bis-Tris pH 7.0 and 10% glycerol) at 4°C as described by Heinemeyer et al. (2004). BN-PAGE was run overnight with an increasing voltage of up to 750 V and 12 mA using cathode buffer (50 mM Tricine, 15 mM Bis-Tris pH 7.0 and 0,02% Coomassie G) and anode buffer (50 mM Bis-Tris pH 7.0) as described by Schagger and von Jagow (1987).

2.15 2D polyacrylamide gel electrophoresis (2D-PAGE)

Samples were fractionated in the first dimension by BN-PAGE as described in 2.14 and gel slices corresponding to the first dimension were incubated in denaturing buffer (125 mM Tris-HCl pH 6.8, 4% SDS and 1% β -mercaptoethanol) for 30 min at room temperature and 5 min at 70°C before running the second dimension. Fractionation in the second dimension was performed in a denaturing SDS-PA gradient gel (10-16% polyacrylamide) as

previously described in 2.3. The 2D gels were stained overnight with colloidal Coomassie and subsequently destained in water. Densitometric analyses of the stained gels were performed using the Lumi Analyst 3.0 (Boehringer, Mannheim, Germany).

2.16 Sucrose gradient centrifugation

Leaves from four-week-old dark adapted *tap38-1* mutant and WT plants were harvested and thylakoids were prepared from non-frozen tissue as described in 2.3. Thylakoids were washed twice with 5 mM EDTA pH 7.8 and diluted to a final chlorophyll concentration of 2 mg/ml. An equal volume of 2% dodecyl- β -D-maltoside (Sigma) (β -DM) was added to the thylakoids and solubilisation was carried out on ice for 10 min. The non-solubilised fraction was pelleted by centrifugation at 16000 *g* for 5 min at 4°C and aliquots of the supernatant were applied on sucrose gradients. The sucrose gradients were prepared by freezing and subsequent thawing at 4°C of 11 ml of 0.4 M sucrose, 20 mM Tricine-NaOH pH 7.5, 0.06% β -DM. The gradients were centrifuged at 39000 rpm (SW40 swing-out rotor) for 21 h at 4°C. In total, 16 fractions were obtained from the gradients with PSI migrating as a distinct band on the bottom of the gradient. WT and *tap38-1* fractions were normalised to the chlorophyll concentration of fraction 16 (PSI) and all fractions were separated on a 16% to 23% SDS-PA gradient gel as described by Schagger and von Jagow (1987).

Primer Name	Sequence (5'-3')
At1G07010_RFPs	CGCCATGGCTTCCCTTTACCTCAATTC
At1G07010_RFPas	CGCCATGGCAATGTAATCTGCAACCTGAAGTTC
At1G07160_RFPs	ATCCATGGCATCGTCTTCAGTTGCCGTTT
At1G07160_RFPas	ATCCATGGCTGCTGCTGCAATACCAACCGGATC
At1G13460_RFPs	ATCCATGGCCTGGAAACAGATTCTGAGTAAG
At1G13460_RFPas	CGCCATGGCATCGAAAACAACACAGCACAAAG
At1G67820_RFPs	ATCCATGGCTAGTACACTTAGCATTG
At1G67820_RFPas	CGCCATGGCACCGAAGCTTACGGTGC
At2G25620_RFPs	ATCCATGGAAGAAACTAGAGGAATTTT
At2G25620_RFPas	TACCATGGCACCTCCGCTTGACCTGGAGCCAATAT
At2G30020_RFPs	ATCCATGGCATCTTGCTCCGTCGCCGTAT
At2G30020_RFPas	ATCCATGGCTGCTGCAGCAACACCAATCGGTATATC
At2G30170_RFPs	ATCCATGGCGATTCCAGTGACG
At2G30170_RFPas	ATCCATGGCTGCTGCTTCTTTAGAGAACAAGGAAGG
At2G35350_RFPs	ATCCATGGGAAGTGGATTCTCCTC
At2G35350_RFPas	CGCCATGGCTCCTCTAAACCCGGTGTGAAGC
At2G40180_RFPs	ATCCATGGCACAACCTCTCAAAGAATC
At2G40180_RFPas	CGCCATGGCAGCCGCCGTTAAGTCAAGCATC
At2G40860_RFPs	ATCCATGGTGATGGAAATTGTGAAAC
At2G40860_RFPas	CGCCATGGCTCCAAACATGTAATTTGGAGGCTTC
At3G02750_RFPs	CGCCATGGGGTCTCTGTTTATCTGCAGAG
At3G02750_RFPas	CGCCATGGCACCCCTCCCAAACAACCATCGCATC
At3G09880_RFPs	ATCCATGGCCTTTAAGAAAATCATGAAAGGTG
At3G09880_RFPas	CGCCATGGCGAAATCGAAAAGGAAACAGC
At3G10940_RFPs	ATCCATGGCCAGTGTGATTGGAAGCAAGAGC
At3G10940_RFPas	CGCCATGGCACCTAGATCATGATGATATTC
At3G19420_RFPs	ATCCATGGCCTCGTCTG AGTCACCGAA
At3G19420_RFPas	CGCCATGGCAGTGTGATTCGTTTGAGGAG
At3G21650_RFPs	ATCCATGGCCATCAAACAGATATTTGGGAAATTAC
At3G21650_RFPas	CGCCATGGCAGGAACATCTCTAAAGCTAGG
At3G26020_RFPs	ATCCATGGGATGGAAACAGATTCTAAGTAAGC
At3G26020_RFPas	TACCATGGCACCTCCAACATCTTTAAAACTCGGCAATG
At3G54930_RFPs	ATCCATGGCCTTCAACAAAATCATAAAACTGG
At3G54930_RFPas	CGCCATGGCCATGTGAGCTTTCTTCATGAAG
At3G63320_RFPs	ATCCATGGTGGAGCTCCGGCAG
At3G63320_RFPas	CGCCATGGCCGGGAAAGGGAATGCCAAG
At4G03415_RFPs	ATCCATGGGGGGTTGTGTGTCGA
At4G03415_RFPas	ATCCATGGCTGCTGCTACACCACAAAATGTCACATCT
At4G15415_RFPs	ATCCATGGCCATCAAAC AGATATTTGG
At4G15415_RFPas	CGCCATGGCCTTCTTGATAAACAGATTAG

At4G27800_RFPs	ATCCATGGCGCTTCTGAGGCCGCATC
At4G27800_RFPas	TACCATGGCAGAGGACGACCCAGCGTGG
At4G33500_RFPs	CGCCATGGCCGATCATTGATTCTTTC
At4G33500_RFPas	CGCCATGGCTGTAGAGACAATTTTCACGAATG
At4G38520_RFPs	ATCCATGGCCCTATCTGGGTTGATGAATTTTC
At4G38520_RFPas	CGCCATGGCTCCATGATCATTGATGAAGCGAG
At5G25510_RFPs	ATCCATGGCCTTTAAGCAGTTTCTGAGTAAAC
At5G25510_RFPas	CGCCATGGCGTCAGAGAAATCAAATGTCAC
At5G36250_RFPs	ATCCATGGGGTCCTGCTTATCATC
At5G36250_RFPas	CGCCATGGCTCCCTCCCAAACAATCATAGCGTC
At5G66080_RFPs	ATCCATGGCCTTATCCCTTTTCTTCAACTTTTTG
At5G66080_RFPas	CGCCATGGCTCCATCGTTGACAAAACGGGAGG
At5G66720_RFPs	ATCCATGGCCTCAGCGACTGCTCTCTCG
At5G66720_RFPas	CGCCATGGCCCTCTCTTCCCAAGTCTC

Table 2.1 List of primers used to amplify the N-terminal coding sequences of the 27 candidate genes to generate the respective dsRED fusion constructs. Forward and reverse primers of the respective genes contain adaptors with *NcoI* cutting sites for cloning into *NcoI* linearised pGJ1425.

AGI accession number	Project Name	T-DNA Insertion Line
At1g67820	<i>pcp8-1</i>	GABI_532F04
At4g33500	<i>pcp12-1</i>	SALK_027267
At3g10940	<i>pcp24-1</i>	CSHL_GT10871
At1g07160	<i>pcp30-1</i>	SALK_071069
At2g30020	<i>pcp34-1</i>	SALK_104445
At2g30170	<i>pcp35-1</i>	SALK_127920
At4g03415	<i>pcp36-1</i>	GABI_439E10
At1g07010	<i>pcp37-1</i>	GABI_313C04

Table 2.2 AGI accession numbers of genes coding for the experimentally identified cpPPs and the corresponding T-DNA insertion lines. Under 'Project Name' the alternative nomenclature used during the screen is indicated. *pcp* – *putative chloroplast protein phosphatase*;

Primer Name	Sequence (5'-3')
Ds3-2	CGATTACCGTATTTATCCCGTTC
LBb1	GCGTGGACCGCTTGCTGCAACT
LBgk1	CCCATTTGGACGTGAATGTAGACAC
pcp8-1_fwd	CTCTCTTGTGACAACAATATGAC
pcp8-1_rev	GCTTCAACTTTCTCCTCCTTCC
pcp12-1_fwd	CCAATTATCATCTTCTTCGTCTAC
pcp12-1_rev	GTTTCTACCTCAACACATCTCG
pcp24-1_fwd	CAGAAATCTGGCGGGAGT
pcp24-1_rev	GGAAACCCCTGGAGCTCTT
pcp30-1_fwd	CGGGTCGGGTTTCTAAAGAT
pcp30-1_rev	GAAACGATCCTCCATAGCTTCTC
pcp34-1_fwd	GGAGTCTATGATGGTCATGG
pcp34-1_rev	TGAACTGGCGTAAAGGGATCAAC
pcp35-1_fwd	CACGCAATCCCTCATCCAGA
pcp35-1_rev	GAGCTTAGTTGGTAAGGACAGTC
pcp36-1_fwd	CTGGAGCAATGGAGAGAAGC
pcp36-1_rev	CCATCGCAAATACTCGACCT
pcp37-1_fwd	GATAGGAGGAGTTCTCAAACC
pcp37-1_rev	GGTCTAGAGTCAAGAACACC

Table 2.3 Primers used for the identification of the homozygous T-DNA insertion lines listed in Table 2.1. The primer combination for the T-DNA insertion is always the reverse primer (_rev) of the respective gene together with the line specific T-DNA insertion primer. CSHL-lines (Ds3-2); SALK-lines (LBb1); GABI-KAT-lines (LBgk1); The gene specific primers are named (_fwd) and (_rev).

3. Results

3.1 Prediction and experimental validation of putative cpPPs

Protein phosphorylation, one of the most frequent posttranslational modifications of proteins, is a major mode of regulation of metabolism, gene expression, and cell architecture. Although phosphorylation of proteins is involved in the regulation of numerous processes in plastids, including photosynthesis, metabolic pathways, the expression of plastid-encoded genes and redox signalling (Baena-Gonzalez et al., 2001; Forsberg and Allen, 2001; Pursiheimo et al., 2001; Bellafiore et al., 2005; Bonardi et al., 2005), the complement of chloroplast protein phosphatases (cpPPs) is largely unknown, except for AtRP1, a bifunctional protein kinase / protein phosphatase involved in the regulation of Arabidopsis pyruvate, orthophosphate dikinase (PPDK) (Chastain et al., 2008).

A first approach to identify novel cpPPs was to screen the TAIR database (<http://www.arabidopsis.org/>; genome release 7) comprising the complete annotated genome of *Arabidopsis thaliana* (Poole, 2007) for genes encoding proteins with a putative protein phosphatase signature. 217 candidate genes were selected and further analysed with respect to the presence of a potential chloroplast transit peptide (cTP). To this purpose a total of nine different prediction algorithms for subcellular localisation (listed in 2.1) were applied on the whole complement of 217 putative protein phosphatases (Table 3.1). The threshold value for a positive cTP-prediction was set to a minimum of four out of nine (4/9) (number of algorithms predicting a cTP/ total number of algorithms applied). This threshold value relies on experiences with previous *in vivo* localisation assays of putative chloroplast kinases (Schliebner et al., 2008) and studies addressing the reliability of prediction algorithms when applied in a combined manner (Richly and Leister, 2004). A further cut-off criterion was that only putative serine (Ser) / threonine (Thr) PPs were considered in the screen, because

most phosphorylated proteins of the thylakoid membrane detected so far are modified at a serine or threonine residue (Forsberg and Allen, 2001). In total, 26 of the initial 217 candidate genes, which met all of these requirements, were selected for further investigations (Table 3.2).

Class	Entire Genome	Predicted cpPPs								
		1/9	2/9	3/9	4/9	5/9	6/9	7/9	8/9	9/9
Ser/Thr	94	38	16	8	5	3	1	1	1	1
Dual-specific	23	14	8	6	6	6	5	3	1	0
PP 2C-type	89	64	38	27	19	15	12	12	9	5
Tyr	6	3	3	3	3	2	2	2	1	0
other	5	3	3	2	2	2	1	1	1	1
total	217	122	68	46	35	28	21	19	13	7

Table 3.1 Protein phosphatase sequences were retrieved from TAIR (<http://www.arabidopsis.org/>; genome release 7). Predictions of chloroplast targeting were performed with the following algorithms: Predotar, TargetP, Protein Prowler, AAIndexLOC, PredSL, SLP-Local, WoLF PSORT, MultiLOC and PCLR (see 2.1). 'n out of 9' indicates the number of predicted cpPPs that have a cTP predicted by at least n of the nine different algorithms. n ranges from 1 to 9. Results are shown separately for the different phosphatase classes. Serine (Ser); Threonine (Thr); Tyrosine (Tyr);

In a second approach, data of different mass spectrometric analyses of the chloroplast proteome or its subfractions were searched for proteins with a protein phosphatase motif (Peltier et al., 2002; Kleffmann et al., 2004; Zybailov et al., 2008; in-house database). This resulted in a list of five putative cpPPs (At1g07010, At2g30170, At3g10940, At4g27800 and At4g33500) overlapping almost completely with the 26 candidate genes from the first approach, except for At4g27800. Interestingly, this additional putative cpPP, derived from the MS database approach, showed a prediction score of only 3/9. The combination of both screens led to a final set of 27 putative cpPPs that were subject to further investigation.

AGI accession number	Prediction (n/9)	actual location
At1g07010	9/9	cp
At1g07160	9/9	cp
At2g30020	9/9	cp
At3g02750	9/9	cm or cyt
At4g33500	9/9	cp
At5g66720	9/9	mt or cyt
At1g67820	8/9	cp
At2g30170	8/9	cp
At3g10940	8/9	cp
At2g35350	7/9	probably cyt
At4g03415	7/9	cp
At5g36250	7/9	mt
At2g25620	5/9	probably mt
At2g40180	5/9	n
At3g19420	5/9	cyt
At3g21650	5/9	cyt
At3g63320	5/9	cyt
At5g25510	5/9	cm or cyt
At1g13460	4/9	cm or cyt
At2g40860	4/9	probably mt
At3g09880	4/9	mt or cyt
At3g26020	4/9	cyt
At3g54930	4/9	cm or cyt
At4g15415	4/9	cyt
At4g38520	4/9	mt
At5g66080	4/9	probably cyt

Table 3.2 List of 26 candidate genes selected for the *in vivo* localisation assay with RFP-fusion proteins in *Arabidopsis* protoplasts. All 26 genes met the following criteria: a putative serine threonine phosphatase motif and a prediction ratio of at least 'four out of nine' (4/9) for a positive cTP-prediction. Under 'actual location' the results of the *in vivo* RFP-localisation study are indicated. cell membrane (cm); chloroplast (cp); cytosol (cyt); mitochondrion (mt); nucleus (n);

The N-terminal coding sequences of the 27 candidate genes comprising their predicted cTPs were cloned in frame with, and immediately upstream of, the red fluorescence protein (RFP) coding sequence of the pGJ1425 vector. Those RFP fusion constructs were used for the transfection of *Arabidopsis* protoplasts followed by fluorescence microscopic analysis (see 2.2). Nine of the 27 RFP fusions could be localised to the chloroplast as shown in Figure 3.1 (see also Table 3.2), whereas the other 18 potential cTPs led to other subcellular targeting of the RFP fusion than the chloroplast (see Table 3.2 and Appendix Figure 1).

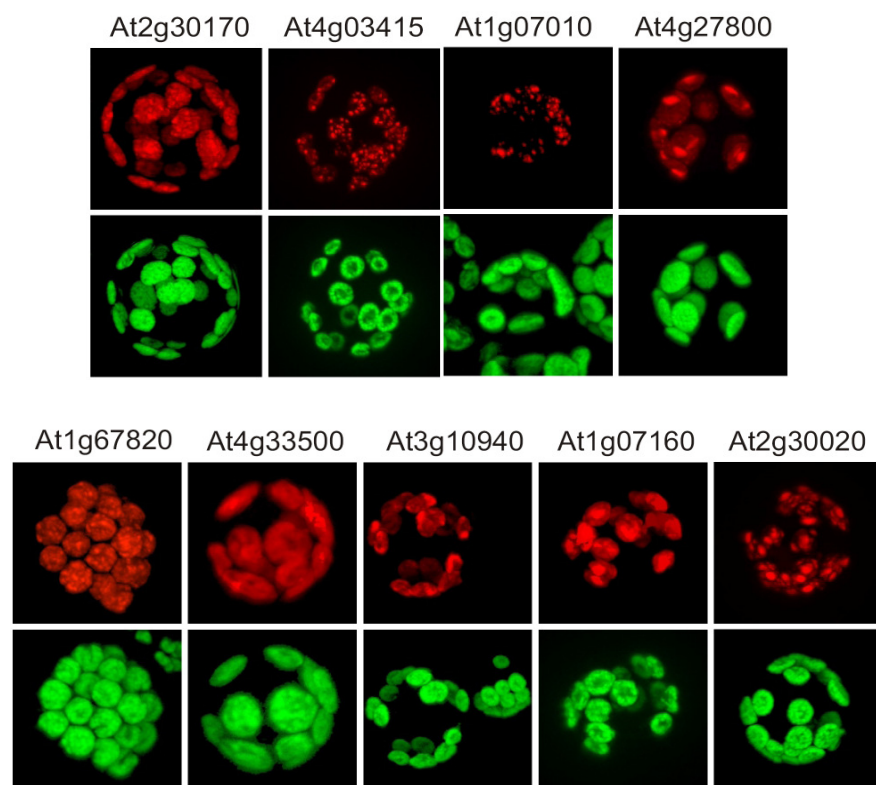


Figure 3.1 Fluorescence micrographs of *Arabidopsis thaliana* protoplasts transfected with N-terminal fusions of the predicted transit peptides of the respective cpPPs to RFP. The pictures are presented in false colour with RFP fluorescence shown in red and chlorophyll autofluorescence in green.

The reliability of cTP prediction for protein phosphatases was quite high, especially when prediction algorithms were applied in a combined manner. This is evident considering the large fraction of putative cpPPs with high prediction scores ($\geq 7/9$) that are actually located in the chloroplast (8 of the 12 tentative cpPPs, Table 3.2).

To investigate whether one of the nine experimentally identified cpPPs plays a role in the reversible phosphorylation of known thylakoid phosphoproteins, one or more T-DNA insertion lines were analysed for each of the respective genes. The T-DNA insertion lines were obtained from publicly available collections and were screened for plants homozygous for the insertion in the respective cpPP gene (Table 2.2 and Figure 3.2).

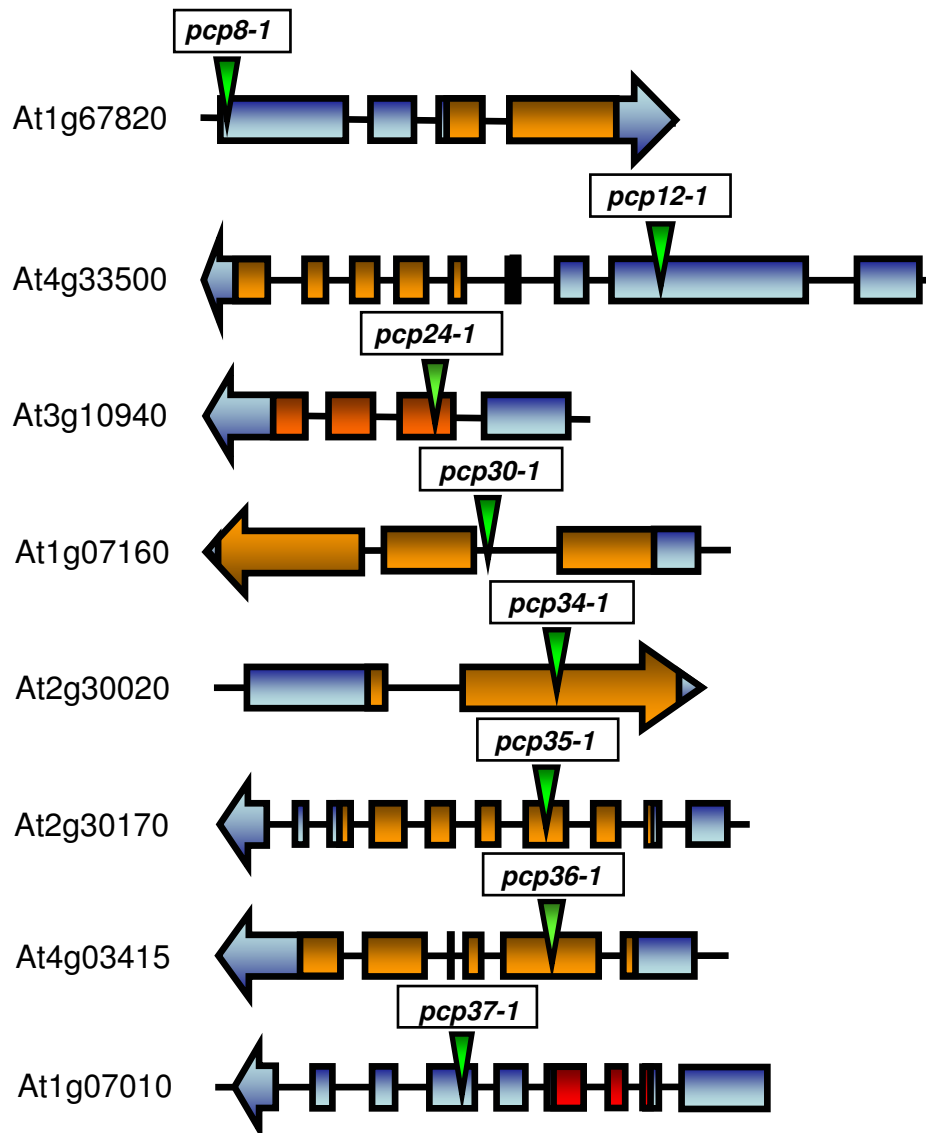


Figure 3.2 Gene structures including T-DNA insertion sites of chloroplast localised protein phosphatases. The coding sequence of the respective gene model is indicated in blue. The colour code of protein phosphatase signatures is as follows: yellow (PP2C signature), orange (dual specific PP signature), red (PP2A signature); Green arrows depict corresponding T-DNA insertion sites of the different genes (see Table 2.2).

Homozygous mutant and WT plants were exposed for predefined time periods to different light conditions [dark (D), low light (LL) and far-red light

(FR), see 2.3], that induce characteristic changes in the phosphorylation state of WT thylakoid proteins (see Figure 3.10a). The T-DNA insertion lines for eight of the nine cpPPs (Figure 3.2) did not show any significant differences in their phosphorylation pattern of PSII core or LHCII proteins in comparison to WT (Figure 3.3).

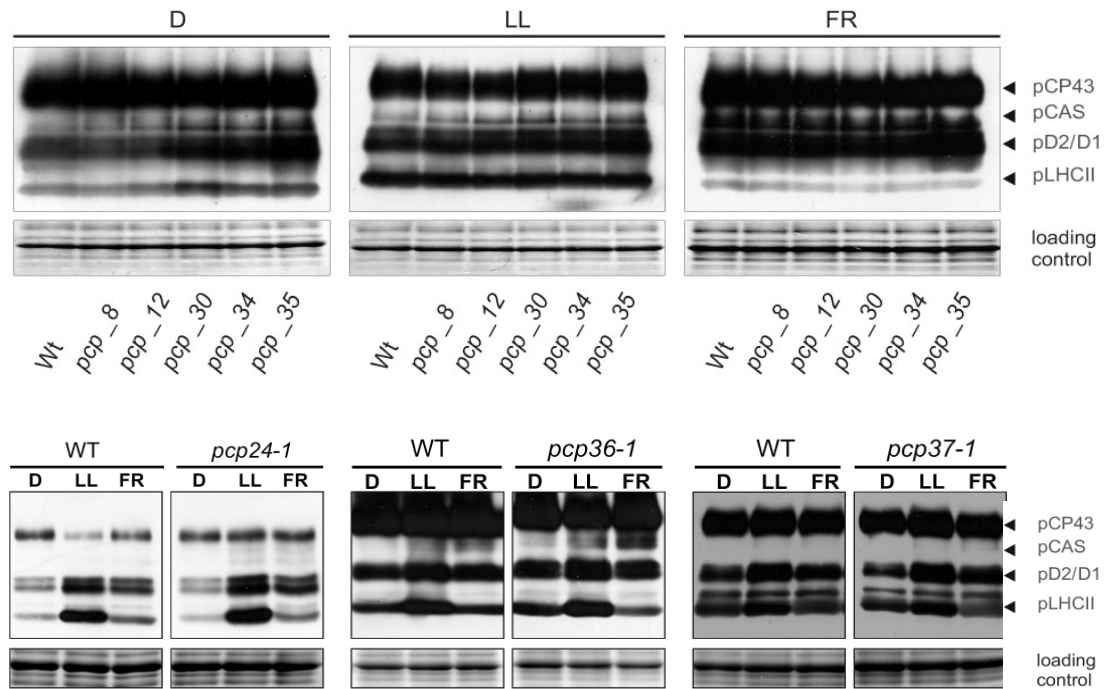


Figure 3.3 Comparison of the level of PSII core and LHCII protein phosphorylation between different T-DNA insertion lines and WT plants. Thylakoid proteins extracted from WT plants and T-DNA insertion lines of the respective cpPPs kept in the dark (D) overnight, subsequently exposed to low light (LL) for 2 h, and then to far-red light (FR) for 2 h were fractionated by SDS-PAGE. Phosphorylation of LHCII and PSII core proteins was detected by immunoblot analysis with a phosphothreonine-specific antibody.

However, the *pcp38-1* and *pcp38-3* mutants with T-DNA insertions in the cpPP At4g27800 displayed a significant difference in the phosphorylation pattern of LHCII (see Figure 3.10 and Appendix Figure 2). Under all applied light conditions a distinct fraction of LHCII remained constantly phosphorylated in the respective mutant plants. In the following, this work concentrates on the in-depth characterisation of the gene locus *At4g27800.1* (later changed to TAP38 - 'Thylakoid associated protein phosphatase of 38 kDa') and the respective T-DNA insertion lines *pcp38-1* (renamed *tap38-2*) and *pcp38-3* (renamed *tap38-1*).

3.2 At4g27800 gene model and expression of splice variants

For *A. thaliana*, three *At4g27800* mRNAs (splice forms) are predicted (Figure 3.4a). To verify their existence and to distinguish between the different splice forms, reverse transcriptase (RT)-PCR analyses were performed. Only *At4g27800.1*, and much less *At4g27800.2*, were detectable in leaves, whereas for the *At4g27800.3* splice variant no signal could be obtained (Figure 3.4a-b). *At4g27800.1* (*TAP38*) is therefore the major isoform in leaves.

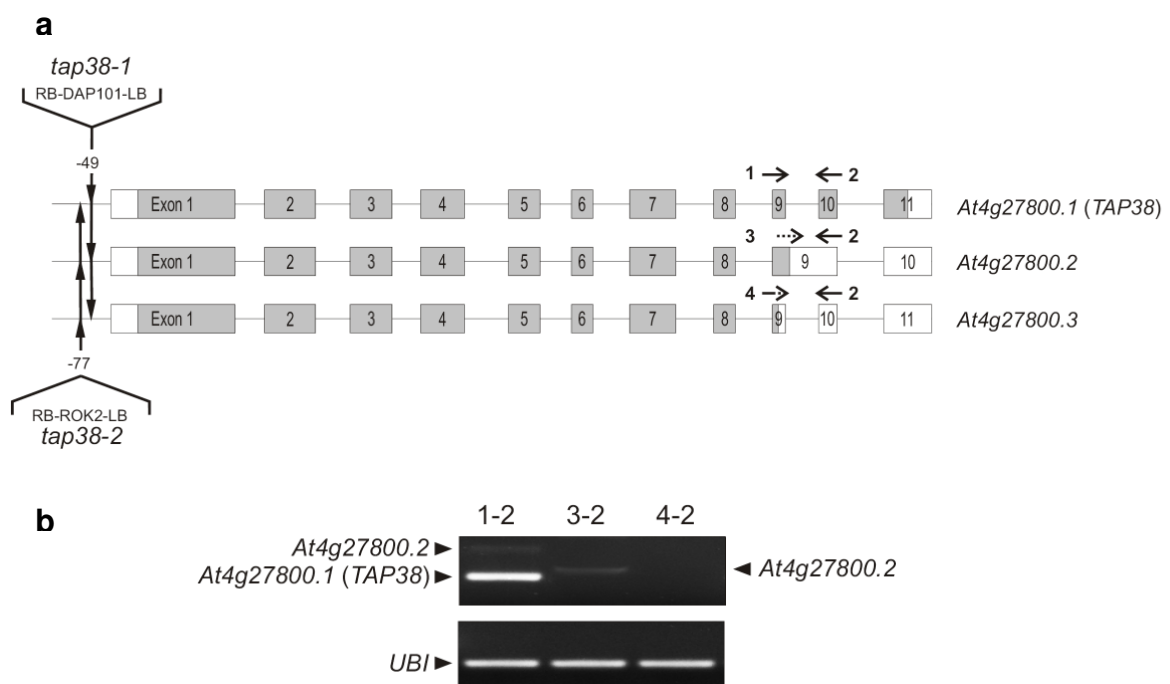


Figure 3.4 Insertion alleles of *At4g27800* and splice variant expression. **a**, T-DNA insertions in the *At4g27800* locus. The different coding sequences of the three splice variants are depicted as grey boxes. The respective 5' and 3' UTRs are shown in white. Introns are indicated as thin lines. Splice variants *At4g27800.1* (*TAP38*) and *At4g27800.3* can be distinguished due to an insertion of four additional nucleotides in exon 9 of *At4g27800.3* leading to a stop codon. Arrows (not drawn to scale) indicate the positions of primer pairs used in PCR analysis. Sequences of primers indicated as 1, 2, 3, and 4 are reported in Methods (2.8). **b**, Semi-quantitative reverse transcriptase (RT)-PCR analysis to verify the presence of the three splice variants in *Arabidopsis* WT leaves. Primer combinations employed in RT-PCR reactions are numbered as in **a**. *Ubiquitin* (*UBI*) was amplified as a control for equal loading. Aliquots (10 μ l) of representative semi-quantitative RT-PCR reactions (30 cycles, see Methods 2.8) were electrophoresed on a 2 % (w/v) agarose gel to differentiate between *At4g27800.1* (*TAP38*) and *At4g27800.2*. Note that for the *At4g27800.3* splice variant no signal could be obtained.

3.3 Subcellular localisation of TAP38

In *Arabidopsis* protoplasts transfected with *At4g27800.1* fused to the entire coding sequence for the Red Fluorescent Protein (RFP), the fusion protein localised to chloroplasts (Figure 3.5a). Thus, the result of the initial RFP fusion assay using only the predicted N-terminal cTP was confirmed. Chloroplast import assays with radioactively labelled *At4g27800.1* confirmed the uptake into the chloroplast with concomitant removal of its cTP. Mature *At4g27800.1* has a molecular weight of ~38 kDa (Figure 3.5b). The sub-fractionation of pea chloroplasts after protein import revealed a predominant localisation of *At4g27800.1* in the membrane fraction (Figure 3.5b). The very weak signal obtained for the stromal fraction is likely to be related to contaminations due to washings of the membrane fraction. This could be confirmed by comparative immunoblot analysis using equal amounts of protein isolations from WT and *tap38-1* mutant plants and probing them with a specific antibody raised against the mature *At4g27800.1* (Figure 3.5c). *At4g27800.1* could be detected in total leaf, chloroplast and thylakoid preparations of WT plants but not in stromal fractions. Taken together, *At4g27800.1* was unambiguously identified as a thylakoid associated protein. Therefore, *At4g27800.1* was renamed TAP38 ('Thylakoid-Associated Phosphatase of 38 kDa'). It is noteworthy, that the putative translation products *At4g27800.2* and *At4g27800.3* (~32 kDa) were undetectable in those preparations (Figure 3.5c).

3.4 Comparison of TAP38 with related protein sequences from higher plants and moss

By screening protein databases, proteins with high homology to TAP38 could be identified in mosses and higher plants, but not in algae or prokaryotes. As characteristic motifs TAP38 and its homologues share a weakly predicted N-terminal chloroplast transit peptide (cTP), a putative transmembrane domain (TM) at their very C-termini and a highly conserved protein phosphatase 2C signature (PP2C) (Figure 3.6).

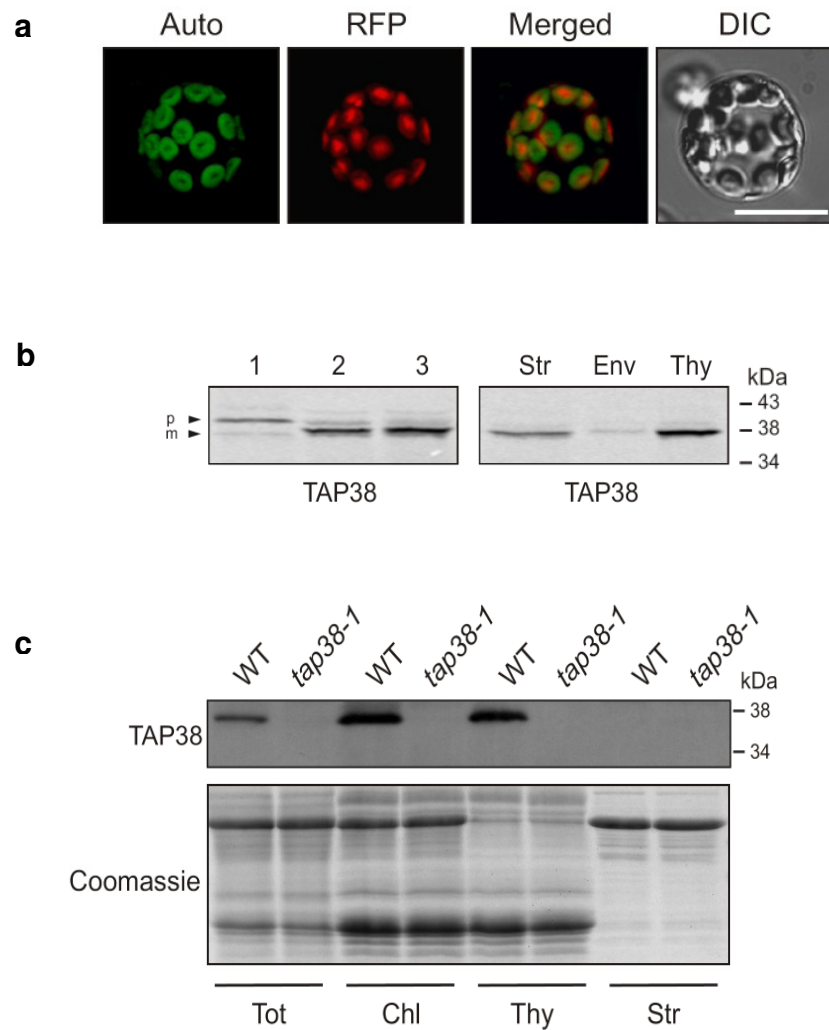


Figure 3.5 Subcellular localisation of TAP38. **a**, Full-length TAP38-RFP was transiently expressed in *Arabidopsis* protoplasts and visualised by fluorescence microscopy. Auto, chlorophyll autofluorescence; RFP, fusion protein; Merged, overlay of the two signals; DIC, differential interference contrast image. Scale bar, 50 μ m. **b**, left panel, 35 S-labelled TAP38 protein, translated *in vitro* (lane 1, 10% translation product), was incubated with isolated chloroplasts (lane 2), which were subsequently treated with thermolysin to remove adhering precursor proteins (lane 3), prior to SDS-PAGE and autoradiography (p, precursor; m, mature protein); right panel, chloroplasts were fractionated after protein import. Str, stroma; Env, envelope; Thy, thylakoids. **c**, Immunoblot analysis of proteins from WT and *tap38-1* leaves. Equal protein amounts were loaded. Tot, total protein; Chl, total chloroplasts; Thy, thylakoid proteins; Str, stromal proteins. Filters were immunolabelled with a TAP38-specific antibody. A replicate gel stained with Coomassie is shown as loading control.

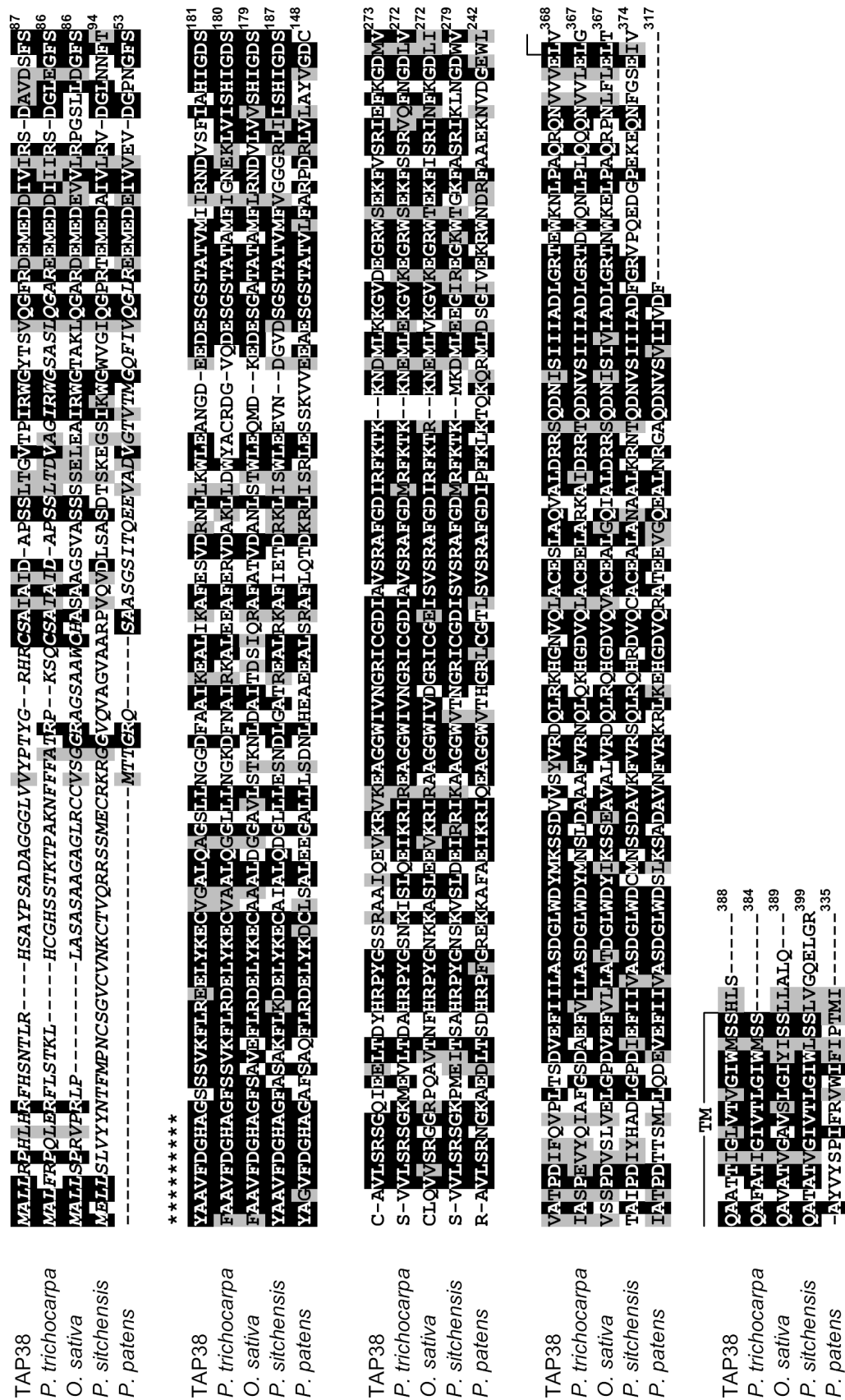


Figure 3.6 Comparison of the TAP38 sequence with those of related proteins from higher plants and moss. In detail the amino acid sequence of the Arabidopsis TAP38 protein (At4g27800) was compared with related sequences from *Populus trichocarpa*

(POPTRDRAFT_250893), *Oryza sativa* (Os01g0552300), *Picea sitchensis* (GenBank: EF676359.1) and *Physcomitrella patens* (PHYPADRAFT_113608). Black boxes highlight strictly conserved amino acids, and gray boxes closely related ones. Amino acids that constitute a protein phosphatase 2C signature are indicated by asterisks. Putative chloroplast transit peptides (cTPs) are indicated in italics, and the potential transmembrane domain (TM) is highlighted.

3.5 Expression of TAP38 in *tap38* mutant and TAP38 overexpressors

As depicted in Figure 3.4a, two *tap38* insertion mutants, *tap38-1* (SAIL_514_C03) and *tap38-2* (SALK_025713), were obtained from T-DNA insertion collections (see 2.4). In *tap38-1* and *tap38-2* plants, the amounts of *TAP38* transcripts were severely reduced to 10% and 13% of WT levels, respectively (Figure 3.7a). Conversely, in transgenic lines carrying the *TAP38* coding sequence under control of the 35S promoter of Cauliflower Mosaic Virus (overexpressor of *TAP38*, *oeTAP38*) (see 2.6), mRNA levels of *TAP38* were much higher than in WT (Figure 3.7a). *TAP38* concentrations reflected the abundance of *TAP38* transcripts: *tap38-1* and *tap38-2* thylakoids had <5% and ~10% of WT levels, respectively, while *oeTAP38* plants displayed >20-fold overexpression (Figure 3.7b).

3.6 State Transitions and 77K measurements

To determine whether *TAP38* is involved in State Transitions, chlorophyll fluorescence was measured in WT, *tap38* and *oeTAP38* leaves (Figure 3.8). Plants were exposed to light conditions that stimulate either state 2 (red light) or state 1 (red and far-red light) (see 2.9.2.1), and the corresponding maximum fluorescence values F_{M2} (state 2) and F_{M1} (state 1) were determined. Because the light intensity chosen to induce State Transitions did not elicit photoinhibition (as monitored by measurements of F_V/F_M - see Figure 3.15b, dark-adapted plants, PAR = 0), changes in F_M can be attributed to State Transitions alone. This allowed us to calculate q_T , the degree of quenching of chlorophyll fluorescence due to State Transitions.

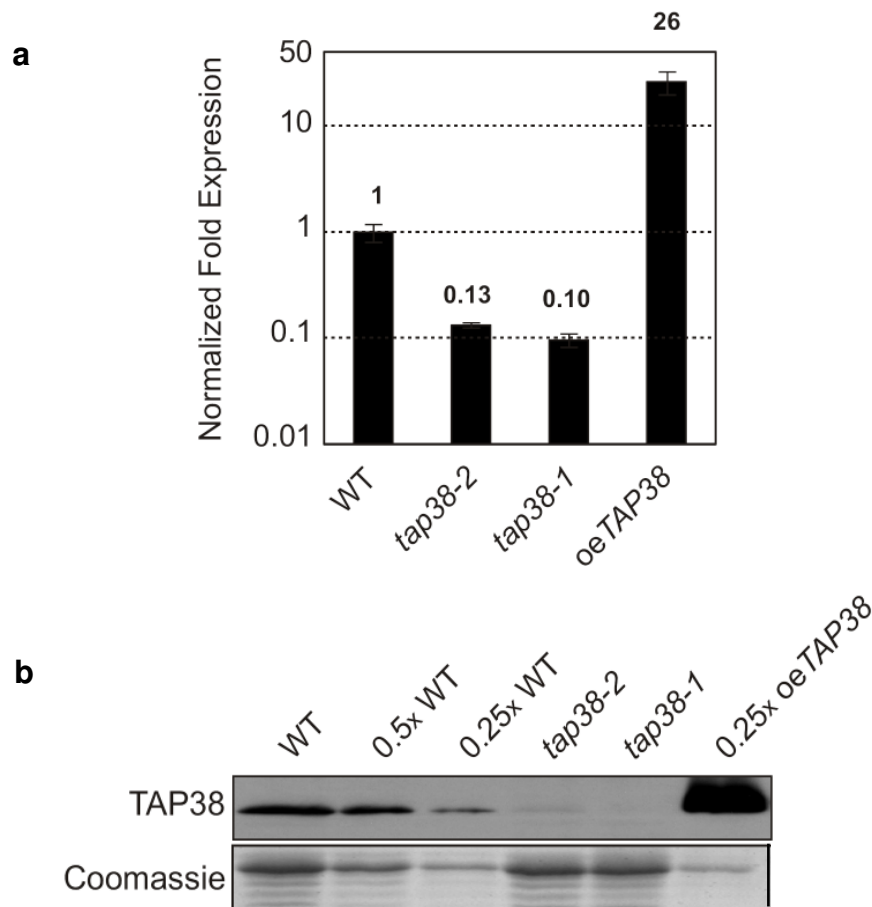


Figure 3.7 TAP38 transcript and protein levels in different genetic backgrounds. **a**, Quantification of *TAP38* mRNAs by real-time PCR in WT, *tap38-1*, *tap38-2* and oe*TAP38* leaves using the primer combination 1-2 (as in Figure 3.4a). **b**, Thylakoid proteins from WT, *tap38* mutants and oe*TAP38* were loaded in each lane. Filters were immunolabelled with a TAP38-specific antibody raised against the mature TAP38 protein (see 2.7). A replicate gel stained with Coomassie is shown as loading control.

In the *tap38* mutants, qT was markedly decreased (*tap38-1*, 0.01 ± 0.004 ; *tap38-2*, 0.02 ± 0.004 ; WT, 0.11 ± 0.001). In *tap38-1* plants complemented with the *TAP38* genomic sequence (including its native promoter), qT values were like WT (0.11 ± 0.005), confirming that State Transitions require TAP38. Interestingly, oe*TAP38* plants exhibited qT values of about 0.01 ± 0.001 , indicating that both absence and excess of TAP38 interfere with the ability to undergo normal State Transitions.

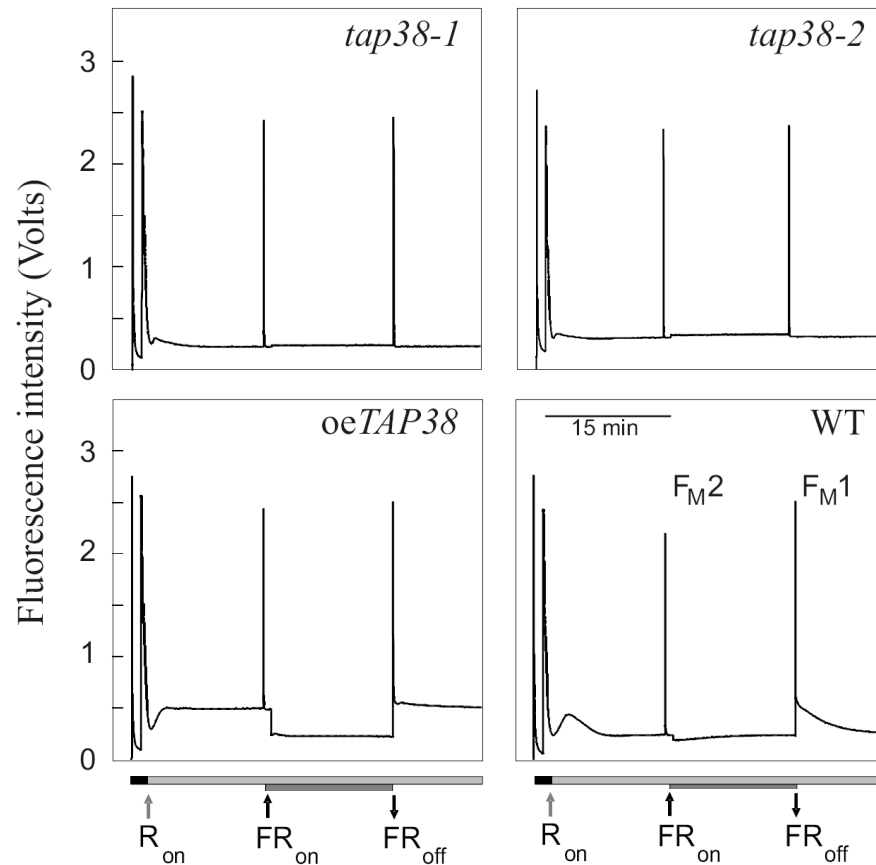


Figure 3.8 TAP38 is required for State Transitions. Red light (R) and red light supplemented with far-red (FR) light were used to induce transitions to state 2 and state 1, respectively. F_{M1} and F_{M2} represent maximal chlorophyll fluorescence levels in states 1 and 2, respectively.

To determine the antenna sizes of PSII and PSI, 77K fluorescence emission spectra were measured under state 1 and state 2 conditions as described (Bellafiore et al., 2005; Tikkanen et al., 2006) (Figure 3.9). The spectra were normalised at 685 nm, the peak of PSII fluorescence. In WT, the transition from state 1 to state 2 was accompanied by a marked increase in relative PSI fluorescence at 730 nm, reflecting the redistribution of excitation energy from PSII to PSI. In contrast, in *tap38* leaves, the PSI fluorescence peak was relatively high even under state 1-promoting conditions, indicating that the mutants were blocked in state 2. Moreover, under state 2-promoting light conditions, the PSI antenna size (expressed as F_{730}/F_{685}) was larger in *tap38* mutants than in WT (*tap38.1*, 1.47; *tap38.2*, 1.45; WT, 1.38; see also Table 3.3). In *oeTAP38* plants the relative fluorescence of PSI hardly increased at all under conditions expected to induce the state 1 \rightarrow state 2

shift (Figure 3.9 and Table 3.3). This behaviour resembles that of *stn7* mutants, which are blocked in state 1 (Bellafiore et al., 2005).

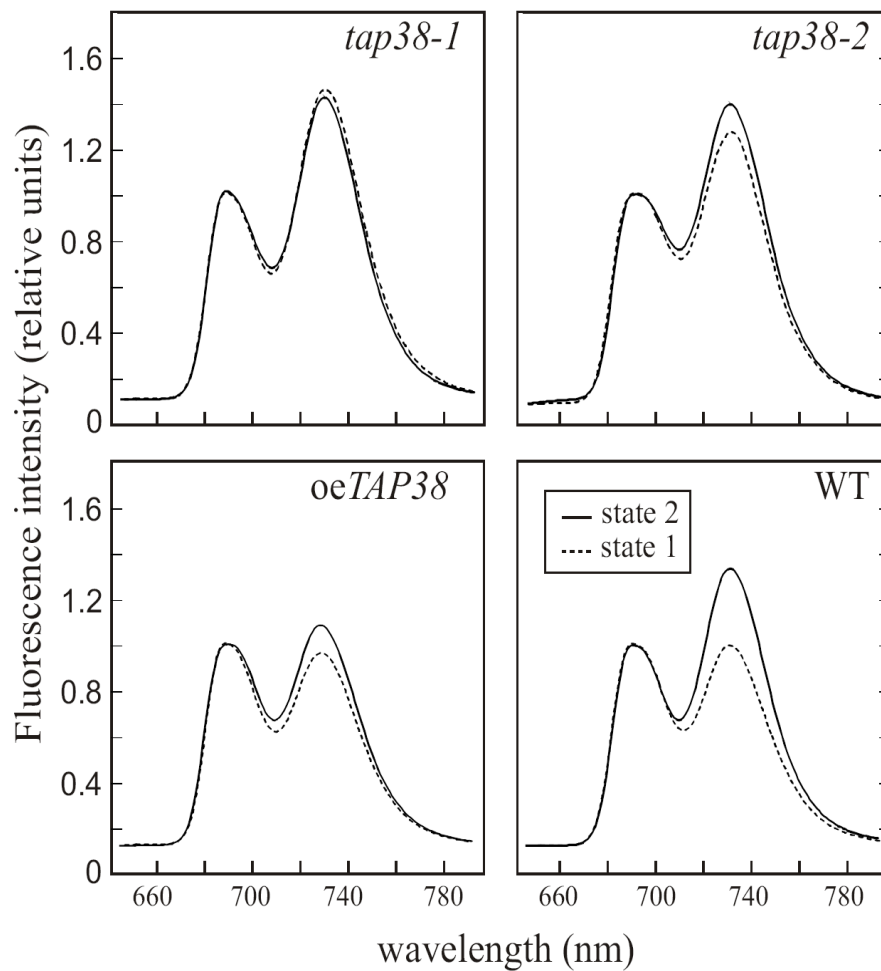


Figure 3.9 Low-temperature (77K) fluorescence emission spectra of thylakoids were recorded after exposure of plants to light inducing either state 1 (dashed lines) or state 2 (solid lines) (see 2.9.2.2). The excitation wavelength was 475 nm and spectra were normalized with reference to the peak height at 685 nm.

	F_{730}/F_{685}	
	state 1	state 2
WT	0.99 ± 0.05	1.38 ± 0.03
<i>tap38-1</i>	1.49 ± 0.04	1.47 ± 0.02
<i>tap38-2</i>	1.32 ± 0.03	1.45 ± 0.04
<i>oeTAP38</i>	0.98 ± 0.02	1.11 ± 0.03

Table 3.3 Energy distribution between PSI and PSII measured as the fluorescence emission ratio at 730 nm and 685 nm (F_{730}/F_{685}) under state 1 and state 2 promoting light conditions.

3.7 Reversible phosphorylation of LHCII

It is generally accepted that State Transitions require reversible phosphorylation of LHCII (Wollman, 2001; Rochaix, 2007; Eberhard et al., 2008). Therefore, the phosphorylation state of LHCII was monitored under light conditions that favour state 1 (dark adaption or far-red light treatment) or state 2 (low light). Plants with abnormal levels of TAP38 and WT plants were dark adapted for 16 h (state 1), then exposed to low light ($80 \mu\text{mol m}^{-2} \text{s}^{-1}$, 8 h) (state 2), and then to far-red light ($4.5 \mu\text{mol m}^{-2} \text{s}^{-1}$, 740 nm) for up to 120 min to induce a return to state 1. Thylakoid proteins were isolated after each treatment, fractionated by SDS-PAGE, and analysed with a phosphothreonine-specific antibody (Figure 3.10, left panels). WT plants showed the expected increase in phosphorylated LHCII (pLHCII) during the transition from state 1 (dark) to state 2 (low light), followed by a progressive decrease in pLHCII upon exposure to far-red light. In *tap38* mutants, levels of pLHCII were aberrantly high at all timepoints, while the *oeTAP38* plants again mimicked the *stn7* phenotype (Bellafiore et al., 2005; Bonardi et al., 2005), displaying constitutively reduced levels of pLHCII.

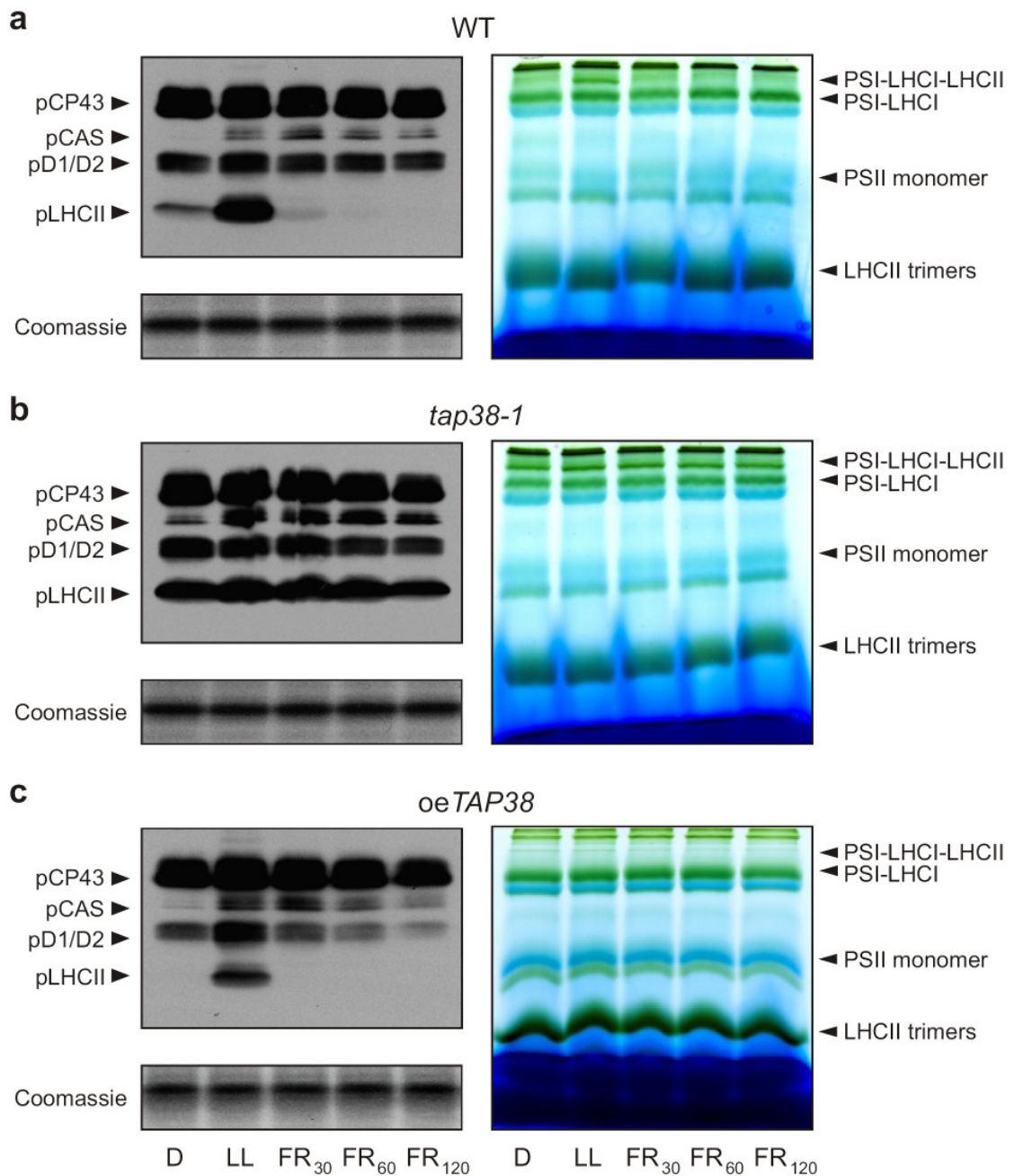


Figure 3.10 Levels of LHCII phosphorylation correlate inversely with TAP38 concentrations. *Left panel*, Thylakoid proteins extracted from WT (**a**), *tap38-1* (**b**) and *oeTAP38* (**c**) plants kept in the dark (D, state 1), subsequently exposed to low light (LL, state 2) and then to far-red light for 30, 60 and 120 min (FR₃₀, FR₆₀, FR₁₂₀; state 1) were fractionated by SDS-PAGE. Phosphorylation of LHCII and PSII core proteins was detected by immunoblot analysis with a phosphothreonine-specific antibody. Replicate gels stained with Coomassie are shown as loading controls. *Right panel*, Thylakoid proteins of WT (**a**), *tap38-1* (**b**) and *oeTAP38* (**c**) plants treated as in the left panel were subjected to BN-PAGE analysis. Accumulation of the state 2 associated PSI-LHCI-LHCII complex correlates with the phosphorylation level of LHCII. Note that *tap38-2* behaves very similarly to *tap38-1* (Appendix Figure 2).

To analyse how the alterations in LHCII phosphorylation in lines lacking or overexpressing TAP38 affect the distribution of the mobile LHCII fraction between the two photosystems, thylakoid protein complexes were subjected to non-denaturing Blue-native (BN) PAGE (Figure 3.10, right panels). The constitutive phosphorylation of LHCII in *tap38* mutants was associated with the presence of a prominent pigment-protein complex of about 670 kDa previously reported to be characteristic for state 2 (Pesaresi et al., 2002; Heinemeyer et al., 2004). 2D-PAGE fractionation showed that the pigment-protein complex consists of PSI and LHCI subunits, together with a portion of pLHCII that associates with PSI upon state 1→ state 2 transition in WT plants (Pesaresi et al., 2009) (see also Figure 3.11). In contrast, *oeTAP38* plants, which are blocked in state 1, failed to form the PSI-LHCI-LHCII complex under all conditions investigated.

Quantification of the different PSI complexes on two-dimensional (2D) PA gels confirmed that the number of PSI complexes associated with LHCII was increased in the *tap38* mutants in comparison to WT (Figure 3.11), supporting the findings obtained from the 77K fluorescence analyses. To clarify whether the LHCII (de-)phosphorylation behaviour in WT plants is directly correlated to the TAP38 protein concentration, TAP38 levels were determined at the same time points as in Figure 3.10. In WT plants, TAP38 was constitutively expressed at similar levels under all applied light conditions (Figure 3.12). Therefore, LHCII (de-)phosphorylation in WT plants seems not to be regulated via adjustment of the TAP38 protein amount.

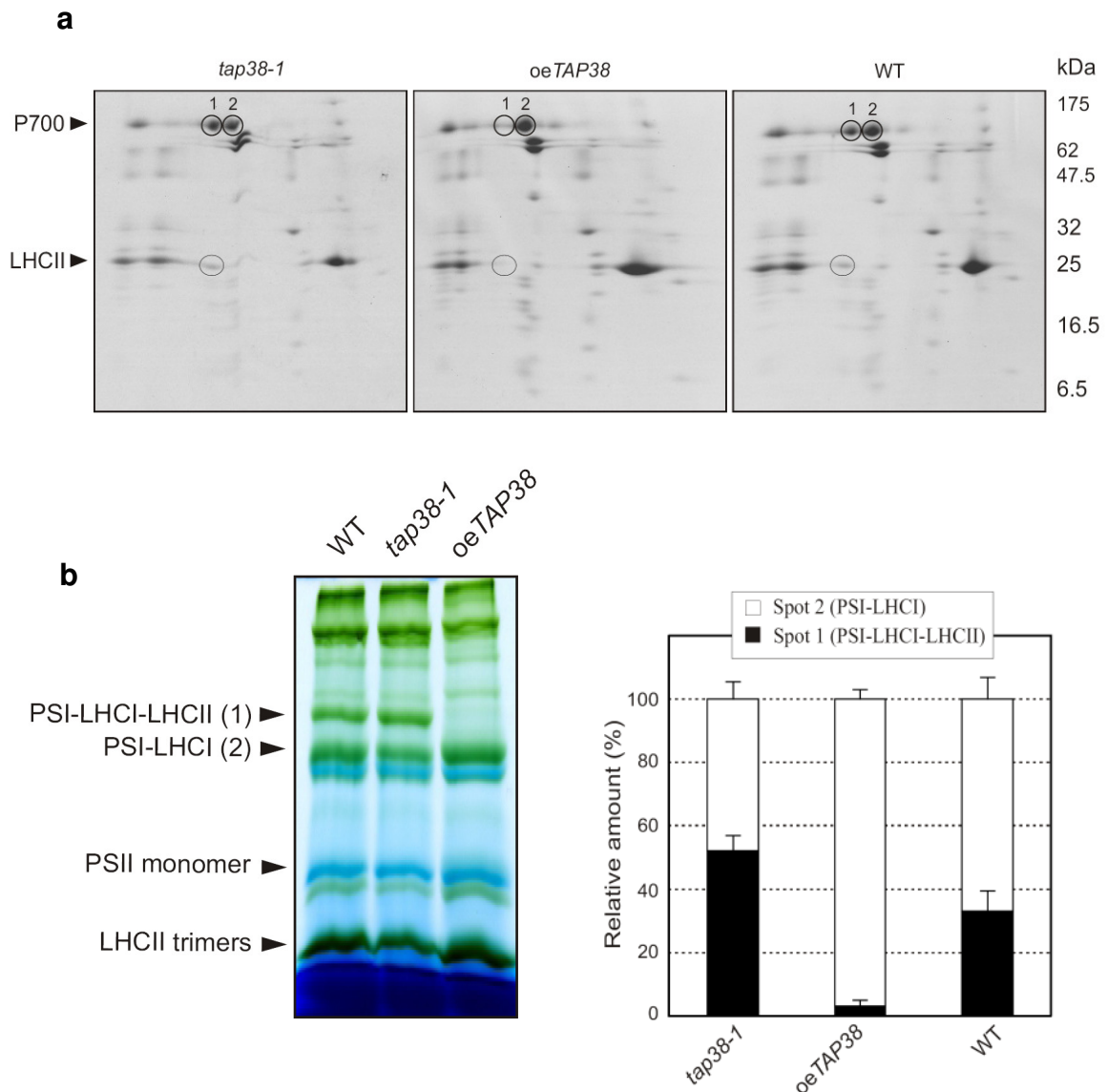


Figure 3.11 Quantification of PSI-LHCI and PSI-LHCI-LHCII complexes under state 2 conditions (low light; $80 \mu\text{mol m}^{-2} \text{s}^{-1}$). **a**, 2D-PAGE of identical amounts of thylakoid proteins isolated from WT, *tap38-1* and *oeTAP38* lines adapted to state 2. Gels were stained with Coomassie. P700, photosystem I reaction centre; LHCII, light-harvesting complex of PSII (the band indicative for the PSI-LHCI-LHCII complex is encircled). **b**, *Left panel*, BN-PAGE of identical amounts of thylakoid proteins from WT, *tap38-1* and *oeTAP38* plants adapted to low light (state 2); *Right panel*, densitometric quantification of the spots representing PSI-LHCI-LHCII (spot 1) and PSI-LHCI (spot 2) in panel **a**. Values are averages of three independent 2D gels for each genotype. Bars indicate standard deviations. Note that *tap38-2* behaves very similarly to *tap38-1*.

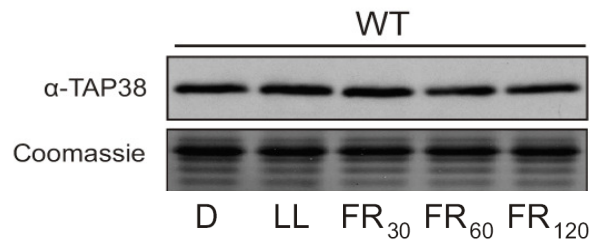


Figure 3.12 TAP38 is constantly expressed under all investigated light conditions (see Figure 3.10). Thylakoid membranes of WT plants exposed to different light conditions were separated by SDS-PAGE. Immunodecoration of the corresponding western was performed using a TAP38 specific antibody raised against the mature protein. A replicate gel stained with Coomassie is shown as loading control.

3.8 Association of TAP38 with a low molecular weight complex

Thylakoids of WT and *tap38-1* plants were solubilised by mild detergent treatment (1% β -DM) and subjected to sucrose gradient centrifugation. The different fractions were separated by SDS-PAGE and probed with a TAP38 specific antibody (Figure 3.13). While fractions 1-5 corresponded mainly to monomeric proteins, fractions 14-16 contained predominantly PSI complexes. TAP38 could be detected in the monomeric and low molecular complex fractions (fractions 4-7). Therefore, at least under the chosen solubilising conditions, TAP38 seems not to be associated to any of the major photosynthetic complexes like PSII, Cyt b_6/f or PSI, but appeared to be predominantly monomeric with a certain fraction possibly being associated to a low molecular weight complex. Similar observations were made by western blot analysis with a TAP38 specific antibody performed on mild detergent (1,5% digitonin) treated thylakoid membranes separated by BN-PAGE (similar to Figure 3.11b, *left panel*). TAP38 was predominantly detected as a monomer in the running front and additionally in a weak band slightly below the LHCII trimer.

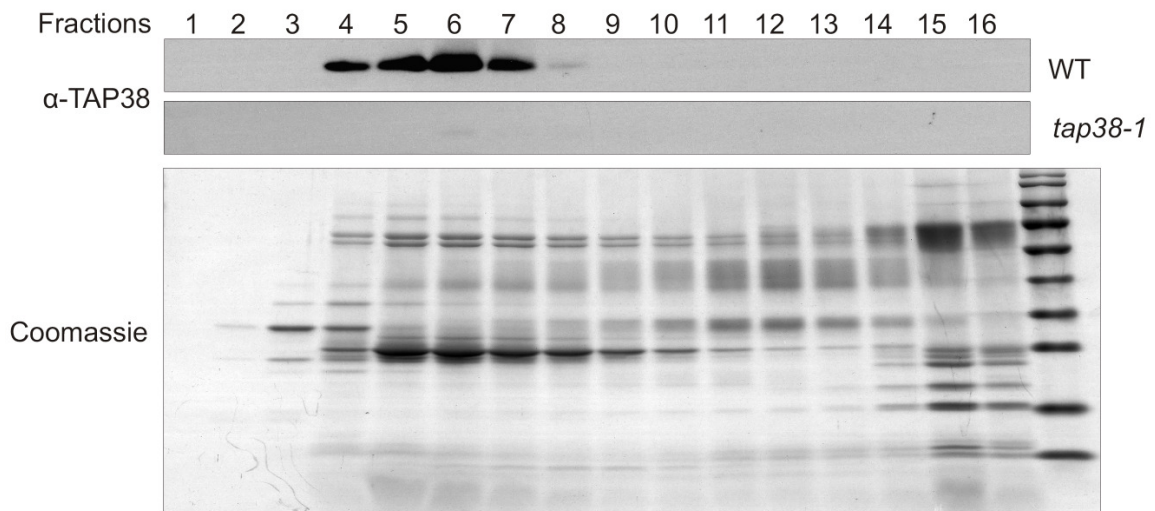


Figure 3.13 TAP38 occurs mainly as a monomer or associated with a low molecular weight complex. Sucrose gradient centrifugation of β -DM treated thylakoid membranes from WT, compared to *tap38-1* mutant, showed the appearance of TAP38 in the monomeric and low molecular complex fractions (4-7). Sucrose gradient fractions were separated by SDS-PAGE. TAP38 was detected by immunoblot analysis with a TAP38 specific antibody. A replicate gel stained with Coomassie is shown as a control for efficient thylakoid solubilisation.

3.9 Growth characteristics and photosynthetic performance

When kept under low light intensities ($80 \mu\text{mol m}^{-2} \text{s}^{-1}$) that favour state 2, *tap38* mutants grew faster than WT plants (Figure 3.14a), whereas *oeTAP38* plants behaved like WT. Detailed measurements revealed that the *tap38* mutants exhibited a constant growth advantage over WT plants, starting at the cotyledon stage (Figure 3.14b). Because this difference might be attributable to an altered photosynthetic performance, parameters of thylakoid electron flow were measured. The fraction of Q_A (the primary electron acceptor of PSII) present in the reduced state (1-qP) was lower in *tap38-1* plants (0.06 ± 0.01) than in WT (0.10 ± 0.01), when both genotypes were grown as in Figure 3.14a and chlorophyll fluorescence was excited with $22 \mu\text{mol m}^{-2} \text{s}^{-1}$ actinic red light. Comparable differences in the redox state of the primary electron acceptor persisted up to $95 \mu\text{mol m}^{-2} \text{s}^{-1}$ actinic red light (Figure 3.15a), indicating that the *tap38-1* mutant can redistribute a

larger fraction of energy to PSI, in accordance with the increase in its antenna size under state 2 (see Figure 3.9, Table 3.3 and Figure 3.11).

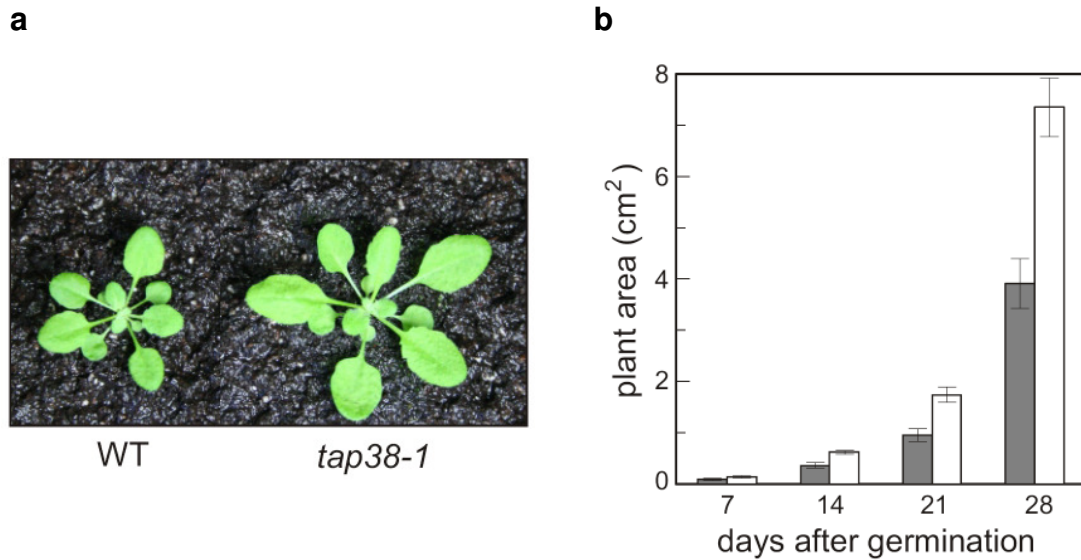


Figure 3.14 Growth characteristics of *tap38* mutant plants. **a**, Phenotypes of 4-week-old *tap38-1* and WT plants grown under low light conditions ($80 \mu\text{mol m}^{-2} \text{s}^{-1}$) on a 12 h / 12 h light / dark regime. **b**, Growth curve. Leaf areas of twenty plants of each genotype (WT, grey bars; *tap38-1*, white bars) were measured over a period of four weeks after germination. Mean values \pm standard deviations (SDs; bars) are shown.

This idea was supported by measurements of the maximum (F_V/F_M) and effective (Φ_{II}) quantum yields of PSII. F_V/F_M remained unaltered in mutant plants (see Figure 3.15b, dark-adapted plants, PAR = 0), indicating WT-like efficiency of mutant PSII complexes. However, Φ_{II} was increased in *tap38-1* (0.75 ± 0.01) relative to WT (0.72 ± 0.01), suggesting that the electron flow through thylakoids was more efficient in *tap38-1* (Figure 3.15b). The improvement in photosynthetic performance of the *tap38* mutants was most pronounced under low and moderate illumination (Figure 3.15a-b), as could be expected from their growth phenotype.

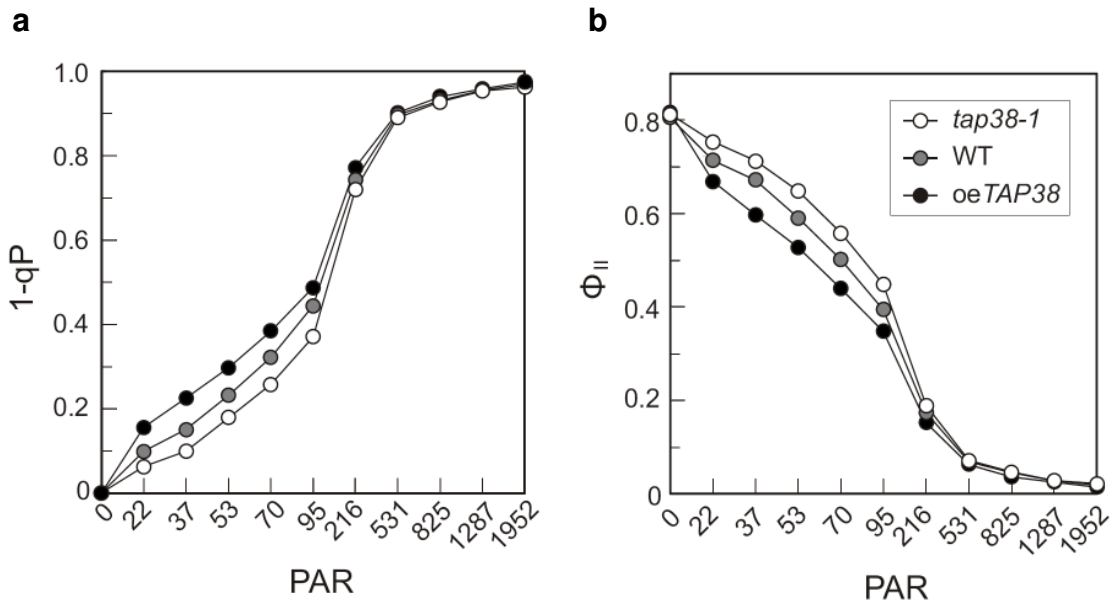


Figure 3.15 Photosynthetic performance of *tap38* mutant plants. **a-b**, Measurements of light dependence of the photosynthetic parameters 1-qP (**a**) and effective quantum yield of PSII (Φ_{II} ; **b**) of plants grown under low light conditions ($80 \mu\text{mol m}^{-2} \text{s}^{-1}$) on a 12 h / 12 h light / dark regime. WT, filled grey circles; *tap38-1*, open circles; *oeTAP38*, filled black circles; PAR, photosynthetically active radiation in $\mu\text{mol m}^{-2} \text{s}^{-1}$. Average values were determined from five independent measurements (SD < 5%). Note that *tap38-2* and *tap38-1* plants behave similarly. However, the *tap38-2* mutant still synthesises some TAP38 (see Figure 3.7b), and its phenotype is slightly less severe.

4. Discussion

4.1 cpPPs - bioinformatic prediction vs experimental confirmation

Considering that around 10% of the nuclear genes in *Arabidopsis* are estimated to encode chloroplast proteins (Leister, 2003), an extension of this extrapolation to the family of protein phosphatases counting around 217 members, results in more than 20 expected cpPPs ($=217/10$) operating in the photosynthetic organelle. Although the genomic approach described in this work led to the identification of nine additional cpPPs, involved in reversible chloroplast protein phosphorylation, the current number of ten confirmed cpPPs (including AtRP1) is still much smaller than the one based on the genome-wide extrapolation and also much smaller than expected based on the cTP predictions for PPs (see Table 3.1).

The combination of nine prediction algorithms most likely led to an increase of false negatives due to the mentioned loss in sensitivity, for the sake of an increase in specificity. One could speculate that the chloroplast as a prokaryotic descendant might have failed to quantitatively adapt to the eukaryotic concept of reversible protein phosphorylation at serine and threonine residues. This could mean that the actual number of PPs in the chloroplast is markedly lower than expected. Nevertheless, only approaches combining less stringent bioinformatic prediction and experimental validation of the subcellular location of proteins as outlined in this work will systematically contribute to identify the entire complement of chloroplast protein phosphatases.

During the initial screen for suitable candidates for the RFP fusion assay, particular attention was paid to the PPM-phosphatase-family (containing PP2C and PP2C-like signatures). Members of that family are known to act as monomeric enzymes with a high substrate specificity and their activity depends on divalent cations (mainly Mn^{2+} and Mg^{2+}) (Cohen, 1989; Das et al., 1996; Moorhead et al., 2007; Xue et al., 2008). It was also shown that

members of the PPM-family are not susceptible to inhibition by microcystin and okadaic acid (Cohen, 1989; Rodriguez, 1998). These characteristics were chosen as cut-off criteria, because so far unsuccessful efforts to identify the LHClI phosphatase(s) using biochemical approaches (Sun et al., 1989; Hammer et al., 1995a; Hast and Follmann, 1996) could at least show that the phosphatase activity is dependent on the presence of aforementioned divalent cations. Furthermore it was shown, that the phosphatase activity could not be inhibited by microcystin and okadaic acid (Sun et al., 1989; Hammer et al., 1995a), phosphatase inhibitors specific for Type 1 and Type 2A protein phosphatases (Cohen, 1989).

The vast majority of chloroplast proteins is targeted to the organelle by an N-terminal signal sequence, the chloroplast transit peptide (cTP), and is imported via the Tic/Toc translocon (Soll and Schleiff, 2004). Therefore, candidate phosphatases for the RFP screen were chosen according to the presence of a transit peptide. For the prediction of cTPs various algorithms have been developed. It was shown that the specificity of combinatorial cTP prediction increases with the number of predictors used. As expected, this gain in specificity occurs at the expense of sensitivity (Richly and Leister, 2004). In this project nine different algorithms for cTP prediction have been employed to the entire complement of 217 PPs encoded in the nuclear genome of *A. thaliana* and a threshold for positive chloroplast prediction of '4 out of 9' predictors was chosen. An additional cut-off criterion was that only putative serine (Ser) / threonine (Thr) PPs were considered, since most phosphorylated proteins of the photosynthetic apparatus detected so far are modified at a serine or threonine residue (Ohad et al., 2001; Vener et al., 2001; Carlberg et al., 2003; Hansson and Vener, 2003). This led to a final selection of 26 protein phosphatases with a putative cTP which were subject to the follow-up RFP-localisation screen. Among the predicted cpPPs, serine/threonine phosphatases were underrepresented whereas PP2C-type PPs dominated (Table 3.1). Showing a prediction score of '3 out of 9' the additional cpPP candidate (TAP38), that resulted from the proteomics database search, was initially not considered because of the decreased sensitivity of the combination of several prediction algorithms. In retrospect, choosing the '4 out of 9' threshold for the approach of combinatorial cTP

prediction led to quite reliable results for protein phosphatases. This becomes evident when looking at the large fraction of tentative cpPPs with high prediction ratios ($\geq 6/9$) that are truly located in the chloroplast (for 8 of the 12 putative cpPPs a chloroplast location could be confirmed, see Table 3.2). In comparison to the reliable results for the cpPPs the phosphorylating complement, the cpPKs, showed a strong discrepancy between prediction and actual subcellular localisation even if a quite stringent prediction threshold ($\geq 6/9$) was applied (Schliebner et al., 2008). Why the combinatorial cTP prediction approach led to predominantly false positive results for the protein kinases needs further investigation. Therefore, it can be concluded that the identification of cpPKs by cTP prediction is very error-prone, whereas cpPPs could be identified in a relatively reliable way.

Previous to our screen for new chloroplast protein phosphatases, only two cpPPs have been known. While AtRP1 exhibits bifunctional PK / PP properties and is capable of (de-)phosphorylation of the regulatory threonine residue of Arabidopsis pyruvate, orthophosphate dikinase (PPDK) (Chastain et al., 2008), the dual specificity protein phosphatase DSP / SEX4 was shown to bind to starch granules and to be involved in the regulation of starch metabolism (Kerk et al., 2006; Niittyla et al., 2006; Sokolov et al., 2006). However, later the function of SEX4 as a chloroplast protein phosphatase had to be revised as it was shown that SEX4 actually functions as a phosphoglucan phosphatase in starch breakdown (Kotting et al., 2009). Furthermore, lacking a conserved motif common to protein phosphatases, AtRP1 cannot be assigned to any of the existing PP classes. It is tempting to speculate that there exist a lot more chloroplast protein phosphatases, like AtRP1, with yet unknown phosphatase motives, which make up for the low number of cpPPs belonging to the known classes of PPs. Thus, the nine newly identified cpPPs are the first described mere protein phosphatases located in plastids that can be allocated to distinct PP classes. Furthermore, TAP38 is the first identified cpPP with a clear assigned function.

While the work described in this thesis aimed to identify potential cpPPs that act on thylakoid membrane proteins, the complement of soluble phosphoproteins was neglected so far. Future analyses of loss-of-function mutants

of the so far uncharacterised cpPPs (see Table 2.2) with respect to soluble chloroplast proteins bear a high potential to further elucidate the importance of reversible phosphorylation in chloroplasts.

4.2 Splice variants of TAP38

Even though the splice variants At4g27800.2 and At4g27800.3 could not be detected in leaf tissue with the generated polyclonal antibodies, there was still a basal level of *At4g27800.2* transcript detectable (Figure 3.3). To analyse whether At4g27800.2 has a function in chloroplasts, At4g27800.2 overexpressing plants will have to be generated for further investigations. Import studies with *in vitro* translated ³⁵S labelled At4g27800.2 could confirm its localisation in plastids (data not shown). Thereby, it seemed as if the protein was only partially processed.

Follow-up analyses will have to clarify, whether any of the two other isoforms (At4g27800.2 and At4g27800.3) are differently expressed in non-green tissue and have regulatory function in plastids others than chloroplasts. Since the level of *At4g27800.2* was reduced in the *tap38* mutants (which should therefore also be the case for *At4g27800.3*) and no obvious additional phenotype besides the defect in State Transitions could be observed, it is likely that At4g27800.2 and At4g27800.3 exert potential functions in regulatory mechanisms that did not become crucial under the chosen conditions.

4.3 LHCII dephosphorylation - thylakoid associated TAP38 vs biochemically identified stromal PP

Former publications postulated the existence of at least two independent chloroplast protein phosphatases (Sun et al., 1989; Hammer et al., 1995a; Hammer et al., 1995b; Hast and Follmann, 1996). Moreover, LHCII dephosphorylation was suggested to be catalysed by two independent protein phosphatases, a membrane bound-one and more predominant, a

stromal PP (Hammer et al., 1995b). Controversely, the results presented in this work rather suggest that TAP38, a thylakoid associated phosphatase, is the sole phosphatase responsible for LHCII dephosphorylation. Although slightly leaky, the *tap38-1* mutant shows a distinct fraction of LHCII in the phosphorylated state under all investigated conditions (Figure 3.10). In case of the presence of a second LHCII phosphatase, one would expect some residual dephosphorylation of LHCII under the applied conditions. An explanation for the previously shown LHCII dephosphorylation activity of the stroma by Hammer et al. (1995a) could be, that the conditions used for stromal preparation led to a release of the possibly just weakly attached TAP38 from the thylakoid membrane resulting in the measured LHCII dephosphorylation capacity of the stromal fractions. To test this hypothesis, thylakoid membranes will have to be treated with different ionic strength to assess the attachment of TAP38 to the thylakoid membrane, including the conditions used by Hammer et al. (1995a) for stromal preparation. A further explanation could be that indeed, a so far unknown stromal protein phosphatase is responsible for the direct dephosphorylation of LHCII, with TAP38 being a regulator of that phosphatase. This scenario would support the later proposed model C (Figure 4.1) for the mode of action of TAP38.

4.4 TAP38 - possible modes of action

One of the major questions to be solved in the future is whether TAP38 negatively regulates the activity of STN7 (e.g. by dephosphorylation of STN7) (Figure 4.1; model A), dephosphorylates LHCII directly (Figure 4.1; model B), or forms part of a phosphorylation / dephosphorylation cascade that controls the activity of the LHCII kinase or phosphatase (Figure 4.1; model C).

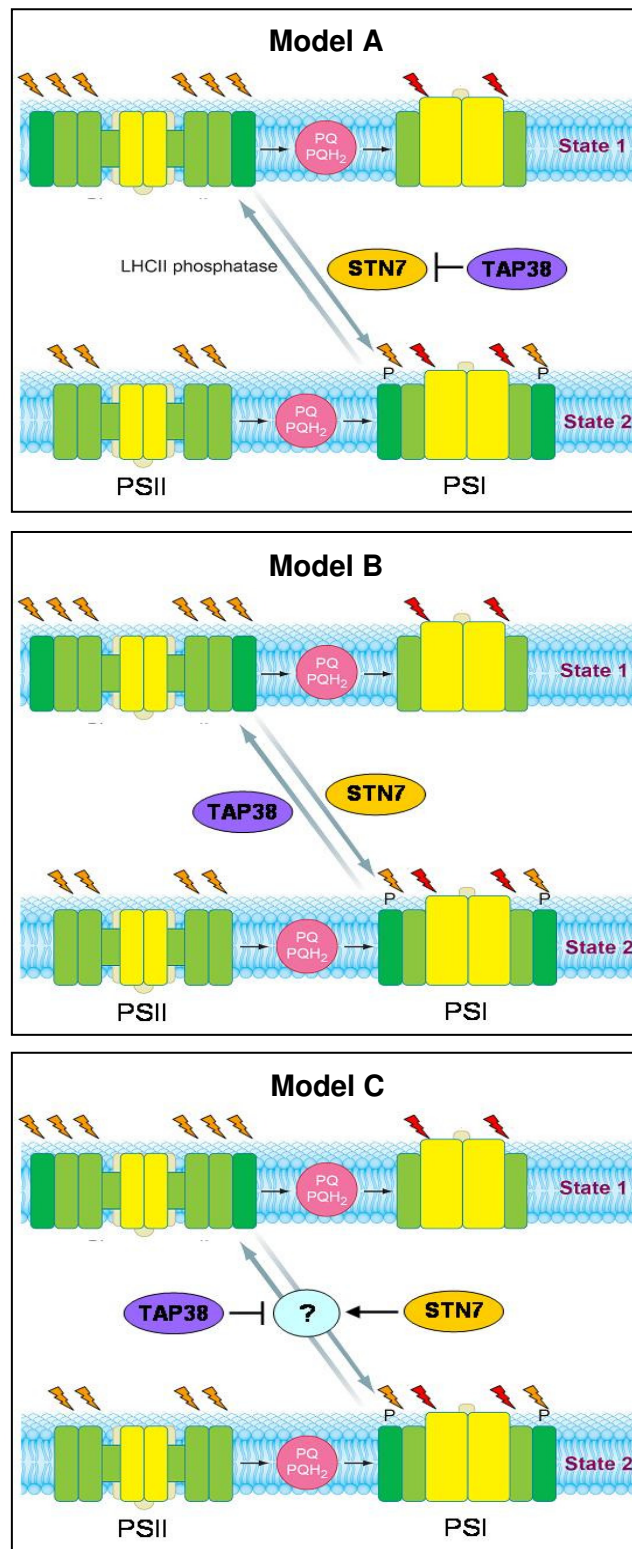


Figure 4.1 Models for potential modes of action of TAP38. **Model A** - TAP38 negatively regulates the activity of STN7 (e.g. by dephosphorylation of STN7); **Model B** - TAP38 directly dephosphorylates LHCII; **Model C** - TAP38 forms part of a phosphorylation / dephosphorylation cascade that controls the activity of the LHCII kinase or phosphatase. Orange flash (PSII favouring light); Red flash (PSI favouring light).

← Activation; ┘ Inhibition; adapted from Allen (2003).

4.4.1 Model A

The observation that *oeTAP38* plants, although showing a >20-fold increase in TAP38 levels, still exhibit residual LHCII phosphorylation (Figure 3.10c), together with the fact that reversible phosphorylation of STN7 has not been demonstrated (Heazlewood et al., 2008), argues in favour of the idea that TAP38 does not inhibit STN7 by dephosphorylation. Therefore, model A (Figure 4.1) is the least likely of the three proposals.

4.4.2 Model B

In different genetic backgrounds (WT, *tap38* mutants and *oeTAP38*) the change of TAP38 levels resulted in a clear change in pLHCII levels. While in *tap38* mutants a strong reduction in TAP38 led to a constantly high level of pLHCII, strong overexpression of TAP38 (*oeTAP38*) severely reduced the amount of pLHCII. However, in WT where pLHCII levels are modulated according to well known and frequently determined patterns (Bellafiore et al., 2005; Bonardi et al., 2005), TAP38 seems to be equally expressed under all applied conditions (Figure 3.12). These results can be explained in two different ways. One possibility could be that TAP38 is constitutively active and directly responsible for the dephosphorylation of LHCII (Figure 4.1; model B). For that, TAP38 would need to be present in a certain concentration range (as it is the case for WT) to constantly dephosphorylate LHCII, whose phosphorylation state would then in the first place be regulated by the activity of the LHCII kinase (STN7). The regulation of STN7 (STN7) on transcript and protein level (Lemeille et al., 2009; Elena Aseeva LMU, personal communication), as well as the regulation of its activity in a redox dependent manner (Wollman, 2001), argues in favour of this scenario. The fact that *tap38* mutant and *oeTAP38* plants, both show a defect in State Transitions (Figure 3.8), whereas in the case of STN7 only the *stn7* mutant and not the *oeSTN7* plants are affected (Elena Aseeva LMU, personal communication), further supports the hypothesis that STN7 is the key factor in regulation. Despite the obvious TAP38 dosage dependence of LHCII dephosphorylation (Figure 3.10), TAP38 activity could anyhow underlay some kind of regulation. However, the strong decrease or

increase of TAP38 levels in *tap38* mutant and *oeTAP38* plants might overstrain this regulatory system.

4.4.3 Model C

Another possibility could be that TAP38 - either as a constitutively active phosphatase or as a phosphatase regulated in a so far unknown way (as mentioned above) - acts in a phosphorylation / dephosphorylation cascade that controls the activity of the LHCII kinase or phosphatase (Figure 4.1; model C).

4.4.4 Arguments in favour of models B and C

The direct dependence of LHCII dephosphorylation upon TAP38 dosage revealed by comparison of *tap38* mutants, WT and *oeTAP38* plants is compatible with both models, model B and C. The very strong phenotypic resemblance of *oeTAP38* plants with *stn7* mutants and *vice versa* (*oeSTN7* with *tap38* mutants) (Elena Asseva LMU, personal communication) additionally supports the idea that TAP38 and STN7 act on the same regulatory level. This could be either because LHCII is the direct substrate of TAP38 and STN7 (Figure 4.1; model A), or because TAP38 and STN7 form part of the aforementioned phosphorylation / dephosphorylation cascade (Figure 4.1; model C).

4.5 Uncoupling of LHCII phosphorylation from PQ redox state

It is known that an increase in the relative size of the reduced fraction of the plastoquinone pool (PQH₂) enhances phosphorylation of LHCII (Allen and Forsberg, 2001; Wollman, 2001; Pesaresi et al., 2002; Ihnatowicz et al., 2008). Depletion of TAP38 in *tap38* mutants, however, increases both LHCII phosphorylation (Figure 3.10b) and PQ oxidation (see 1-qP values in Figure 3.15a). This discrepancy can be resolved by assuming that the enhanced oxidation of PQ caused by the increase in PSI antenna size (and LHCII phosphorylation) in *tap38* plants is not sufficient to down-regulate the LHCII

kinase to such an extent that it can compensate for the decline in LHCII dephosphorylation.

4.6 Putative interaction partners of TAP38

Under the quite mild solubilising conditions applied in this work (see 2.14 and 2.16), TAP38 could not be detected in association with any higher molecular weight complex (Figure 3.13). However, TAP38 might still be weakly attached to major photosynthetic complexes under physiological conditions. A counter-argument is that TAP38 was not only present as a monomer after solubilisation with 1% β -DM and 1.5% digitonin, but also associated to some unknown components of the thylakoid membrane. This can be deduced from Western blots showing that TAP38 penetrates somewhat deeper into the sucrose gradient than the major fraction of monomeric proteins (Figure 3.13). Also a weak additional TAP38-containing band just below the LHCII trimer (in BN-PAGEs similar to Figure 3.10) could be observed besides the major monomeric signal migrating with the running front. To definitely answer the question whether putative TAP38 interaction partners exist, assays will have to be performed that either stabilise weak protein interactions before solubilisation steps or that can purify potential interaction partners under physiological conditions. In the meantime, monospecifically purified epitope antibodies against TAP38 were generated, which can be used for Co-Immunoprecipitation assays, in order to identify potential direct interaction partners under physiological conditions. Another possibility is to use crosslinking reagents to covalently link proteins to TAP38 that only weakly interact under physiological conditions. Both kinds of assays will help to identify putative interaction partners.

It has been shown by photosynthetic measurements and BN-PAGE (Figure 3.11) that the lack of TAP38 does not affect the general organisation of the photosynthetic apparatus or its activity. In return, it is of high interest to understand whether the accumulation of TAP38 is dependent on its association to one of the major photosynthetic complexes like PSII, Cyt b_6/f , PSI and/or ATPase. To answer this question, the presence of TAP38

protein will have to be investigated in mutants lacking the different photosynthetic complexes. The appropriate assortment of mutants could be the following: *hcf136*, *petc*, *psad1psad2* and *atpd*; *hcf136* lacks a PSII assembly / stability factor and therefore PSII complexes cannot accumulate (Plücken et al., 2002); In *petc* the gene coding for the Rieske protein is non-functional and the mutant lacks the entire Cyt b_6/f complex (Maiwald et al., 2003); *psad1psad2* lacks both PSI-D isoforms (Ihnatowicz et al., 2004) and as a consequence the entire PSI complex; *atpd* was chosen as a mutant that is missing the ATPase due to a mutation in the gene coding for the ATPase δ subunit (Maiwald et al., 2003). An accumulation of TAP38 independent from the presence of any of the major complexes would suggest a stable integration of TAP38 in the thylakoid membrane. Contrarily, the lack of TAP38 in one of the mutants would provide an indication of a direct association of TAP38 with the respective complex. Preliminary results suggest an association of TAP38 with the Cyt b_6/f complex, which again would strengthen the idea of a close proximity of TAP38 and STN7, given that STN7 is also absent when Cyt b_6/f is missing (Elena Asseva LMU, personal communication).

Another candidate interaction partner of TAP38 in *Arabidopsis* is AtCYP38. The AtCYP38 ortholog in spinach, TLP40, a cyclophilin-like peptidyl-prolyl isomerase, is a negative regulator of a thylakoid membrane protein phosphatase involved in dephosphorylation of the PSII core proteins (Rokka et al., 2000). Like TLP40, AtCYP38 was shown to be a thylakoid membrane attached luminal protein possessing a phosphatase binding domain. Moreover, AtCYP38 - deficient thylakoids also exhibited strong reduction in the *in vivo* phosphorylation levels of PSII phosphoproteins, particularly D1 and D2 (Sirpiö et al., 2008).

Interestingly, *AtCYP38* mutant plants displayed a similar phosphorylation pattern like *oeTAP38* plants. Besides a strong dephosphorylation of LHCII, which in the case of *AtCYP38* deficient plants resulted from inhibition of the respective LHCII kinase (Rintamäki et al., 2000), also the PSII core proteins, mainly D1 and D2, showed an increased dephosphorylation (Figure 3.10c).

However, there are arguments against a possible interaction of TAP38 with AtCYP38, or at least a function of both in the same regulatory pathway. It was shown before that a purified enzyme that interacts with TLP40 exhibits characteristics typical of eukaryotic Ser / Thr phosphatases of the PP2A-type. The purified enzyme was inhibited by okadaic acid and microcystin and was recognised by a polyclonal antibody raised against a recombinant catalytic subunit of human PP2A (Vener et al., 1999). TAP38 however belongs to the PPM-family of phosphatases. Nevertheless, it cannot be excluded, that AtCYP38 also interacts with phosphatases others than the PP2A one.

Under elevated temperatures TLP40 dissociates from the thylakoid membrane, which leads to an increase in the dephosphorylation of PSII core proteins. To clarify whether the resembling phenotypes of *AtCYP38* – deficient and *oeTAP38* plants are truly not due to a defect in the same reaction pathway, dephosphorylation experiments under increased temperatures will have to be performed to assess a potentially enhanced phenotype for *oeTAP38* plants. The already initiated characterisation of Δ AtCYP38/*tap38-1* and Δ AtCYP38/*oeTAP38* lines will also shed light on a potential interaction of those two proteins. A further possible way to elucidate a direct interaction between the two thylakoid associated proteins TAP38 and AtCYP38 would be a split ubiquitin assay (Pasch et al., 2005).

4.7 Does TAP38 - like STN7 - function in LTR?

Besides its function in short-term acclimation by modulating the phosphorylation state of LHCII, STN7 also plays a key role in adjusting the stoichiometry of the two photosystems, the so called long-term response (LTR) (Bonardi et al., 2005; Dietzel et al., 2008). In contrast to rearrangements of the antennae structure during State Transitions, the photosystem stoichiometry adjustment requires hours and days and redirects imbalances in excitation energy by changing the relative amounts of the two photosystems (Fujita, 1997). The Chl fluorescence parameter F_S/F_M (ratio between steady-state and maximum fluorescence), as well as

the Chl a/b ratio, were found to be useful for assessing the ability of plants to perform a proper LTR (Pfannschmidt et al., 2001; Fey et al., 2005b) because both ratios exhibit characteristic differences between plants acclimated to PSI light or PSII light. The F_S/F_M parameter reflects the structural differences in the photosynthetic apparatus, and its value typically increases after acclimation of WT plants to PSI light and decreases after acclimation to PSII light. The Chl a/b ratio also reflects the photosystem organisation of the photosynthetic complexes and behaves in the opposite manner in WT plants - being high after acclimation to PSII light and low in PSI light. The *stn7* mutant of *Arabidopsis* did not show such differences, indicating that this mutant lacks not only the ability to perform State Transitions but also LTR (Bonardi et al., 2005).

Even though, showing controverse LHCII phosphorylation levels, *tap38* and *stn7* mutants are equally defective in the short-term acclimation process. Furthermore, *oeTAP38* plants imitate the *stn7* mutant phenotype regarding short-term acclimation. These observations, together with the favoured idea (represented by models B and C of Figure 4.1) that TAP38 and STN7 act on the same regulatory level, lead to the speculation that *tap38* mutants might also be affected in their ability to perform a proper long-term response. However, because both *tap38* mutant lines contain residual levels of TAP38 protein (Figure 3.7b), LTR could anyhow be functional, although a true knock out of TAP38 might lead to a loss in LTR ability. A potential complete knock-out T-DNA insertion line for TAP38 is currently under investigation and will help to resolve this open question. It is known that LTR, as well as State Transitions, are triggered by the redox state of the PQ pool. Most species investigated exhibit enhanced expression of the PSI reaction centre genes *psaA* and *psaB* (encoding the P700 apoproteins) upon reduction of the PQ pool or a respective repression upon its oxidation. As shown by the 1-qP measurements (Figure 3.15a) the *tap38* mutants display a rather oxidised PQ pool in comparison to WT plants when grown under PSII light conditions. However, according to BN-PAGE analyses there is no obvious decrease in the total amount of PSI visible in the *tap38* mutants compared to WT (Figure 3.11). This can be seen as an additional hint for a defect in LTR. RT-PCR and Western blot analyses on the transcript and protein

levels of PSI and PSII core subunits will also help to elucidate the potential involvement of TAP38 in LTR.

In case TAP38 also acts in LTR, this would be a strong hint that STN7 and TAP38 act antagonistically at the very same regulatory level regarding photosynthetic acclimation. Further this would mean, that there has to be at least another substrate of TAP38 different from LHCII, since it was shown by Pesaresi et al. (2009) that neither the phosphorylation state of LHCII nor any other conformational changes caused by State Transitions are crucial for LTR.

4.8 Which protein took over the function of TAP38 in *Chlamydomonas*?

Future analyses should also clarify which protein phosphatase replaces the role of TAP38 in *Chlamydomonas*, which apparently lacks a *TAP38* orthologue. There are three genes coding for putative phosphatases present in *Chlamydomonas* (Gene IDs: 5724767, 5722431 and 5724961) with rather low homologies to TAP38, that could have taken over its function. Only the analysis of loss-of-function lines for all three candidate genes will help to finally answer this question.

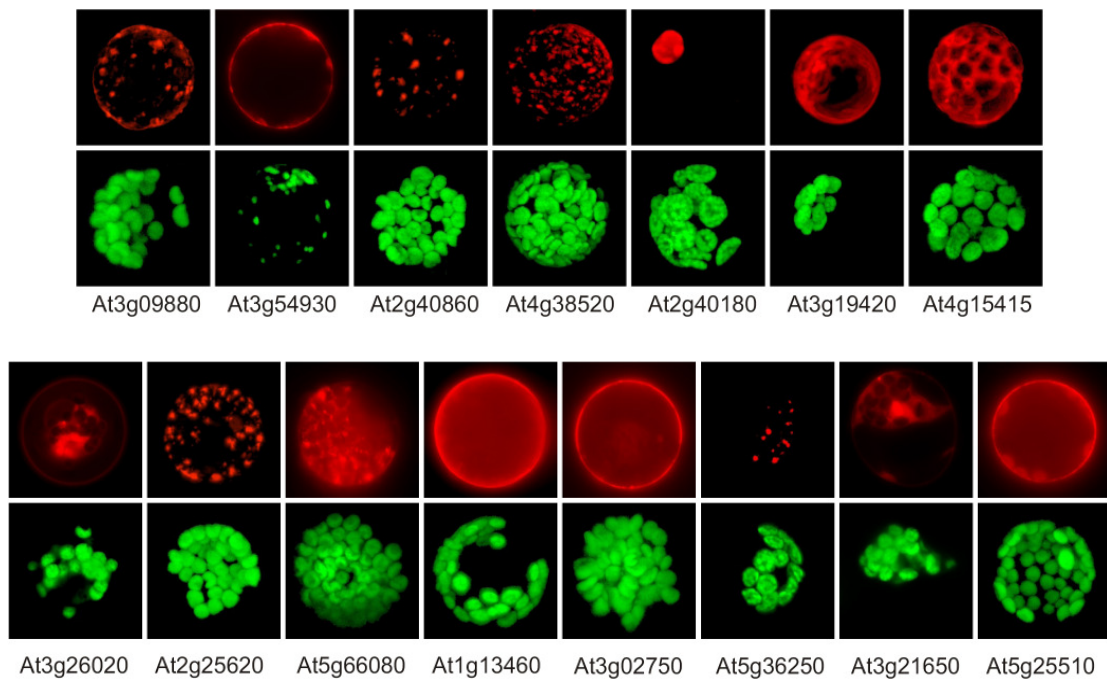
4.9 Enhanced photosynthetic performance and growth phenotype of *tap38* mutants

The enhanced photosynthetic performance indicated by an increase in Φ_{II} (Figure 3.15b), as well as the growth advantage of the *tap38* mutants under constant moderate PSII light, can be attributed to the redistribution of a larger fraction of energy to PSI. This is in accordance with the increase in its antenna size under the applied state 2 light conditions (see Figure 3.9, Table 3.3 and Figure 3.11). The improvement in photosynthetic performance of the *tap38* mutants was most pronounced under low and moderate illumination (Figure 3.15), as expected from their growth

phenotype. It would be interesting to see, whether *oeSTN7* plants also show an enhanced growth phenotype under similar light conditions compared to WT plants.

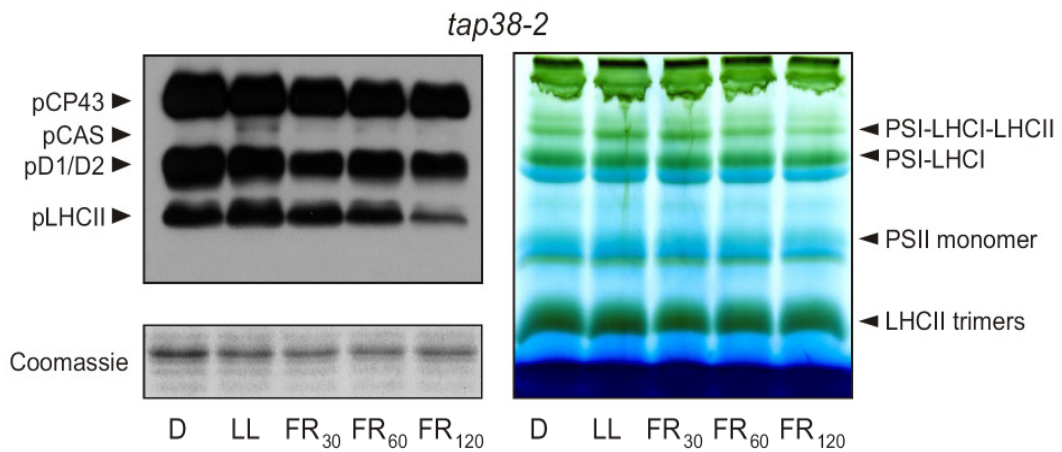
From the aspect of evolution an enhanced photosynthetic performance of loss-of-function mutants is not favourable. However, under natural conditions constant light regimes are rather unlikely to occur and it can be expected that the *tap38* mutants would rather exhibit a fitness disadvantage in comparison to WT plants. This is also the case for the *stn7* mutant, which is marginally affected in its development and fitness when grown under field conditions (Frenkel et al., 2007). Under variable environmental conditions various adaptational mechanisms have evolved that allow plants to optimise their photosynthetic performance. Nowadays however mankind is able to stably control environmental conditions as is the case with modern greenhouses. In this respect some adaptational mechanisms of plants (e.g. State Transitions) might not be necessary for optimal photosynthetic performance anymore, or could even have disadvantageous effects under optimised light conditions. Therefore, factors, like TAP38, that exert a regulatory function on the photosynthetic performance of plants will get into the focus of agronomical interest. Since a considerable proportion of world's crop production is realised in spacious greenhouses under controlled growth conditions (e.g. light, temperature and humidity) and an increase in biomass production is a valuable trait for many plant applications, e.g. oral vaccines or plantibody production (Daniell, 2006), the knockout of TAP38 could represent an economically interesting application.

Appendix 1



Appendix Figure 1 Collection of fluorescence micrographs of *A. thaliana* protoplasts transfected with N-terminal fusions of the predicted transit peptides of the respective cpPPs to dsRED. The pictures are presented in false colour with RFP fluorescence shown in red and chlorophyll autofluorescence in green.

Appendix 2



Appendix Figure 2 Left panel, Thylakoid proteins extracted from *tap38-2* plants kept in the dark (D, state 1), subsequently exposed to low light (LL, state 2), and then to far-red light for 30, 60 and 120 min (FR₃₀, FR₆₀, FR₁₂₀; state 1) were fractionated by SDS-PAGE. Phosphorylation of LHCII and PSII core proteins was detected by immunoblot analysis with a phosphothreonine-specific antibody. Right panel, Thylakoid proteins of *tap38-2* plants treated as in the left panel were subjected to BN-PAGE analysis. Accumulation of the state 2 associated PSI-LHCI-LHCII complex correlates with the phosphorylation level of LHCII.

References**A**

Abramoff, M.D., Magelhaes, P.J., and Ram, S.J. (2004). Image Processing with ImageJ. *Biophotonics International* **11**, 36-42.

Allen, J. (2002). Photosynthesis of ATP-electrons, proton pumps, rotors, and poise. *Cell* **110**, 273-276.

Allen, J.F. (1992). Protein phosphorylation in regulation of photosynthesis. *Biochim Biophys Acta* **1098**, 275-335.

Allen, J.F. (1995). Thylakoid protein phosphorylation, state 1 - state 2 transitions, and photosystem stoichiometry adjustment: redox control at multiple levels of gene expression. *Physiol Plant* **93**, 196-205.

Allen, J.F. (2003). Botany. State transitions-a question of balance. *Science* **299**, 1530-1532.

Allen, J.F., and Pfannschmidt, T. (2000). Balancing the two photosystems: photosynthetic electron transfer governs transcription of reaction centre genes in chloroplasts. *Philos Trans R Soc Lond B Biol Sci* **355**, 1351-1359.

Allen, J.F., and Forsberg, J. (2001). Molecular recognition in thylakoid structure and function. *Trends Plant Sci* **6**, 317-326.

Alonso, J.M., Stepanova, A.N., Leisse, T.J., Kim, C.J., Chen, H., Shinn, P., Stevenson, D.K., Zimmerman, J., Barajas, P., Cheuk, R., Gadrinab, C., Heller, C., Jeske, A., Koesema, E., Meyers, C.C., Parker, H., Prednis, L., Ansari, Y., Choy, N., Deen, H., Geralt, M., Hazari, N., Hom, E., Karnes, M., Mulholland, C., Ndubaku, R., Schmidt, I., Guzman, P., Aguilar-Henonin, L., Schmid, M., Weigel, D., Carter, D.E., Marchand, T.,

Risseuw, E., Brogden, D., Zeko, A., Crosby, W.L., Berry, C.C., and Ecker, J.R. (2003). Genome-wide insertional mutagenesis of *Arabidopsis thaliana*. *Science* **301**, 653-657.

Aronsson, H., and Jarvis, P. (2002). A simple method for isolating import-competent *Arabidopsis* chloroplasts. *FEBS Lett* **529**, 215-220.

B

Baena-Gonzalez, E., Baginsky, S., Mulo, P., Summer, H., Aro, E.M., and Link, G. (2001). Chloroplast transcription at different light intensities. Glutathione-mediated phosphorylation of the major RNA polymerase involved in redox-regulated organellar gene expression. *Plant Physiol* **127**, 1044-1052.

Baginsky, S., Tiller, K., and Link, G. (1997). Transcription factor phosphorylation by a protein kinase associated with chloroplast RNA polymerase from mustard (*Sinapis alba*). *Plant Mol Biol* **34**, 181-189.

Baniulis, D., Yamashita, E., Zhang, H., Hasan, S.S., and Cramer, W.A. (2008). Structure-function of the cytochrome b6f complex. *Photochem Photobiol* **84**, 1349-1358.

Bassi, R., dal Belin Peruffo, A., Barbato, R., and Ghisi, R. (1985). Differences in chlorophyll-protein complexes and composition of polypeptides between thylakoids from bundle sheaths and mesophyll cells in maize. *Eur J Biochem* **146**, 589-595.

Bellafiore, S., Barneche, F., Peltier, G., and Rochaix, J.D. (2005). State transitions and light adaptation require chloroplast thylakoid protein kinase STN7. *Nature* **433**, 892-895.

Ben-Shem, A., Frolow, F., and Nelson, N. (2003). Crystal structure of plant photosystem I. *Nature* **426**, 630-635.

Boden, M., and Hawkins, J. (2005). Prediction of subcellular localization using sequence-biased recurrent networks. *Bioinformatics* 2279 - 2286.

Bonardi, V., Pesaresi, P., Becker, T., Schleiff, E., Wagner, R., Pfannschmidt, T., Jahns, P., and Leister, D. (2005). Photosystem II core phosphorylation and photosynthetic acclimation require two different protein kinases. *Nature* **437**, 1179-1182.

Bonaventura, C., and Myers, J. (1969). Fluorescence and oxygen evolution from *Chlorella pyrenoidosa*. *Biochim Biophys Acta* **189**, 366-383.

C

Campbell, N.A. (1997). *Biologie*. (Heidelberg; Berlin; Oxford: Spektrum Akademischer Verlag GmbH).

Carlberg, I., Hansson, M., Kieselbach, T., Schroder, W.P., Andersson, B., and Vener, A.V. (2003). A novel plant protein undergoing light-induced phosphorylation and release from the photosynthetic thylakoid membranes. *Proc Natl Acad Sci U S A* **100**, 757-762.

Casadio, R., Martelli, P.L., and Pierleoni, A. (2008). The prediction of protein subcellular localization from sequence: a shortcut to functional genome annotation. *Brief Funct Genomic Proteomic* **7**, 63-73.

Chastain, C.J., Xu, W., Parsley, K., Sarath, G., Hibberd, J.M., and Chollet, R. (2008). The pyruvate, orthophosphate dikinase regulatory proteins of *Arabidopsis* possess a novel, unprecedented Ser/Thr protein kinase primary structure. *Plant J* **53**, 854-863.

Chuartzman, S.G., Nevo, R., Shimoni, E., Charuvi, D., Kiss, V., Ohad, I., Brumfeld, V., and Reich, Z. (2008). Thylakoid membrane remodeling during state transitions in *Arabidopsis*. *Plant Cell* **20**, 1029-1039.

Clough, S.J., and Bent, A.F. (1998). Floral dip: a simplified method for *Agrobacterium*-mediated transformation of *Arabidopsis thaliana*. *Plant J* **16**, 735-743.

Cohen, P. (1989). The structure and regulation of protein phosphatases. *Annu Rev Biochem* **58**, 453-508.

D

DalCorso, G., Pesaresi, P., Masiero, S., Aseeva, E., Schünemann, D., Finazzi, G., Joliot, P., Barbato, R., and Leister, D. (2008). A complex containing PGRL1 and PGR5 is involved in the switch between linear and cyclic electron flow in *Arabidopsis*. *Cell* **132**, 273-285.

Daniell, H. (2006). Production of biopharmaceuticals and vaccines in plants via the chloroplast genome. *Biotechnol J* **1**, 1071-1079.

Das, A.K., Helps, N.R., Cohen, P.T., and Barford, D. (1996). Crystal structure of the protein serine/threonine phosphatase 2C at 2.0 Å resolution. *EMBO J* **15**, 6798-6809.

Delosme, R., Beal, D., and Joliot, P. (1994). Photoacoustic detection of flash-induced charge separation in photosynthetic systems - spectral dependence of the quantum yield. *Biochim Biophys Acta* **1185**, 56-64.

Delosme, R., Olive, J., and Wollman, F.A. (1996). Changes in light energy distribution upon state transitions: An *in vivo* photoacoustic study of the wild type and photosynthesis mutants from *Chlamydomonas reinhardtii*. *Biochim Biophys Acta* **1273**, 150-158.

Depege, N., Bellafiore, S., and Rochaix, J.D. (2003). Role of chloroplast protein kinase Stt7 in LHCII phosphorylation and state transition in *Chlamydomonas*. *Science* **299**, 1572-1575.

Dietzel, L., Bräutigam, K., and Pfannschmidt, T. (2008). Photosynthetic acclimation: state transitions and adjustment of photosystem stoichiometry-functional relationships between short-term and long-term light quality acclimation in plants. *FEBS J* **275**, 1080-1088.

Dovzhenko, A., and Koop, H.U. (2003). Sugarbeet (*Beta vulgaris* L.): shoot regeneration from callus and callus protoplasts. *Planta* **217**, 374-381.

E

Eberhard, S., Finazzi, G., and Wollman, F.A. (2008). The dynamics of photosynthesis. *Annu Rev Genet* **42**, 463-515.

Emanuelsson, O., Nielsen, H., Brunak, S., and von Heijne, G. (2000). Predicting subcellular localization of proteins based on their N-terminal amino acid sequence. *J Mol Biol* **300**, 1005-1016.

F

Fey, V., Wagner, R., Brautigam, K., and Pfannschmidt, T. (2005a). Photosynthetic redox control of nuclear gene expression. *J Exp Bot* **56**, 1491-1498.

Fey, V., Wagner, R., Brautigam, K., Wirtz, M., Hell, R., Dietzmann, A., Leister, D., Oelmüller, R., and Pfannschmidt, T. (2005b). Retrograde plastid redox signals in the expression of nuclear genes for chloroplast proteins of *Arabidopsis thaliana*. *J Biol Chem* **280**, 5318-5328.

Fleischmann, M.M., Ravanel, S., Delosme, R., Olive, J., Zito, F., Wollman, F.A., and Rochaix, J.D. (1999). Isolation and characterization of photoautotrophic mutants of *Chlamydomonas reinhardtii* deficient in state transition. *J Biol Chem* **274**, 30987-30994.

Forsberg, J., and Allen, J.F. (2001). Protein tyrosine phosphorylation in the transition to light state 2 of chloroplast thylakoids. *Photosynth Res* **68**, 71-79.

Frenkel, M., Bellafiore, S., Rochaix, J.D., and Jansson, S. (2007). Hierarchy amongst photosynthetic acclimation responses for plant fitness. *Physiologia Plantarum* **129**, 455-459.

Fristedt, R., Carlberg, I., Zygadlo, A., Piippo, M., Nurmi, M., Aro, E.M., Scheller, H.V., and Vener, A.V. (2009). Intrinsically unstructured phosphoprotein TSP9 regulates light harvesting in *Arabidopsis thaliana*. *Biochemistry* **48**, 499-509.

Fujita, Y. (1997). A study on the dynamic features of photosystem stoichiometry: Accomplishments and problems for future studies. *Photosynthesis Research* **53**, 83-93.

H

Haldrup, A., Jensen, P.E., Lunde, C., and Scheller, H.V. (2001). Balance of power: a view of the mechanism of photosynthetic state transitions. *Trends Plant Sci* **6**, 301-305.

Hammer, M.F., Sarath, G., and Markwell, J. (1995a). Dephosphorylation of the thylakoid membrane light-harvesting complex-II by a stromal protein phosphatase. *Photosynthesis Research* **45**, 195-201.

Hammer, M.F., Sarath, G., Osterman, J.C., and Markwell, J. (1995b). Assessing modulations of stromal and thylakoid light-harvesting complex-II phosphatase activities with phosphopeptide substrates. *Photosynthesis Research* **44**, 107-115.

Hankamer, B., Barber, J., and Boekema, E.J. (1997). Structure and Membrane Organization of Photosystem II in Green Plants. *Annu Rev Plant Physiol Plant Mol Biol* **48**, 641-671.

Hansson, M., and Vener, A.V. (2003). Identification of three previously unknown *in vivo* protein phosphorylation sites in thylakoid membranes of *Arabidopsis thaliana*. *Mol Cell Proteomics* **2**, 550-559.

Hast, T., and Follmann, H. (1996). Identification of two thylakoid-associated phosphatases with protein phosphatase activity in chloroplasts of the soybean (*Glycine max*). *Journal of Photochemistry and Photobiology B-Biology* **36**, 313-319.

Heazlewood, J.L., Durek, P., Hummel, J., Selbig, J., Weckwerth, W., Walther, D., and Schulze, W.X. (2008). PhosPhAt: A Database of phosphorylation sites in *Arabidopsis thaliana* and a plant specific phosphorylation site predictor. *Nucleic Acids Research* **38**, 1015-1021.

Heinemeyer, J., Eubel, H., Wehmhöner, D., Jänsch, L., and Braun, H.P. (2004). Proteomic approach to characterize the supramolecular organization of photosystems in higher plants. *Phytochemistry* **65**, 1683-1692.

Hoglund, A., Donnes, P., Blum, T., Adolph, H.W., and Kohlbacher, O. (2006). MultiLoc: prediction of protein subcellular localization using N-terminal targeting sequences, sequence motifs and amino acid composition. *Bioinformatics*, 1158-1165.

Horton, P., Park, K.J., Obayashi, T., Fujita, N., Harada, H., Adams-Collier, C.J., and Nakai, K. (2007). WoLF PSORT: protein localization predictor. *Nucleic Acids Research*, W585-587.

I

Ihnatowicz, A., Pesaresi, P., Lohrig, K., Wolters, D., Müller, B., and Leister, D. (2008). Impaired photosystem I oxidation induces STN7-dependent phosphorylation of the light-harvesting complex I protein Lhca4 in *Arabidopsis thaliana*. *Planta* **227**, 717-722.

Ihnatowicz, A., Pesaresi, P., Varotto, C., Richly, E., Schneider, A., Jahns, P., Salamini, F., and Leister, D. (2004). Mutants of photosystem I subunit D of *Arabidopsis thaliana*: effects on photosynthesis, photosystem I stability and expression of nuclear genes for chloroplast functions. *Plant J* **37**, 839-852.

J

Jach, G., Binot, E., Frings, S., Luxa, K., and Schell, J. (2001). Use of red fluorescent protein from *Discosoma* sp. (dsRED) as a reporter for plant gene expression. *Plant J* **28**, 483-491.

Jarvis, P. (2004). Organellar proteomics: chloroplasts in the spotlight. *Curr Biol* **14**, R317-319.

Jarvis, P., and Soll, J. (2002). Toc, tic, and chloroplast protein import. *Biochim Biophys Acta* **1590**, 177-189.

Jensen, P.E., Gilpin, M., Knoetzel, J., and Scheller, H.V. (2000). The PSI-K subunit of photosystem I is involved in the interaction between light-harvesting complex I and the photosystem I reaction center core. *J Biol Chem* **275**, 24701-24708.

Jensen, P.E., Haldrup, A., Zhang, S., and Scheller, H.V. (2004). The PSI-O subunit of plant photosystem I is involved in balancing the excitation pressure between the two photosystems. *J Biol Chem* **279**, 24212-24217.

K

Kanervo, E., Suorsa, M., and Aro, E.M. (2005). Functional flexibility and acclimation of the thylakoid membrane. *Photochem Photobiol Sci* **4**, 1072-1080.

Kerk, D., Conley, T.R., Rodriguez, F.A., Tran, H.T., Nimick, M., Muench, D.G., and Moorhead, G.B. (2006). A chloroplast-localized dual-specificity protein phosphatase in *Arabidopsis* contains a phylogenetically dispersed and ancient carbohydrate-binding domain, which binds the polysaccharide starch. *Plant J* **46**, 400-413.

Kleffmann, T., Russenberger, D., von Zychlinski, A., Christopher, W., Sjölander, K., Gruissem, W., and Baginsky, S. (2004). The *Arabidopsis thaliana* Chloroplast Proteome Reveals Pathway Abundance and Novel Protein Functions. *Current Biology* **14**, 354-362.

Kleffmann, T., von Zychlinski, A., Russenberger, D., Hirsch-Hoffmann, M., Gehrig, P., Gruissem, W., and Baginsky, S. (2007). Proteome dynamics during plastid differentiation in rice. *Plant Physiol* **143**, 912-923.

Koop, H.U., Steinmuller, K., Wagner, H., Rossler, C., Eibl, C., and Sacher, L. (1996). Integration of foreign sequences into the tobacco plastome via polyethylene glycol-mediated protoplast transformation. *Planta* **199**, 193-201.

Kotting, O., Santelia, D., Edner, C., Eicke, S., Marthaler, T., Gentry, M.S., Comparot-Moss, S., Chen, J., Smith, A.M., Steup, M., Ritte, G., and Zeeman, S.C. (2009). STARCH-EXCESS4 is a laforin-like Phosphoglucan phosphatase required for starch degradation in *Arabidopsis thaliana*. *Plant Cell* **21**, 334-346.

L

Laemmli, U.K. (1970). Cleavage of structural proteins during the assembly of the head of bacteriophage T4. *Nature* **227**, 680-695.

Laugesen, S., Bergoin, A., and Rossignol, M. (2004). Deciphering the plant phosphoproteome: tools and strategies for a challenging task. *Plant Physiol Biochem* **42**, 929-936.

Leister, D. (2003). Chloroplast research in the genomic age. *Trends Genet* **19**, 47-56.

Lemeille, S., Willig, A., Depege-Fargeix, N., Delessert, C., Bassi, R., and Rochaix, J.D. (2009). Analysis of the chloroplast protein kinase Stt7 during state transitions. *PLoS Biol* **7**, e45.

Liu, Y.G., Mitsukawa, N., Oosumi, T., and Whittier, R.F. (1995). Efficient isolation and mapping of *Arabidopsis thaliana* T-DNA insert junctions by thermal asymmetric interlaced PCR. *Plant J* **8**, 457-463.

Lodish, H., Berk, A., Zipursky, S.L., Matsudaira, P., Baltimore, D., and Darnell, J.E. (2000). *Molecular cell biology*, S. Tenney, ed (New York: W.H. Freeman and Company).

Lunde, C., Jensen, P.E., Haldrup, A., Knoetzel, J., and Scheller, H.V. (2000). The PSI-H subunit of photosystem I is essential for state transitions in plant photosynthesis. *Nature* **408**, 613-615.

M

Maiwald, D., Dietzmann, A., Jahns, P., Pesaresi, P., Joliot, P., Joliot, A., Levin, J.Z., Salamini, F., and Leister, D. (2003). Knock-out of the genes coding for the Rieske protein and the ATP-synthase delta-subunit of

Arabidopsis. Effects on photosynthesis, thylakoid protein composition, and nuclear chloroplast gene expression. *Plant Physiol* **133**, 191-202.

Matsuda, S., Vert, J.P., Saigo, H., Ueda, N., Toh, H., and Akutsu, T.A. (2005). novel representation of protein sequences for prediction of subcellular location using support vector machines. *Protein Science*, 2804-2813.

Maxwell, K., and Johnson, G.N. (2000). Chlorophyll fluorescence-a practical guide. *J Exp Bot* **51**, 659-668.

Melis, A. (1991). Dynamics of photosynthetic membrane composition and function. *Biochim Biophys Acta* **1058**, 87-106.

Moorhead, G.B., Trinkle-Mulcahy, L., and Ulke-Lemee, A. (2007). Emerging roles of nuclear protein phosphatases. *Nat Rev Mol Cell Biol* **8**, 234-244.

Munekage, Y., Hojo, M., Meurer, J., Endo, T., Tasaka, M., and Shikanai, T. (2002). PGR5 is involved in cyclic electron flow around photosystem I and is essential for photoprotection in *Arabidopsis*. *Cell* **110**, 361-371.

Murata, N. (1969). Control of excitation transfer in photosynthesis. I. Light-induced change of chlorophyll a fluorescence in *Porphyridium cruentum*. *Biochim Biophys Acta* **172**, 242-251.

N

Nada, A., and Soll, J. (2004). Inner envelope protein 32 is imported into chloroplasts by a novel pathway. *J Cell Sci* **117**, 3975-3982.

Nelson, N., and Yocum, C.F. (2006). Structure and function of photosystems I and II. *Annu Rev Plant Biol* **57**, 521-565.

Nield, J., Orlova, E.V., Morris, E.P., Gowen, B., van Heel, M., and Barber, J. (2000). 3D map of the plant photosystem II supercomplex obtained by cryoelectron microscopy and single particle analysis. *Nat Struct Biol* **7**, 44-47.

Niittyla, T., Comparot-Moss, S., Lue, W.L., Messerli, G., Trevisan, M., Seymour, M.D., Gatehouse, J.A., Villadsen, D., Smith, S.M., Chen, J., Zeeman, S.C., and Smith, A.M. (2006). Similar protein phosphatases control starch metabolism in plants and glycogen metabolism in mammals. *J Biol Chem* **281**, 11815-11818.

Nilsson, A., Stys, D., Drakenberg, T., Spangfort, M.D., Forsen, S., and Allen, J.F. (1997). Phosphorylation controls the three-dimensional structure of plant light harvesting complex II. *J Biol Chem* **272**, 18350-18357.

O

Ohad, I., Vink, M., Zer, H., Herrmann, R.G., and Andersson, B. (2001). Novel aspects on the regulation of thylakoid protein phosphorylation. In *Regulation of Photosynthesis*, E.M. Aro and B. Andersson, eds (Dordrecht: Kluwer Academic Publishers), pp. 419-432.

Olsen, J.V., Blagoev, B., Gnad, F., Macek, B., Kumar, C., Mortensen, P., and Mann, M. (2006). Global, *in vivo*, and site-specific phosphorylation dynamics in signaling networks. *Cell* **127**, 635-648.

P

Pasch, J.C., Nickelsen, J., and Schünemann, D. (2005). The yeast split-ubiquitin system to study chloroplast membrane protein interactions. *Appl Microbiol Biotechnol* **69**, 440-447.

Peltier, J.B., Emanuelsson, O., Kalume, D.E., Ytterberg, J., Friso, G., Rudella, A., Liberles, D.A., Soderberg, L., Roepstorff, P., von Heijne, G.,

and van Wijk, K.J. (2002). Central functions of the luminal and peripheral thylakoid proteome of *Arabidopsis* determined by experimentation and genome-wide prediction. *Plant Cell* **14**, 211-236.

Pesaresi, P., Lunde, C., Jahns, P., Tarantino, D., Meurer, J., Varotto, C., Hirtz, R.D., Soave, C., Scheller, H.V., Salamini, F., and Leister, D. (2002). A stable LHCII-PSI aggregate and suppression of photosynthetic state transitions in the *psae1-1* mutant of *Arabidopsis thaliana*. *Planta* **215**, 940-948.

Pesaresi, P., Hertle, A., Pribil, M., Kleine, T., Wagner, R., Strissel, H., Ihnatowicz, A., Bonardi, V., Scharfenberg, M., Schneider, A., Pfannschmidt, T., and Leister, D. (2009). Balancing of excitation energy distribution between photosystems: functional relationship of state transitions to long-term photosynthetic acclimation. *Plant Cell*, accepted.

Petsalaki, E.I., Bagos, P.G., Litou, Z.I., and Hamodrakas, S.J. (2006). PredSL: a tool for the N-terminal sequence-based prediction of protein subcellular localization. *Genomics Proteomics Bioinformatics*, 48-55.

Pfannschmidt, T. (2003). Chloroplast redox signals: how photosynthesis controls its own genes. *Trends Plant Sci* **8**, 33-41.

Pfannschmidt, T., Schutze, K., Brost, M., and Oelmüller, R. (2001). A novel mechanism of nuclear photosynthesis gene regulation by redox signals from the chloroplast during photosystem stoichiometry adjustment. *J Biol Chem* **276**, 36125-36130.

Plücker, H., Müller, B., Grohmann, D., Westhoff, P., and Eichacker, L.A. (2002). The HCF136 protein is essential for assembly of the photosystem II reaction center in *Arabidopsis thaliana*. *FEBS Letters* **532**, 85-90.

Poole, R.L. (2007). The TAIR database. *Methods Mol Biol* **406**, 179-212.

Porra, R.J. (2002). The chequered history of the development and use of simultaneous equations for the accurate determination of chlorophylls a and b. *Photosynth Res* **73**, 149-156.

Pursiheimo, S., Mulo, P., Rintamäki, E., and Aro, E.M. (2001). Coregulation of light-harvesting complex II phosphorylation and lhcb mRNA accumulation in winter rye. *Plant J* **26**, 317-327.

Puthiyaveetil, S., Kavanagh, T.A., Cain, P., Sullivan, J.A., Newell, C.A., Gray, J.C., Robinson, C., van der Giezen, M., Rogers, M.B., and Allen, J.F. (2008). The ancestral symbiont sensor kinase CSK links photosynthesis with gene expression in chloroplasts. *Proc Natl Acad Sci U S A* **105**, 10061-10066.

R

Richly, E., and Leister, D. (2004). An improved prediction of chloroplast proteins reveals diversities and commonalities in the chloroplast proteomes of Arabidopsis and rice. *Gene* **329**, 11-16.

Rintamäki, E., Kettunen, R., and Aro, E.M. (1996). Differential D1 dephosphorylation in functional and photodamaged photosystem II centers. Dephosphorylation is a prerequisite for degradation of damaged D1. *J Biol Chem* **271**, 14870-14875.

Rintamäki, E., Martinsuo, P., Pursiheimo, S., and Aro, E.M. (2000). Cooperative regulation of light-harvesting complex II phosphorylation via the plastoquinol and ferredoxin-thioredoxin system in chloroplasts. *Proc Natl Acad Sci U S A* **97**, 11644-11649.

Rintamäki, E., Salonen, M., Suoranta, U.M., Carlberg, I., Andersson, B., and Aro, E.M. (1997). Phosphorylation of light-harvesting complex II and photosystem II core proteins shows different irradiance-dependent

regulation in vivo. Application of phosphothreonine antibodies to analysis of thylakoid phosphoproteins. *J Biol Chem* **272**, 30476-30482.

Rochaix, J.D. (2007). Role of thylakoid protein kinases in photosynthetic acclimation. *FEBS Lett* **581**, 2768-2775.

Rodriguez, P.L. (1998). Protein phosphatase 2C (PP2C) function in higher plants. *Plant Mol Biol* **38**, 919-927.

Rokka, A., Aro, E.M., Herrmann, R.G., Andersson, B., and Vener, A.V. (2000). Dephosphorylation of photosystem II reaction center proteins in plant photosynthetic membranes as an immediate response to abrupt elevation of temperature. *Plant Physiol* **123**, 1525-1536.

S

Saito, H. (2001). Histidine phosphorylation and two-component signaling in eukaryotic cells. *Chem Rev* **101**, 2497-2509.

Sambrook, J., Fritsch, E.F., and Maniatis, T. (1989). *Molecular cloning*. (New York: Cold Spring Harbor Laboratory Press).

Schägger, H., and von Jagow, G. (1987). Tricine-sodium dodecyl sulfate-polyacrylamide gel electrophoresis for the separation of proteins in the range from 1 to 100 kDa. *Anal Biochem* **166**, 368-379.

Schein, A.I., Kissinger, J.C., and Ungar, L.H. (2001). Chloroplast transit peptide prediction: a peek inside the black box. *Nucleic Acids Res* **29**, E82.

Schliebner, I., Pribil, M., Zühlke, J., Dietzmann, A., and Leister, D. (2008). A survey of chloroplast protein kinases and phosphatases in *Arabidopsis thaliana*. *Curr Genomics* **9**, 184-190.

Sessions, A., Burke, E., Presting, G., Aux, G., McElver, J., Patton, D., Dietrich, B., Ho, P., Bacwaden, J., Ko, C., Clarke, J.D., Cotton, D., Bullis, D., Snell, J., Miguel, T., Hutchison, D., Kimmerly, B., Mitzel, T., Katagiri, F., Glazebrook, J., Law, M., and Goff, S.A. (2002). A high-throughput Arabidopsis reverse genetics system. *Plant Cell* **14**, 2985-2994.

Shikanai, T. (2007). Cyclic electron transport around photosystem I: genetic approaches. *Annu Rev Plant Biol* **58**, 199-217.

Sirpio, S., Khrouchtchova, A., Allahverdiyeva, Y., Hansson, M., Fristedt, R., Vener, A.V., Scheller, H.V., Jensen, P.E., Haldrup, A., and Aro, E.M. (2008). AtCYP38 ensures early biogenesis, correct assembly and sustenance of photosystem II. *Plant J* **55**, 639-651.

Small, I., Peeters, N., Legeai, F., and Lurin, C. (2004). Predotar: A tool for rapidly screening proteomes for N-terminal targeting sequences. *Proteomics* **4**, 1581-1590.

Sokolov, L.N., Dominguez-Solis, J.R., Allary, A.L., Buchanan, B.B., and Luan, S. (2006). A redox-regulated chloroplast protein phosphatase binds to starch diurnally and functions in its accumulation. *Proc Natl Acad Sci U S A* **103**, 9732-9737.

Soll, J., and Schleiff, E. (2004). Protein import into chloroplasts. *Nat Rev Mol Cell Biol* **5**, 198-208.

Stengel, A., Soll, J., and Bölter, B. (2007). Protein import into chloroplasts: new aspects of a well-known topic. *Biol Chem* **388**, 765-772.

Sun, G., Bailey, D., Jones, M.W., and Markwell, J. (1989). Chloroplast Thylakoid Protein Phosphatase Is a Membrane Surface-Associated Activity. *Plant Physiol* **89**, 238-243.

T

Tantoso, E., and Li, K.B. (2007). AAIndexLoc: predicting subcellular localization of proteins based on a new representation of sequences using amino acid indices. *Amino Acids*.

Tetlow, I.J., Wait, R., Lu, Z., Akkasaeng, R., Bowsher, C.G., Esposito, S., Kosar-Hashemi, B., Morell, M.K., and Emes, M.J. (2004). Protein phosphorylation in amyloplasts regulates starch branching enzyme activity and protein-protein interactions. *Plant Cell* **16**, 694-708.

Tikkanen, M., Nurmi, M., Suorsa, M., Danielsson, R., Mamedov, F., Styring, S., and Aro, E.M. (2008). Phosphorylation-dependent regulation of excitation energy distribution between the two photosystems in higher plants. *Biochim Biophys Acta* **1777**, 425-432.

Tikkanen, M., Piippo, M., Suorsa, M., Sirpiö, S., Mulo, P., Vainonen, J., Vener, A.V., Allahverdiyeva, Y., and Aro, E.M. (2006). State transitions revisited—a buffering system for dynamic low light acclimation of *Arabidopsis*. *Plant Mol Biol* **62**, 779-793.

Towbin, H., Staehelin, T., and Gordon, J. (1979). Electrophoretic transfer of proteins from polyacrylamide gels to nitrocellulose sheets: procedure and some applications. *Proc Natl Acad Sci U S A* **76**, 4350-4354.

V

Vainonen, J.P., Hansson, M., and Vener, A.V. (2005). STN8 protein kinase in *Arabidopsis thaliana* is specific in phosphorylation of photosystem II core proteins. *J Biol Chem* **280**, 33679-33686.

Vener, A.V. (2007). Environmentally modulated phosphorylation and dynamics of proteins in photosynthetic membranes. *Biochim Biophys Acta* **1767**, 449-457.

Vener, A.V., Ohad, I., and Andersson, B. (1998). Protein phosphorylation and redox sensing in chloroplast thylakoids. *Curr Opin Plant Biol* **1**, 217-223.

Vener, A.V., Harms, A., Sussman, M.R., and Vierstra, R.D. (2001). Mass spectrometric resolution of reversible protein phosphorylation in photosynthetic membranes of *Arabidopsis thaliana*. *J Biol Chem* **276**, 6959-6966.

Vener, A.V., van Kan, P.J., Rich, P.R., Ohad, I., and Andersson, B. (1997). Plastoquinol at the quinol oxidation site of reduced cytochrome *b_f* mediates signal transduction between light and protein phosphorylation: thylakoid protein kinase deactivation by a single-turnover flash. *Proc Natl Acad Sci U S A* **94**, 1585-1590.

Vener, A.V., Rokka, A., Fulgosi, H., Andersson, B., and Herrmann, R.G. (1999). A cyclophilin-regulated PP2A-like protein phosphatase in thylakoid membranes of plant chloroplasts. *Biochemistry* **38**, 14955-14965.

W

Waagemann, K., and Soll, J. (1991). Characterization of the import apparatus in isolated outer envelopes of chloroplasts. *Plant Journal*, 149-159.

Walters, R.G. (2005). Towards an understanding of photosynthetic acclimation. *J Exp Bot* **56**, 435-447.

Wollman, F.A. (2001). State transitions reveal the dynamics and flexibility of the photosynthetic apparatus. *EMBO J* **20**, 3623-3630.

X

Xue, T., Wang, D., Zhang, S., Ehrling, J., Ni, F., Jakab, S., Zheng, C., and Zhong, Y. (2008). Genome-wide and expression analysis of protein phosphatase 2C in rice and Arabidopsis. *BMC Genomics* **9**, 550.

Z

Zer, H., and Ohad, I. (2003). Light, redox state, thylakoid-protein phosphorylation and signaling gene expression. *Trends Biochem Sci* **28**, 467-470.

Zito, F., Finazzi, G., Delosme, R., Nitschke, W., Picot, D., and Wollman, F.A. (1999). The Qo site of cytochrome b6f complexes controls the activation of the LHCII kinase. *EMBO J* **18**, 2961-2969.

Zybailov, B., Rutschow, H., Friso, G., Rudella, A., Emanuelsson, O., Sun, Q., and van Wijk, K.J. (2008). Sorting signals, N-terminal modifications and abundance of the chloroplast proteome. *PLoS ONE* **3**, e1994.

Acknowledgements

I am especially grateful to Prof. Dr. Dario Leister for funding, supervising and supporting my work and his trust in me, especially during times of uncertainty of the project's outcome. I have hopefully learned from his persistence.

I would like to thank Prof. Dr. Jörg Nickelsen for taking over the "Zweitgutachten".

I dearly want to thank Dr. Paolo Pesaresi for being a seemingly inexhaustible source of ideas. I appreciated the fruitful discussions we had, his endless motivation for science and his personal commitment towards the end of this work. For sure there will be a spare room for him also in the future.

To Prof. Dr. Roberto Barbato and Dr. Paolo Pesaresi for the generation of TAP38 antibodies in record time.

To Alexander Hertle for the quick realisation of the *in vitro* import studies and his inexhaustible optimism he readily shared with his colleagues.

To Angie for introducing me to the lab. Her willingness to help with words and deeds is unique.

To all colleagues of my lab for sharing good and bad times and your buffers.

To my dear office mates who readily took care of my continuously increasing caffeine dosage towards the end of this work and gratefully overlooked my recent absent-mindedness.

To my parents, who always believed in me, although I always had to tell them that there are still untouched resources. Here they are!

To Jutta, my better half, who gave me all the support it took to get this work done.

Curriculum vitae

PERSONAL DATA

Name: Mathias Pribil
Date of birth: 19 th of May 1979
Place of birth: Augsburg, Germany
Citizenship: German

RESEARCH EXPERIENCE

May 2006 – July 2009

Ludwig-Maximilians-University Munich (Germany)
Department Biology I, Botany
PhD in “Regulation of Photosynthesis in *Arabidopsis thaliana* via reversible protein phosphorylation”.
Supervisor Prof. Dr. Dario Leister

January 2005 – December 2005

The University of Queensland, Brisbane (Australia)
Research Project “Characterisation of transgenic sugarcane cultivars in respect of gibberellic acid biosynthesis”
(completed at the biotechnology laboratories of BSES Ltd.)
Supervisor Dr. Prakash Lakshmanan

EDUCATION

2000 – 2006

Ludwig-Maximilians-University of Munich (Germany)
Studies of Biology
Diploma thesis “Molecular characterisation of transgenic sugarcane over-expressing *Phaseolus coccineus* GA2-oxidase”
Supervisor Prof. Dr. Hans-Ulrich Koop
Diploma in Biology – Diplom Biologe (Univ.) Final grade 1.1

1999 - 2000

University of Augsburg, Germany
Studies of Educational Sciences

1989 –1998

Justus-von-Liebig-Grammar school of Neusaess, Germany
Majors: Chemistry and English
A-levels, Final grade 2.5

PUBLICATIONS

Pribil, M., Pesaresi, P., Hertle, A., Barbato, R., and Leister, D. (2009). Role of chloroplast protein phosphatase TAP38 in LHCII dephosphorylation and thylakoid electron flow. *Science*, submitted.

Pesaresi, P., Hertle, A., Pribil, M., Kleine, T., Wagner, R., Strissel, H., Ihnatowicz, A., Bonardi, V., Scharfenberg, M., Schneider, A., Pfannschmidt, T., and Leister, D. (2009). Balancing of excitation energy distribution between photosystems: functional relationship of state transitions to long-term photosynthetic acclimation. *Plant Cell*, accepted.

Hald, S., Pribil, M., Leister, D., Gallois, P., and Johnson, G.N. (2008). Competition between linear and cyclic electron flow in plants deficient in Photosystem I. *Biochim Biophys Acta* **1777**, 1173–1183.

Schliebner, I.*, Pribil, M.*, Zühlke, J., Dietzmann, A., and Leister, D. (2008). A survey of chloroplast protein kinases and phosphatases in *Arabidopsis thaliana*. *Curr Genomics* **9**, 184-190.

Pribil, M., Hermann, S.R., Dun, G.D., Karno, Ngo, C., O'Neill, S., Wang, L., Bonnett, G.D., Chandler, P.M., Beveridge, C.A., and Lakshmanan, P. (2007). Altering Sugarcane Shoot Architecture through genetic engineering: Prospects for increasing cane and sugar yield. *Proc. Aust. Soc. Sugar Cane Technol.* **29**

* authors contributed equally

publications related to this thesis

Declaration / Ehrenwörtliche Versicherung

Hiermit versichere ich, dass ich die vorliegende Arbeit selbständig und nur unter Verwendung der angegebenen Hilfsmittel und Quellen angefertigt habe. Der Autor hat zuvor nicht versucht, anderweitig eine Dissertation einzureichen oder sich einer Doktorprüfung zu unterziehen. Die Dissertation wurde keiner weiteren Prüfungskommission weder in Teilen noch als Ganzes vorgelegt.

München, 13. Juli 2009

.....

Mathias Pribil